GFZ

Helmholtz-Zentrum
POTSDAM

HELMHOLTZ-ZENTRUM POTSDAM
DEUTSCHES
GEOFORSCHUNGSZENTRUM

Ludwig Ballani, Dietrich Stromeyer,
Hans Greiner-Mai, Jan M. Hagedoorn

The geomagnetic nonharmonic downward continuation method (NHDC)

Basics, details, special cases and some applications

Scientific Technical Report STR12/08

www.gfz-potsdam.de

HELMHOLTZ
GEMEINSCHAFT

Imprint

Helmholtz Centre Potsdam
GFZ German Research Centre for Geosciences

Telegrafenberg
D-14473 Potsdam

Printed in Potsdam, Germany
June 2012

ISSN 1610-0956

DOI: 10.2312/GFZ.b103-12088
URN: urn:nbn:de:kobv:b103-12088

This work is published in the GFZ series
Scientific Technical Report (STR)
and electronically available at GFZ website
www.gfz-potsdam.de > News > GFZ Publications

Ludwig Ballani, Dietrich Stromeyer,
Hans Greiner-Mai, Jan M. Hagedoorn

The geomagnetic nonharmonic downward continuation method (NHDC)

Basics, details, special cases and some applications

Scientific Technical Report STR12/08

Abstract

It is of high interest to know the magnetic field, measured at the earth surface or by satellites, in the earth deep interior, especially at the core-mantle boundary (CMB). This knowledge is of relevance for the determination of fluid motions at the top of the outer core, the estimation of diffusion and the geomagnetic spectrum, as well as in calculations of the electromagnetic core-mantle coupling torques or in studying the behaviour of geomagnetic jerk components near the CMB.

The presented procedure of nonharmonic downward continuation (NHDC) is a strong theoretical method, an illposed inverse initial boundary value problem, which determines the given outer geomagnetic field or the secular variation in the deep earth interior. It accounts for a prescribed mantle conductivity model depending on the radius. Boundary values are given only on one, the upper (outer) side of the radial interval.

We discuss the theoretical background of the method, referring to the intensively investigated inverse heat conduction problem in the field of parabolic differential equations, and adapt it to the geomagnetic downward continuation problem. Some historical remarks on the early trials in developing this method around the year 1980 are outlined.

After investigating the limited possibilities for analytical solutions, we present the numerical algorithm, which uses the integral equation approach, combined with a special regularization variant. It can be implemented on the basis of finite differences or the finite-element technique.

This algorithm enables simulations setting up simple function types (e.g. oscillations, time polynomials). In addition, approximative approaches help to reveal the analytical dependence of the solution on the conductivity function, e.g. its impact on the phase shifts or time shifts, which are different for radial and tangential magnetic field components.

A couple of new applications are addressed, e.g. to check the divergence condition for the magnetic field at the CMB and the way to make diffusion studies near the CMB. On the basis of NHDC, we derive a new formula for the geomagnetic spectrum at the CMB, which shows in its approximated form the influence of the mantle conductivity model. Finally, some remarks on future possibilities in the field of geomagnetic downward continuation are added.

Keywords

geomagnetic field, geomagnetic secular variation, downward continuation, core-mantle boundary, fluid outer core, electrical mantle conductivity, magnetic diffusion, geomagnetic spectrum, inverse boundary value problem

Table of Contents

Abstract 1

Table of Contents 4

1 Introduction 5

2 Geomagnetic frame 7
- 2.1 The mantle induction equation . . . 7
- 2.2 An extension of the model : Adding the upper layer of the fluid outer core . . . 9

3 Downward field continuation 11
- 3.1 Mathematical tasks . . . 11
- 3.2 Harmonic downward continuation . . . 12
- 3.3 Nonharmonic downward continuation . . . 13
- 3.4 Solution by an integral equation . . . 14
- 3.5 Transformation of the one-dimensional induction (diffusion) equation . . . 15
- 3.6 Solution: Analytical possibility . . . 17
- 3.7 Hadamard's criteria on correctness . . . 18
  - 3.7.1 Existence and uniqueness . . . 18
  - 3.7.2 Temporal instability . . . 18
  - 3.7.3 Stability estimates . . . 20
- 3.8 A sketch on the history of the geomagnetic nonharmonic downward continuation . . . 21

4 The NHDC method 25
- 4.1 Algorithm . . . 25
- 4.2 Solution by finite elements . . . 27
- 4.3 Error estimation . . . 31

5 Special cases: Solutions for special function setups ('Simulations') 33
- 5.1 Time polynomial setups . . . 33
- 5.2 Periodical Gauss coefficients . . . 35
  - 5.2.1 Basics . . . 35
  - 5.2.2 Amplitude and phase shift for B_r with a periodical setup at $r = R_\sigma$ . . . 36
  - 5.2.3 Amplitude and phase shift for B_ϑ with a periodical setup at $r = R_\sigma$ . . . 37
- 5.3 Finite Fourier series . . . 38

6 Data based setups: Approximative solutions 41
- 6.1 Up and downward continuation solution schemes . . . 41
- 6.2 Upward and downward continuation of field components . . . 43
- 6.3 Periodical perturbation setups: Amplitudes and phases . . . 44
- 6.4 Downward continuation of temporally local extrema . . . 45

7 Impact of the conductivity function 47

8 Applications **51**
8.1 Divergence of the geomagnetic field at the CMB 51
8.2 Geomagnetic spectra and geomagnetic energy at the CMB 52
8.3 Diffusion studies 56

9 Overcoming the limitations **61**

References **69**

1 Introduction

Only a few phenomena originating from the deep earth interior can be directly observed at the earth surface. Among them are the sufficiently long-periodic subdecadal and decadal variations (1 a. . . 100 a) of the temporally variable earth-magnetic field. Measurements of different type of the earth magnetic field vector are known from about the year 1600 (Jacobs, 1987a). Since several years global field measurements are provided by means of satellites (MAGSAT, ØRSTED, CHAMP, see e.g. Reigber et al., 2002; Olsen, 2002) and will be continued by future satellite missions as the SWARM mission.

However, only one portion of the magnetic field, the so-called poloidal part, is observable in principle outside the earth. Nevertheless, it represents important geophysical boundary values depending on the wavelength for properties of the earth crust, the mantle and the earth core. Especially detailed investigations are possible concerning the electrical conductivity (Kuvshinov, 2012), and for processes ongoing in the core-mantle boundary zone or in the fluid outer core as the fluid motions. Thus also the modelling of the field generating dynamo process is supported (Krause & Rädler, 1980; Bloxham & Jackson, 1991; Backus et al., 1996) and indirect ways for the determination of the unknown toroidal field part (Hagedoorn et al., 2010).

Another global phenomenon of interest is the explanation of the rotational behavior of the layered earth body composed of media with different rheology down to the inner core. The modelling consists in applying the conservation law for the angular momentum which is usually done by including and balancing all the models of mass transfers, angular momenta, loading effects and coupling torques. The electromagnetic coupling between the earth core and mantle due to Lorentz torques, including magnetic field variations, fluid motions and induced currents which act in the decadal spectral range, is one candidate of possible coupling mechanisms explaining corresponding variations in the earth rotation vector (Greiner-Mai, 1993; Holme, 1998; Hagedoorn & Greiner-Mai, 2008).

All these modelling tasks have the requirement in common to need and to derive the deep earth magnetic field using only earth surface or outer space field data. Thus this task belongs to the class of the typical geophysical field downward continuation problems known also for gravity, heat flow and gas exploration. These problems are boundary value problems but with partly unknown (lower) boundary values, i.e. they have to be classified as inverse boundary value problems often being illposed.

The geomagnetic frame is given by the induction equation for the poloidal magnetic field which is derived from the Maxwell equations in the quasi-static approximation. It is a parabolic differential equation here formulated for a spherical shell and treated – after some decomposition – in one local dimension for a finite interval of the radial variable. The geomagnetic downward continuation means that the input data (time functions), the boundary values, are given only on one – here the upper (earth surface) – side of the radial interval like the inverse heat conduction problem (the sideways heat equation problem or more general the 'non-characteristic Cauchy problem'). The other one, the internal (deeper) boundary is inaccessible for measurements and the values there have to be determined. In addition to the analogy to the usually studied inverse heat conduction problem, our 'diffusion' equations have a radially variable coefficient function being the radially variable electrical conductivity. While only for constant conductivity coefficients (the simplest case) approximative analytical solutions can be given in the form of infinite series solutions connected with the so-called ϑ-functions, the general downward continuation problem can be only solved by a numerical procedure. Because of the partially relative weak conductivities, recently assumed and discussed for the earth mantle, this downward continuation problem is often neglected and replaced with the harmonic downward continuation (zero-conductivity) for which in the one-dimensional case simple analytical formulae can be applied. To stress the difference to this limitation we have introduced the term 'nonharmonic downward continuation'(NHDC) for the general case to be considered here (for some numerical results, applications and comparisons see Ballani et al., 2002; Greiner-Mai

et al., 2004).

Some analytic theory around this problem in geomagnetism can be found in Smylie (1965) and in an expanded form in Gubbins (1996). An approximative numerical method for the nonharmonic downward continuation using a series setup ('perturbation theory') was studied in Benton & Whaler (1983). Related early papers were given by Braginsky & Fishman (1977) and Zhdanov et al. (1980). There are also some contributions in this field by Stadelmann (2001,2006); Stadelmann & Weidelt (2005b,a).

In the intensively studied field of the inverse heat conduction problems, the specific basic statements, especially on the properties as the stability of this inverse boundary value problem, were developed. Accounting for locally and temporally variables in finite intervals and including also coefficient functions in the differential equation, being the characteristics in the NHDC, corresponding statements were derived in papers by Manselli & Miller (1980), Knabner & Vessella (1987, 1988) and Engl & Manselli (1989). Similar to our problem, but alternatively solved, is one of the computed examples in (Berntsson, 1999), who treats an inverse problem for a parabolic differential equation with a locally variable coefficient. General surveys with many references on the inverse heat conduction problem are given in Dinh & Gorenflo (1991) and (Reinhardt & Seiffarth, 1993). Some recent mathematical work is found by Vessella (1997) and Francini (2000).

The main features of the downward continuation problem presented here were discussed (for an easier) inverse heat conduction problem by Eldén (1983, 1995). His outline inspired us to follow a solution approach via an integral equation formulation.

The NHDC method was developed as of the years 1994/1995. A short article on the basic structure of the method (Ballani et al., 1995), first theoretical studies and applications followed after some conference presentations with mathematical background details (Ballani et al., 1999) and the extension of the method to the fluid outer core (Greiner-Mai et al., 2001). The first fundamental and detailed article (Ballani et al., 2002) studied the effect of nonharmonic downward continuation for the B_r field component at the CMB and also in a layer of the fluid outer core ('passive upper layer'). However, for this component the deviations from the until then conventional harmonic case and also from results of the perturbation theory of Benton & Whaler (1983) were really very weak, so that the method for this case could not fully convince. A further progress became an expansion of the method combined with prescribed velocities in the fluid outer core, where in the depth range of 50 km to 100 km at its numerical boundaries very strong effects (because of the high conductivity in the core) were determined. For this task, the method was reformulated in the more compact complex notation (Greiner-Mai et al., 2004). The significant effects arising in the tangential field or secular variation components could be studied for the electromagnetic core-mantle coupling (Greiner-Mai et al., 2007), where the condition $\sigma(r) \neq 0$ is absolutely required, and in the study of the jerk 1991 at the CMB (Ballani et al., 2010). For the three components could be demonstrated that the jerk components concerning their time shifts behave up to a certain degree as oscillating secular variation components.

The structure of this report is as follows: We present the geomagnetic frame (Ch. 2). In Ch. 3 at first we sketch the connection between boundary value problem and field continuation and viewing all possible cases. After a brief summary of the harmonic downward continuation, we define the nonharmonic downward continuation and discuss the possibilities of solution in different formulations. We illustrate the limitations for pure analytical solutions, study the three principal Hadamard condition, especially the temporal instability, and survey the historical attempts to find a downward continuation method. Ch. 4 is devoted to the details of our solution method added by some basics to introduce finite elements. The NHDC method is further studied (Ch. 5) using special simulating setups with simple analytic functions. The following chapter (Ch. 6) treats in a complementary way approximative setups giving approximative solutions which allow to study such properties as phase shifts of oscillations or time shifts of extremal points at downward continuation. Special aspects on the impact of a given conductivity function at NHDC can be found in Ch. 7. There are also some new applications (Ch. 8) of the NHDC method concerning the divergence test at the CMB, the derivation of a new formula for the geomagnetic spectrum at the CMB accounting for a prescribed mantle conductivity function, and the calculation of diffusion near the CMB. Finally, we discuss some limitations of the method connected with some chances for future developments (Ch. 9).

Geomagnetic frame | 2

2.1 The mantle induction equation

The description and the study of electromagnetic phenomena, proceeding in the earth mantle, require the use of the theoretical frame of Maxwell equations, (e.g. Backus et al., 1996; Jacobs, 1987b). It consists of the differential equations

$$\operatorname{curl} \mathbf{H} = \mathbf{J} + \frac{\partial}{\partial t}\mathbf{D}\,, \tag{2.1}$$

$$\operatorname{curl}\, \mathbf{E} = -\frac{\partial}{\partial t}\mathbf{B}\,, \tag{2.2}$$

$$\operatorname{div} \mathbf{B} = 0\,, \tag{2.3}$$

$$\operatorname{div} \mathbf{D} = \rho\,, \tag{2.4}$$

with the constitutive equation and Ohm's law

$$\mathbf{B} = \mu\mathbf{H}\,, \qquad \mathbf{J} = \sigma\mathbf{E}\,. \tag{2.5}$$

The quantities $\mathbf{H}$, $\mathbf{B}$, $\mathbf{E}$, $\mathbf{D}$, $\mathbf{J}$, μ, σ, ρ denote the magnetic field, the magnetic flux density, the electric field, the electric displacement, the electric current density, the permeability, the (mantle) conductivity, and the charge density, respectively. If in addition to the earth mantle the fluid outer core with its motions is involved, then the Maxwell equations have to be extended by motion terms, the fluid velocity $\mathbf{u}$, yielding the magnetohydrodynamic approximation by replacing Ohm's law with the expanded version

$$\mathbf{J} = \sigma\left(\mathbf{E} + \mathbf{u} \times \mathbf{B}\right)\,. \tag{2.6}$$

In the following, only the time scale of decadal variations (1 to 100 years) is considered, therefore the electric displacement currents $\partial/\partial t\mathbf{D}$ can be neglected and the first law (2.1) is replaced by

$$\operatorname{curl} \mathbf{H} = \mathbf{J}\,. \tag{2.7}$$

Thus, instead of the full Maxwell form of the basic equations the so-called pre-Maxwell frame (also called 'quasi-static approximation') forms the theoretical starting point.

The vectorial induction equation of the mantle is derived from (2.1) with (2.7) and (2.5) by eliminating $\mathbf{J}$ and the electric field $\mathbf{E}$, to reduce the involved number of fields leaving the magnetic flux, $\mathbf{B}$,

$$\operatorname{curl}\left(\frac{1}{\mu\,\sigma}\,\operatorname{curl}\,\mathbf{B}\right) \;=\; -\frac{\partial}{\partial t}\mathbf{B},\,. \tag{2.8}$$

We will assume a spherical symmetric conductivity function σ, i.e., $\sigma = \sigma(r)$. This assumption enables to move $1/(\mu\,\sigma)$ in front of the differential operator (see 8.44). Together with the equation $\operatorname{div}\mathbf{B} = 0$, (2.3), the flux density $\mathbf{B}$ can be orthogonally decomposed into toroidal and poloidal parts $\mathbf{B_t}, \mathbf{B_p}$, which are generated by two scalar functions $S(r,\vartheta,\varphi,t)$ and $T(r,\vartheta,\varphi,t)$ as follows

$$\mathbf{B} \;=\; \mathbf{B_t} \,+\, \mathbf{B_p} \;=\; \operatorname{curl}\left(\mathbf{r}T\right) \,+\, \operatorname{curl}\,\operatorname{curl}\left(\mathbf{r}S\right)\,. \tag{2.9}$$

This decomposition is unique, if on any sphere with radius r the normalization conditions

$$\oiint T\,\sin\vartheta\,d\vartheta\,d\varphi \;=\; 0 \quad \text{and} \quad \oiint S\,\sin\vartheta\,d\vartheta\,d\varphi \;=\; 0 \tag{2.10}$$

are fulfilled (e.g. Krause & Rädler, 1980; Backus, 1986; Schmitt, 1995).

As the toroidal field vanishes outside a conductor, it is difficult to observe it on (near) the earth surface and its downward continuation requires additional assumptions (Hagedoorn et al., 2010). Thus, all considerations in the following are confined to the poloidal field part.

Using known formulae of vector analysis, we find the relation between the poloidal vector field $\mathbf{B_p}$ and the poloidal scalar function S

$$\mathbf{B_p} = -\,\mathbf{r}\,\Delta S \,+\, \nabla\,\frac{\partial}{\partial r}(r\,S), \tag{2.11}$$

where Δ and ∇ are the Laplacean and the Nabla operators, respectively. If the operator

$$\Omega \,=\, \frac{1}{\sin\vartheta}\,\frac{\partial}{\partial\vartheta}\left(\sin\vartheta\,\frac{\partial}{\partial\vartheta}\right) \,+\, \frac{1}{\sin^2\vartheta}\,\frac{\partial^2}{\partial\varphi^2} \tag{2.12}$$

means the Laplacean on the unit sphere the single vector components of $\mathbf{B_p} = (B_r, B_\vartheta, B_\varphi)$ (formulas (19,20,21) in Benton & Whaler, 1983) can be expressed by

$$B_r = -\frac{1}{r}\,\Omega\,S\,, \qquad B_\vartheta = \frac{1}{r}\,\frac{\partial}{\partial\vartheta}\left(\frac{\partial}{\partial r}(r\,S)\right)\,, \qquad B_\varphi = \frac{1}{r\sin\vartheta}\,\frac{\partial}{\partial\varphi}\left(\frac{\partial}{\partial r}(r\,S)\right)\,. \tag{2.13}$$

With relation (2.11) the vectorial induction equation (2.8) passes into a scalar induction equation

$$\Delta\,S = \mu_0\,\sigma(r)\,\dot{S}, \tag{2.14}$$

which has the form of a parabolic partial differential equation, under physical point of view being a diffusion or heat conduction equation. For non-conducting mantle shells ($\sigma(r) \equiv 0$) the Laplace equation holds

$$\Delta\,S = 0. \tag{2.15}$$

The scalar function S can be expanded for any fixed radius r into a series of surface spherical harmonic functions, $\{P_{nm}(\cos\vartheta)\cos m\varphi, P_{nm}(\cos\vartheta)\sin m\varphi\}$ where P_{nm} are the associated Legendre functions and N the truncation index:

$$S(r,\vartheta,\varphi,t) = \sum_{n=1}^{N}\sum_{m=0}^{n}\left(S^c_{nm}(r,t)\cos m\varphi \,+\, S^s_{nm}(r,t)\sin m\varphi\right)P_{nm}(\cos\,\vartheta)\,. \tag{2.16}$$

Because of the eigenvalue equation

$$\Omega\left(P_{nm}(\cos\vartheta)\left\{\begin{array}{c}\cos\,m\varphi\\ \sin\,m\varphi\end{array}\right\}\right) \,=\, -n(n+1)\,P_{nm}(\cos\vartheta)\left\{\begin{array}{c}\cos\,m\varphi\\ \sin\,m\varphi\end{array}\right\} \tag{2.17}$$

and equation (2.14), we find corresponding to a separation of the form $f(r,t)\cdot g(\vartheta,\varphi)$ and due to the orthogonality of the spherical harmonics, the fully decoupled one-dimensional induction equations for the single spherical harmonic modes $S^{c,s}_{nm}(r,t)$ as 1-D parabolic partial differential equations ($n = 1,\ldots,N; m = 0,\ldots,n$)

$$\frac{\partial^2 S^{c,s}_{nm}}{\partial r^2} \,+\, \frac{2}{r}\,\frac{\partial S^{c,s}_{nm}}{\partial r} \,-\, \frac{n(n+1)}{r^2}\,S^{c,s}_{nm} = \mu_0\,\sigma_(r)\,\dot{S}^{c,s}_{nm} \tag{2.18}$$

or the elliptic differential equations for vanishing conductivity

$$\frac{\partial^2 S^{c,s}_{nm}}{\partial r^2} \,+\, \frac{2}{r}\,\frac{\partial S^{c,s}_{nm}}{\partial r} \,-\, \frac{n(n+1)}{r^2}\,S^{c,s}_{nm} = 0\,. \tag{2.19}$$

It has to be remarked that only the magnetic vector component B_r (2.13) is directly governed by scalar function S while the components B_ϑ, B_φ also include the derivative $\frac{\partial}{\partial r}(r\,S)$, which needs the additional calculation of derivatives in the general nonharmonic case (2.14) resp. (2.18).

In detail we have the geomagnetic component formulae expressed by the single spherical harmonic modes $S^{c,s}_{nm}(r,t)$ resp. by their radial partial derivatives

$$B_r = \sum_{n=1}^{N}\sum_{m=0}^{n}\left(\frac{1}{r}S^c_{nm}(r,t)\cos m\varphi + \frac{1}{r}S^s_{nm}(r,t)\sin m\varphi\right) n(n+1)\ P_{nm}(cos\vartheta), \tag{2.20}$$

$$B_\vartheta = \sum_{n=1}^{N}\sum_{m=0}^{n}\left(\frac{1}{r}\frac{\partial}{\partial r}(r\ S^c_{nm}(r,t))\cos m\varphi + \frac{1}{r}\frac{\partial}{\partial r}(r\ S^s_{nm}(r,t))\sin m\varphi\right)\frac{dP_{nm}(cos\vartheta)}{d\vartheta}, \tag{2.21}$$

$$B_\varphi = \sum_{n=1}^{N}\sum_{m=0}^{n}\left(\frac{1}{r}\frac{\partial}{\partial r}(r\ S^s_{nm}(r,t))\cos m\varphi - \frac{1}{r}\frac{\partial}{\partial r}(r\ S^c_{nm}(r,t))\sin m\varphi\right) m\ \frac{P_{nm}(cos\vartheta)}{\sin\vartheta}. \tag{2.22}$$

The structure of the two types of corresponding (r,t)-depending coefficients – here abbreviated by $\beta^r_{nm}(r,t)$ and $\beta^{\vartheta,\varphi}_{nm}(r,t)$ resp. – yields to

$$\beta^r_{nm}(r,t) = \frac{S^{c,s}_{nm}(r,t)}{r} \quad \text{and} \quad \beta^{\vartheta,\varphi}_{nm}(r,t) = \frac{S^{c,s}_{nm}(r,t)}{r} + \frac{\partial\, S^{c,s}_{nm}(r,t)}{\partial r}. \tag{2.23}$$

We do not use here the more precise notations $\beta^{r,c,s}_{nm}, \beta^{\vartheta,\varphi,c,s}_{nm}$ contrary to Sec. 8.2.

Remark: Coefficients $S^{c,s}_{nm}, g_{nm}, h_{nm}$ and associated Legendre functions P_{nm} should be coordinated in their normalization, Ferrers-Neumann (FN) or Schmidt-quasinormalization (SchmQ), (e.g. Kautzleben, 1965). Special notes are not given in the single sections. For the polynomials with different normalization holds

$$\lambda_{nm}\, P^{FN}_{nm} \ = \ P^{SchmQ}_{nm}\,. \tag{2.24}$$

See (3.5), (3.8) and further conversion formulae in Sec. 8.2.

2.2 An extension of the model : Adding the upper layer of the fluid outer core

The combined treatment of electromagnetism and moving media with velocity $\mathbf{v}$ in the fluid outer core is provided by an expanded induction equation, including now the so-called Lorentz term,

$$\mathrm{curl}\,[(\mu_0\sigma)^{-1}\,\mathrm{curl}\ \mathbf{B}] - \mathrm{curl}(\mathbf{v}\times\mathbf{B}) = -\dot{\mathbf{B}}\,. \tag{2.25}$$

Thus a kinematic modelling in a shell of thickness d, $r\in[R_c-d, R_c]$, beneath the core-mantle boundary is possible with prescribed velocity $\mathbf{v}$.

If the special setup for the velocity $\mathbf{v}$

$$\mathbf{v} = (0,0,\omega(r))\times\mathbf{r} \tag{2.26}$$

is introduced into the vector differential equation (2.25), with a given function $\omega(r)$ a differential rotation in this layer is described. All the decompositions applied above for the mantle case, lead finally to pairs of coupled differential equations (for each n and m) for the functions S^c_{nm}, S^s_{nm} (Greiner-Mai et al., 2004)

$$\frac{\partial^2 S^c_{nm}}{\partial r^2} + \frac{2}{r}\frac{\partial S^c_{nm}}{\partial r} - \frac{n(n+1)}{r^2}S^c_{nm} - m\,\mu_0\,\sigma(r)\,\omega(r)\,S^s_{nm} = \mu_0\,\sigma(r)\,\dot{S}^c_{nm} \tag{2.27}$$

$$\frac{\partial^2 S^s_{nm}}{\partial r^2} + \frac{2}{r}\frac{\partial S^s_{nm}}{\partial r} - \frac{n(n+1)}{r^2}S^s_{nm} + m\,\mu_0\,\sigma(r)\,\omega(r)\,S^c_{nm} = \mu_0\,\sigma(r)\,\dot{S}^s_{nm}\,. \tag{2.28}$$

They describe the effect of prescribed motion due to the function $\omega(r)$ on the diffusion of the magnetic field variations beginning upwards from this outer core layer. This can be used for the study of this layer.

A really dynamical description which can lead to geodynamo models would be reached by adding the Navier-Stokes equation accounting for the momentum balance of the fluid medium in the outer core (cf. Krause & Rädler, 1980; Backus et al., 1996). In this frame 'inverse dynamo problems' can also be studied (e.g. Stefani & Gerbeth, 2000).

3 Downward field continuation

3.1 Mathematical tasks

Our area of modelling is the earth mantle or additionally an upper layer of the fluid outer core, which does not change this situation principally, i.e. the equations (2.14) and (2.15) and also (2.18) and (2.19)resp. have to be studied in a spherical shell

$$M = \{(r, \vartheta, \varphi) : R_c \le r \le R_E, -\pi/2 \le \vartheta \le \pi/2, -\pi \le \varphi \le \pi\}$$

Its boundary ∂M consists of an inner and an outer part, which are the spherical surfaces at both ends of the r-interval: $r = R_E$ and $r = R_c$. **Continuation** of the magnetic field – which is here represented by the scalar function S – shall refer to the connection between time functions on these boundaries $S(R_c, \vartheta, \varphi, t)$ and $S(R_E, \vartheta, \varphi, t)$. Two directions can be distinguished:

Upward continuation calculates a time function at the upper side of the shell from a given time function giver on the lower side of the shell.

$$S(R_c, \vartheta, \varphi, t) \quad \longrightarrow \quad S(R_E, \vartheta, \varphi, t) \quad (3.1)$$

Vice versa, **downward continuation** uses an outer time function to determine an unknown time function on the lower side of the spherical shell.

$$S(R_E, \vartheta, \varphi, t) \quad \longrightarrow \quad S(R_c, \vartheta, \varphi, t) \quad (3.2)$$

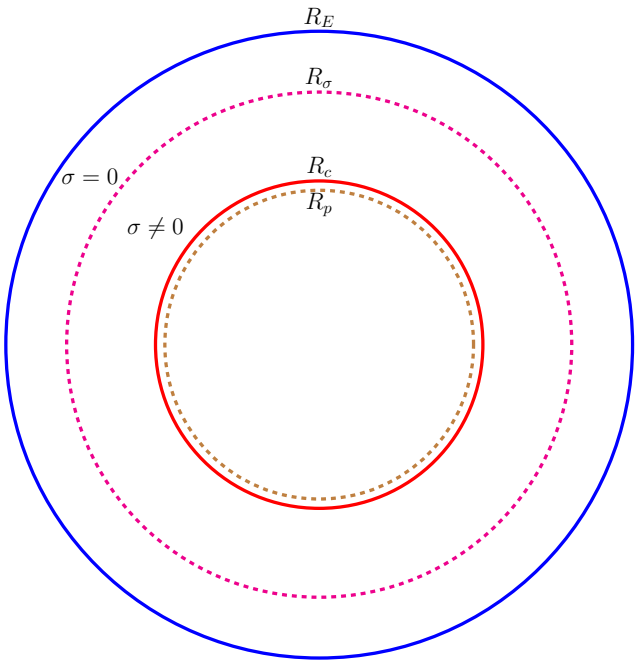

Figure 3.1: Earth mantle model geometry with radii used : $R_E = 6371$ km, $R_\sigma = 5485$ km, $R_c = 3485$ km and (inside the fluid outer core) $R_p = R_c - d$ with $d \le 100$ km.

To understand the background of these tasks it is useful to remember a few basics of boundary value problems of parabolic differential equations of second order (here eq. (2.14)). The classical case for an initial-boundary value value problem can be solved uniquely and stable, i.e. 'well-posed' in the sense of Hadamard, if an initial condition and a boundary value function for the **whole boundary** is given. (For precise details see standard textbooks treating boundary value problems of partial differential equations.) Moreover, it is also possible to prescribe boundary values of different kind (first, second or third kind) for **different parts of the whole boundary** (see e.g. Cannon, 1984). In our case of the earth mantle, we get a well-posed task if we assume, e.g., boundary value functions at R_c of second kind, $\phi_2(t) = \partial S/\partial r(R_c, \vartheta, \varphi, t)$, and at R_E of first kind, $\phi_1(t) = S(R_E, \vartheta, \varphi, t)$.

In contrary to this, it is typically for the (geophysical) **continuation** problems that **not all parts** of the boundary are (can be) **supported** with a boundary value function (input data). However, under these conditions the boundary value problem can not be longer solved in the usual way. This applies for the unknown geomagnetic field at the CMB, and to a great extent for the well-known inverse heat conduction problems mainly because of the inaccessibility to measurements (e.g. Eldén, 1983).

The situation can be improved by using an additional boundary value function (of another type e.g. of 2nd or 3rd kind) which originates from a further physical indication at those parts of the boundary which are already supported by a boundary value function (e.g. of 1st kind).

That means that now the whole boundary consists of two different parts: one part supported by two boundary values (e.g. at R_E : $S(R_E, \vartheta, \varphi, t)$), $\frac{\partial S}{\partial r}(R_E, \vartheta, \varphi, t)$ and the remaining other one without support by boundary value data (e.g. at R_c). Such problems for partial differential equations are illposed because of their temporal instability, but are in our case uniquely solvable (e.g. Tsutsumi, 1965; Dinh & Gorenflo, 1991), see also below Sec. 3.7.

The possible continuation problems with boundary values

$$\text{of first kind} \quad \phi_1(t) = S(r, \vartheta, \varphi, t) \quad \text{and of second kind} \quad \phi_2(t) = \frac{\partial S}{\partial r}(r, \vartheta, \varphi, t) \tag{3.3}$$

with r specified to one of the two possible locations $r = R_E$ or $r = R_c$, are contained in the following table, which shows all constellations for the two boundary kinds at the earth surface and at the CMB

case	$r = R_c$	$r = R_E$
1	ϕ_1, ϕ_2	
2	ϕ_1	ϕ_2
3		ϕ_1, ϕ_2
4	ϕ_2	ϕ_1

The cases 1 and 2 can be classified as upward continuation problems (Smylie, 1965; Backus, 1983), 3 and 4 are downward continuation problems. The cases 1 and 3 are one-sided unstable (illposed) boundary value problems while the cases 2 and 4 are well-posed problems. Only two of these cases are of relevance in the following and were studied in the literature, case 2 as upward continuation and case 3 as downward continuation. The cases 1 and 4 could be of importance, e.g., if inner geomagnetic dynamo data and outer magnetic data would be studied in combination.

Our main intention is to study case 3 in detail, i.e. its properties and some applications in different situations.

3.2 Harmonic downward continuation

The simplest case arises, if the mantle conductivity is set to be zero through the whole mantle, which is very often assumed by many authors, i.e., the mantle is an insulator and does not permit any magnetic diffusion.

The geomagnetic potential V, related to the magnetic flux by $\mathbf{B_p} = -\nabla V$, is given by

$$V(r, \vartheta, \varphi, t) = R_E \sum_{n=1}^{N} \sum_{m=0}^{n} \left(g_{nm}(t) \cos m\varphi + h_{nm}(t) \sin m\varphi\right) \lambda_{nm} P_{nm}(\cos \vartheta) \left(\frac{R_E}{r}\right)^{n+1}, \tag{3.4}$$

(e.g. Ch. 4, p.255, Jacobs, 1987a), with P_{nm} in Ferrers-Neumann normalization and with λ_{nm} as Schmidt's quasi-normalization coefficients defined by

$$\lambda_{nm} = \left((2 - \delta_{0m}) \frac{(n-m)!}{(n+m)!}\right)^{1/2} \text{with } \delta_{ik} = \begin{cases} 1 & i = k \\ 0 & i \neq k \end{cases} \text{ (Kronecker's symbol).} \tag{3.5}$$

Via the connection to the poloidal scalar S

$$V = -\frac{\partial}{\partial r}(rS) \tag{3.6}$$

the relation for **harmonic downward continuation** of S

$$S(r, \vartheta, \varphi, t) = \sum_{n,m} \left(C^c_{nm}(t)\, r^{-n-1} \cos m\varphi + C^s_{nm}(t)\, r^{-n-1} \sin m\varphi\right) P_{nm}(\cos \vartheta) \tag{3.7}$$

can be derived. It gives the result simply by inserting the wanted radius $r, R_c \leq r \leq R_E$. Our proper data, contained in global geomagnetic field models, are the time-dependent Gauss coefficients $g_{nm}(t)$,$h_{nm}(t)$ valid for the earth surface $\mathrm{r} = \mathrm{R_E}$ given in the usual Schmidt quasi-normalisation. They are related to the time-dependent coefficients $C^{c,s}_{nm}(t)$ by

$$C^{c,s}_{nm}(t) \;=\; \left\{ \begin{array}{c} g_{nm}(t) \\ h_{nm}(t) \end{array} \right\} \frac{\lambda_{nm}}{n}\; R_E^{n+2}\,. \tag{3.8}$$

In this analytical form, harmonic downward continuation is clearly unique, but can also be temporally unstable. (The problem in the background is the (illposed) Cauchy problem for the Laplace equation applied to a spherical shell. The identity (3.7) for $r = R_E$ represents the upper boundary value.) The time structure given by the Gauss coefficients at the earth surface is for each degree n and order m kept, but is newly scaled at downward continuation corresponding to the special degree n.

3.3 Nonharmonic downward continuation

Together with the two boundary values and an initial condition the following initial-boundary value problem describes the task of **nonharmonic downward continuation** for determining $S(R_c, \vartheta, \varphi, t)$ (compare case 3 in the table above). At the moment the radius R_σ can be any radius between R_c and $\mathrm{R_E}$.

$$\Delta\, S = \mu_0\, \sigma(r)\, \dot{S}\,, \qquad R_c < r < R_\sigma\,, \qquad 0 \leq t \leq T \tag{3.9}$$

with the boundary conditions

$$S(R_\sigma, \vartheta, \varphi, t) = \phi_1(t)\,, \qquad \frac{\partial S(R_\sigma, \vartheta, \varphi, t)}{\partial r} = \phi_2(t)$$

and the initial condition

$$S(r, 0) \;=\; \psi(r).$$

Inserting the general representation for S (2.16) leads to **decomposed nonharmonic downward continuation tasks**, based on decoupled differential equations, and formulated for the single mode $S^{c,s}_{nm}(r,t)$ for determining $S^{c,s}_{nm}(R_c, t)$

$$\frac{\partial^2 S^{c,s}_{nm}}{\partial r^2} + \frac{2}{r}\frac{\partial S^{c,s}_{nm}}{\partial r} - \frac{n(n+1)}{r^2} S^{c,s}_{nm} \;=\; \mu_0 \sigma(r)\, \frac{\partial S^{c,s}_{nm}}{\partial t}\,, \quad R_c < r < R_\sigma\,, \quad 0 \leq t \leq T \tag{3.10}$$

with the boundary conditions

$$S^{c,s}_{nm}(R_\sigma, t) \;=\; \phi^{c,s}_{1,nm}(t)\,, \qquad \frac{\partial S^{c,s}_{nm}}{\partial r}(R_\sigma, t) \;=\; \phi^{c,s}_{2,nm}(t)$$

and initial conditions

$$S^{c,s}_{nm}(r, 0) \;=\; \psi^{c,s}_{nm}(r).$$

Remarks about these tasks:

1. Theinitial conditions $\psi(\mathrm{r})$ resp. $\psi^{c,s}_{nm}(r)$ are necessary, but they can be freely chosen. However their influence dominates the solution only at the beginning of the time interval and is diminishing with elapsing time.

2. Of course, the boundary values have to be connected with the data which can be time functions or discrete values. The radial derivatives (boundary values of second kind) can be approximated e.g. by finite differences formed by the data. Also the applications of other numerical techniques, e.g. splines, are possible.

3. An important special case is given, if the shell situated above of the conducting mantle shell is nonconducting (between R_E and R_σ) and its surface is identical with the earth surface: The decisive point to derive boundary value functions is the continuity of the magnetic field $\mathbf{B}_p = (B_r, B_\vartheta, B_\varphi)$ at R_σ, the spherical interface between a nonconducting and a conducting mantle shell.

   This continuity holds always for $\mathbf{B_p}$ (e.g. §3 Sommerfeld, 1961) and is transferred by the radial component B_r to S and by the tangential components of $\mathbf{B_p}$ to $\partial S/\partial r$.

   The relations valid at R_σ

$$S(R_\sigma, \vartheta, \varphi, t) = \sum_{n,m} \left(C^c_{nm}(t)\cos(m\varphi) + C^s_{nm}(t)\sin(m\varphi)\right) R_\sigma^{-n-1}\, P_{nm}(\cos\vartheta), \tag{3.11}$$

$$\frac{\partial S(R_\sigma, \vartheta, \varphi, t)}{\partial r} = \sum_{n,m} \left(C^c_{nm}(t)\cos(m\varphi) + C^s_{nm}(t)\sin(m\varphi)\right)(-n-1)R_\sigma^{-n-2}P_{nm}(\cos\vartheta) \tag{3.12}$$

   show the detailed situation for this continuity: The right sides are the harmonic downward continuity results for the radial position R_σ, respectively. The left sides present the searched upper boundary value for the nonconducting mantle shell in problem (3.9).

4. Analogously to these both identities hold for the **single modes from** (3.11), (3.12) for problem (3.10) the relations (using the decomposition of S (2.16))

$$S^{c,s}_{nm}(R_\sigma, t) = C^{c,s}_{nm}(t) R_\sigma^{-n-1}, \tag{3.13}$$

$$\frac{\partial\, S^{c,s}_{nm}(R_\sigma, t)}{\partial r} = C^{c,s}_{nm}(t)(-n-1)R_\sigma^{-n-2}\,. \tag{3.14}$$

   Obviously the last two relations can be combined due to the close analytical connections between them: By inserting the left side of (3.13) into the right side of (3.14) a boundary value of third kind at R_σ is generated:

$$\frac{\partial S^{c,s}_{nm}}{\partial r}(R_\sigma, t) \;+\; \frac{n+1}{R_\sigma}\, S^{c,s}_{nm}(R_\sigma, t) \;=\; 0$$

   It can used instead of the boundary value of second kind and thus avoids the direct data input. Thus, these **decomposed nonharmonic downward continuation tasks**, having decoupled differential equations, can de formulated for the single modes $S^{c,s}_{nm}$ for determining $S^{c,s}_{nm}(R_c, t)$

$$\frac{\partial^2 S^{c,s}_{nm}}{\partial r^2} + \frac{2}{r}\frac{\partial S^{c,s}_{nm}}{\partial r} - \frac{n(n+1)}{r^2} S^{c,s}_{nm} \;=\; \mu_0\sigma(r)\,\frac{\partial S^{c,s}_{nm}}{\partial t}\,, \quad R_c < r < R_\sigma\,, \quad 0 \le t \le T \tag{3.15}$$

   with the boundary conditions

$$S^{c,s}_{nm}(R_\sigma, t) \;=\; \phi^{c,s}_{nm}(t)\,, \qquad \frac{\partial S^{c,s}_{nm}}{\partial r}(R_\sigma, t) \;+\; \frac{n+1}{R_\sigma}\, S^{c,s}_{nm}(R_\sigma, t) \;=\; 0$$

   and initial conditions

$$S^{c,s}_{nm}(r, 0) \;=\; \psi^{c,s}_{nm}(r).$$

   $\phi^{c,s}_{nm}$ are the boundary values derived by harmonic continuation of the geomagnetic surface potential field downward to this boundary at $r = R_\sigma$.

3.4 Solution by an integral equation

Another solution possibility connected directly with the downward continuation task (table 1, case 3) is to transfer the problem given as initial-value problem (3.9) or (3.10), respectively, to an equivalent Volterra integral equation of the first kind. This requires an homogeneous initial condition, which can be reached by subtraction of an appropriate stable, two-side (well-posed) boundary value problem (see Sec. 4.1, step(i)). One possible way to such an integral equation was described by Smylie (1965) (see Sec. 3.6 and the formulae (3.39), (3.40)) ($u(r,t) := S^{c,s}_{nm}(r,t)$)

$$\phi(t) = u(R_\sigma, t) \;=\; \int_0^t k(t-\tau)\, f(\tau) d\tau, \qquad f(t) = u(R_c, t) \tag{3.16}$$

This integral equation interconnects the upper (known) boundary function $\phi(t) = u(R_\sigma, t)$ and the unknown function $f(t) = u(R_c, t)$ (see eq. (4.1)). The information on the geometry of the problem, on the conductivity function and on the second boundary condition is 'contained' in the kernel k(t) (Cannon, 1984; Eldén, 1983).

Under analytical point of view, especially the explicite determination and applying the kernel function k(t) itself for the integration, this approach however remains of limited importance (see Sec. 3.6). On the other hand, the integral equation approach turns out to be numerically advantageous, so that a practicable algorithm for nonharmonic downward continuation can be realized starting with this origin (see Section 4.1 'Algorithm').

3.5 Transformation of the one-dimensional induction (diffusion) equation

The decomposed one-dimensional diffusion equation (3.10) can be found by Smylie (1965) and by Backus (1983), who study the problem of upward continuation. In dependency of special applications and a further analytical or numerical handling it can be useful to transform this equation, i.e. to exchange of the local variable r as well as the whole function $S^{c,s}_{nm}(r,t)$. $S^{c,s}_{nm}(r,t)$ shall be abbreviated by $u(r,t)$ in the following. If a confusion is impossible we use also the shortened notation $u_t := (\partial/\partial t)\, u$ etc.

The whole equation can be presented in different forms: For the application of the finite element approach (weak formulation) only a **simple reshaping** to a symmetric form is necessary. The sign is chosen due to the convention for weak solutions of elliptical differential equations. In general form we have

$$-\frac{\partial}{\partial r}\left(p(r)\frac{\partial}{\partial r}u\right) + b(r)\, u = c(r)\, u_t \ , \tag{3.17}$$

which is here specified to

$$\frac{\partial}{\partial r}\left(r^2\frac{\partial}{\partial r}u\right) - n(n+1)u = \mu_0\, r^2\, \sigma\, u_t \tag{3.18}$$

showing now a changed right hand side. Smylie (1965) presents another possibility to compress the derivation terms with

$$\frac{1}{r}\,\frac{\partial^2}{\partial r^2}\Big(r\, u\Big) - \frac{n(n+1)}{r^2}\, u = \mu_0\, \sigma\, u_t \ . \tag{3.19}$$

By the classical differential calculus it is possible to **reduce** our differential equation finally **leaving only two terms**, each one on each side. Backus (1983) has found and applied such a completed transformation formula with well tuned constants providing then the optimal analytical result. Unfortunately there were no hints to understand the details of this derivation. In the following, we will show the basic steps which could be of general interest.

1. To elucidate the background we start with the general differential equation

$$u_{rr} \ + \ a(r)\, u_r \ + \ b(r)\, u \ = \ c(r)\, u_t. \tag{3.20}$$

We try to **scale the unknown function** $u(r,t)$ by introducing the factor $w(r)$ and the new function by

$$y(r,t) \ = \ u(r,t) \ \cdot \ w(r). \tag{3.21}$$

After having expressed the derivation terms the new differential equation for $y(r,t)$ has the general form

$$y_{rr} \ + \ \left(-\frac{2w_r}{w} + a(r)\right)\, y_r \ + \ \left(-\frac{w_{rr}}{w} + \frac{2(w_r)^2}{w^2} - \frac{w_r}{w}a(r) + b(r)\right)\, y \ = \ c(r)\, y_t \ . \tag{3.22}$$

We search now that scale factor $w(r)$ so that the coefficient of y in this differential equation vanishes, that is to find an analytical solution of the corresponding ordinary differential equation:

$$-\frac{w_{rr}}{w} + \frac{2(w_r)^2}{w^2} - \frac{w_r}{w}a(r) + b(r) \ = \ 0 \tag{3.23}$$

In our case, after specifying the functions $a(r)$ and $b(r)$ (see eq. (3.10)),

$$-\frac{w_{rr}}{w} + \frac{2(w_r)^2}{w^2} - \frac{w_r}{w}\cdot\frac{2}{r} - \frac{n(n+1)}{r^2} = 0 \tag{3.24}$$

can be solved at least by an ansatz $w(r) = A \cdot r^k$ which gives the two solutions

$$w(r) = A \cdot r^{n+1} \quad \text{and} \quad \mathrm{w(r) = A \cdot r^{-n}}. \tag{3.25}$$

We can restrict here only to the first one. Inserting it leads to the shortened differential equation

$$y_{rr} - \left(\frac{2n}{r}\right) y_r = \mu_0\,\sigma\,y_t\ . \tag{3.26}$$

Because the factor A does not appear, it can be freely chosen.

This reduced differential equation is connected with an **important interpretation**: The setup $S_{nm} = u_{nm} = y_{nm}(r,t)\cdot r^{-n-1}$, with S_{nm} from (2.16) and (3.10) means a decomposition into the physical (diffusive) part y_{nm} and geometric part r^{-n-1}. The latter one corresponds to the harmonic downward continuation (3.7). But this setup is also identical with the transformation of the differential equation by scaling (3.21), (3.22) (using the first solution of (3.24) $w(r) = A\cdot r^{n+1}$) which leads to the reduced equation (3.26). Thus this equation for $y_{nm}(r,t)$ exactly describes the pure physical (diffusive) downward continuation (see Rotanova et al., 1991).

2. For a **second transformation step** we look again at a general differential equation

$$v_{rr} + d(r)\,v_r + e(r)\,v = f(r)\,v_t\ . \tag{3.27}$$

We assume that the **coordinate transformation** $x = x(r)$ and its opposite $r = r(x)$ to be smooth enough for inversion. After changing the variable r in the differential equation (3.27) we have (writing $r' = dr/dx$)

$$\mathrm{v_{xx} + \left(-\frac{r''}{r'} + d(x)\,r'\right) v_x + e(x)\,(r')^2\,v = f(x)\,(r')^2\,v_t\ .} \tag{3.28}$$

Specifying to our case (eq. (3.10)) and now considering the coefficient of the first derivative requires to solve the differential equation

$$r''\cdot r' + 2n\cdot(r')^2 = 0 \tag{3.29}$$

to find the condition for vanishing the term by a suited coordinate. This equation can be directly solved by the technique of the separation of variables. The general result

$$r^{2n+1} = c_1\cdot x + c_2 \tag{3.30}$$

has two free constants. Finally, we get equation (3.27) (in its shortest version)

$$v_{xx} = \mu_0\,\sigma(x)\,(c_1x + c_2)^{-\frac{4n}{2n+1}}\,v_t\ . \tag{3.31}$$

3. The described two transformation steps can only demonstrate the way to simplifications. In every case, the precondition is the analytical solvability of the concerned differential equations. The free parameters have to be adapted to the special case, as f.i. the upward or the downward continuation and for a useful range of the variable.

   It is possible to **combine both steps** into one step using the more general framework on substitution in differential expressions (see f.i. Bronshtein et al., 2004, p.398). Therefore, we recapitulate the transformations of Backus (1983) in a compacted form. With

$$r = R_c(1+x)^{\frac{1}{2n+1}} = \phi(x,y)\,,\quad u(r,t) = y(x,t)(1+x)^{-\frac{n+1}{2n+1}} = \psi(x,y) \tag{3.32}$$

applied to the specified equation (3.20) follows the reduced equation as given by Backus (1983)

$$y_{xx} = \mu_0\,\frac{R_c^2}{(2n+1)^2}\,\sigma(x)\,(1+x)^{-\frac{4n}{2n+1}}\,y_t\ . \tag{3.33}$$

4. The effect of an appropriate fixing of the constants (c_1, c_2) of relation (3.31) changes the original r-interval $[R_c,\ R_\sigma]$ into the x-interval $[0,\ (R_\sigma/R_c)^{2n+1} - 1]$.

5. It is interesting that the boundary value of the 3rd kind (see second boundary condition in (3.10)) by the pure coordinate transformation keeps the type. But applying the multiplication (scaling) transformation of the function, the second boundary value change always to a homogeneous one of second kind (see e.g. in (3.9) the second boundary condition with $\phi_2(t) = 0$).

3.6 Solution: Analytical possibility

We present the reformulation of the inverse problem (3.10) as an integral equation and ask for an analytical solution. The linear relation between the known and unknown time functions can be found by a suitable integral transform applied to the parabolic differential equation in (3.10), e.g. using the Laplace transform,

$$\mathcal{L}(u) = \tilde{u}(r,s) := \int_0^\infty u(r,t)\,\mathrm{e}^{-\mathrm{st}}\,\mathrm{dt}, \quad \mathrm{s} \in \mathbb{C} \quad \text{(complex numbers)}\,. \tag{3.34}$$

We get the following two-point boundary value problem for an ordinary differential equation

$$\frac{\partial^2 \tilde{u}}{\partial\, r^2} + \frac{2}{r}\frac{\partial \tilde{u}}{\partial r} + \left(-\mu_0\,\sigma(r)s - \frac{n(n+1)}{r^2}\right)\tilde{u} = -\mu_0\,\sigma(r)\,\psi(r), \tag{3.35}$$

$$\tilde{u}(R_\sigma, s) = \tilde{\phi}(s) \qquad \text{and} \qquad \frac{\partial \tilde{u}(R_\sigma, s)}{\partial r} = -\frac{n+1}{R_\sigma}\,\tilde{\phi}(s). \tag{3.36}$$

Assuming a zero initial condition $\psi(r)$ yields

$$\tilde{u}(R_\sigma, s) = \frac{1}{\tilde{v}(R_c, s)} \cdot \tilde{u}(R_c, s), \tag{3.37}$$

where $\tilde{v}(R_c, s)$ fulfills the differential equation (3.35), but with the boundary values

$$\tilde{v}(R_\sigma, s) = 1 \qquad \text{and} \qquad \frac{\partial \tilde{v}(R_\sigma, s)}{\partial r} = -\frac{n+1}{R_\sigma}\,. \tag{3.38}$$

Thus, the kernel $k(t)$ for the convolution equation (a Volterra integral equation of first kind, see (4.1))

$$\phi(t) = k(t) * u(R_c, t) \tag{3.39}$$

can be determined via

$$k(t) = \mathcal{L}^{-1}\left(\frac{1}{\tilde{v}(R_c, s)}\right). \tag{3.40}$$

Further insight into the structure of $\tilde{k}(s)$ is reached by introducing the general solution of (3.35) with the bases functions $Z_1(r, s, \sigma, n), Z_2(r, s, \sigma, n)$. Thus, the transformed convolution reads as (Z' means here the r-derivative)

$$\tilde{u}(R_\sigma, s) = \frac{Z_1(R_\sigma, s)Z_2'(R_\sigma, s) - Z_2(R_\sigma, s)Z_1'(R_\sigma, s)}{Z_1(R_c, s)Z_2'(R_\sigma, s) - Z_2(R_c, s)Z_1'(R_\sigma, s)} \cdot \tilde{u}(R_c, s)\,. \tag{3.41}$$

The numerator often can be simplified to a constant due to a kind of addition theorem which is connected with Abel's formula for the Wronskian determinant, e.g. in the case of Bessel functions. If no closed analytical inverse Laplace transform of (3.41) exists, usually the residue theorem provides a series solution for the kernel and therefore also for the integral equation. The main problem hereby is to determine the sequence of the roots from transcendental equations (for an application see Smylie, 1965). While the transformed problem (3.35, 3.36) appears as a stable one, the temporal instability of the original downward continuation problem is hidden in the application of the inverse Laplace transform.

For a very simple example, we sketch the analytical solution structure: Assuming the conductivity as $\sigma(r) = \sigma_0 = \mathrm{const}$ and the index as $n = 0$ (This index is however not of relevance for the magnetic field!),

the homogeneous differential equation (3.35) passes via the substitution $\tilde{w} = r \cdot \tilde{u}$ into the well studied standard form

$$\frac{\partial^2 \tilde{w}}{\partial r^2} = \mu_0 \sigma_0 \frac{\partial \tilde{w}}{\partial t} \,. \tag{3.42}$$

Then, adapting the boundary values (3.36), a series representation for the kernel can be found

$$k(t) = \frac{R_c \pi}{\mu_0 \sigma_0 R_\sigma (R_\sigma - R_c)^2} \sum_{j=0}^{\infty} (-1)^n (2j+1) \exp\left(-\frac{(2j+1)^2 \pi^2 t}{4\mu_0 \sigma_0 (R_\sigma - R_c)^2} \right) \,, \tag{3.43}$$

which corresponds to a transformed result of Carslaw & Jaeger (1992, p. 104). This series structure is directly connected with the theory of Theta functions, here with the function ϑ_2 (Spanier & Oldham, 1987),

$$\vartheta_2(\nu, x) = 2 \sum_{j=0}^{\infty} \exp(-(j+1/2)^2 \pi^2 x) \cos(2(j+1/2)\nu\pi) \,.$$

A solution for a two-point boundary value problem with boundary values of the first and third kind (compare (3.36)), can be found in Doetsch (1937). This solution uses analytical results of the inverse Laplace transform and shows that for $n = 0$ the kernel $k(t)$ is proportional to the derivative $\partial\vartheta_2/\partial x$.

In summary, the analytical possibilities concerning the magnetic downward continuation, especially for the relevant cases $n \geq 1$, are strongly limited to special cases, e.g. constant conductivity, time-harmonic case, exponential decay, so that in general a numerical treatment is absolutely necessary.

3.7 Hadamard's criteria on correctness

3.7.1 Existence and uniqueness

Statements concerning the first two correctness criteria of Hadamard, the existence and the uniqueness of the solution of (3.10) and (3.45), hold under relatively weak requirements. They are characterized by conditions for the locally variable coefficient, the initial and boundary functions in the differential equation on finite intervals for both variables. Results were published e.g. by Tsutsumi (1965), Knabner & Vessella (1987), Reinhardt & Seiffarth (1993) and Francini (2000), (For further details see Ballani et al., 1999).

Representatively, the following result (Theorem 1, p. 297, Dinh Nho Hào, 1994) proves that a unique local weak solution of (3.10) exists, which belongs to an adapted Sobolev space, under the conditions

(i) initial condition: $\psi(r) \in L_2[R_c, R_\sigma]$

(ii) coefficient (conductivity function): $\sigma(r) \in W^{1,\infty}[R_c, R_\sigma]$ (Sobolev-Raum) with $0 < \gamma < \sigma(r) < \infty$

(iii) the boundary function $\phi(t)$ belongs to special spaces of smooth functions ('Holmgren classes 2'/ 'Gevrey class of order 2').

The last condition means for our problem: As every finite data series can be identified with an appropriate polynomial, the input data function $\phi(t)$, normally given as a data point series, taken from a B-spline interpolated Gauss coefficient, has not to fulfill an additional smoothness condition.

Thus, the theoretical background gives enough reliability for numerical processing. Data and coefficients are given in discrete form on finite intervals, i.e. the smoothness conditions can be always assumed as fulfilled because their appropriate representation by polynomials or splines.

3.7.2 Temporal instability

Reformulating of the downward continuation problem as an integral equation (see above Sec. 3.4) can help to understand some details of the instability. Altogether, there are three aspects which have to be distinguished:

- The inverse of a smoothing compact (integral) operator especially amplifies the high frequency part of the input data (see (3.45)) (concerning the known instability of the inverse heat conduction problem, see Knabner & Vessella, 1987; Dinh Nho Hào, 1994; Vessella, 1997).
- Because the integral operator is of the convolution type, i.e. the unknown function in the integral equation can be more and more poorer reconstructed the nearer the time points are situated to the end of the time interval. Therefore supporting information is needed.
- In some cases a limited numerical influence can also come from the (in some cases very high) magnitude of the electrical conductivity $\sigma(r)$ as a coefficient function in the differential equation.

Before illustrating the high-frequency instability, we want to investigate the **temporal sensitivity** of the problem of downward continuation in a simple way. We split up the initial boundary value problem by subtracting the harmonic downward continuation, being a temporally stable problem, from the original problem (3.10). The remaining problem represents a further form of our original inverse problem (3.10), which still carries the instability property and thus enables an insight in these effects. Taking the time-dependent coefficient $C^{\mathrm{c,s}}_{n,m}(t)$ used for the harmonic downward continuation ((3.7), (3.8)), the function $R^{\mathrm{c,s}}_{n,m}(r,t)$

$$R^{\mathrm{c,s}}_{n,m}(r,t) := S^{\mathrm{c,s}}_{n,m}(r,t) - C^{c,s}_{n,m}(t)\; r^{-n-1} \tag{3.44}$$

describes the difference between nonharmonic and harmonic downward continuation. This function fulfills the now inhomogeneous parabolic differential equation

$$\frac{\partial^2 R^{\mathrm{c,s}}_{nm}}{\partial r^2} + \frac{2}{r}\frac{\partial R^{\mathrm{c,s}}_{nm}}{\partial r} - \frac{n(n+1)}{r^2} R^{\mathrm{c,s}}_{nm} = \mu_0\,\sigma(r)\frac{\partial R^{c,s}_{n,m}}{\partial t} + \mu_0\,\sigma(r)\frac{\partial C^{\mathrm{c,s}}_{n,m}}{\partial t}\; r^{-n-1}\,, \tag{3.45}$$

$$R^{\mathrm{c,s}}_{n,m}(R_\sigma,t) = 0, \qquad \frac{\partial}{\partial r}R^{c,s}_{n,m}(R_\sigma,t) = 0, \qquad 0 \le t \le T \tag{3.46}$$

$$R^{c,s}_{n,m}(r,0) = 0, \qquad R_c \le r \le R_\sigma$$

but with homogeneous initial and boundary conditions. To find the solution $R^{c,s}_{n,m}(R_c,t)$ from (3.45) and (3.46) is an inverse boundary value problem with the same boundary value structure as (3.10). However, the reduced problem shows clearly that the solution is only controlled by the **inhomogeneity** of the differential equation (3.45), $\mu_0\,\sigma(r)\partial C^{c,s}_{n,m}/\partial t\; r^{-n-1}$, which consists of the **first time derivative of the data functions**. As it is the exclusive data source for the solution of the initial-boundary value problem, it illustrates the sensitive reactions on temporal changes in the data, especially in the high frequency parts.

To get more into the details of the **temporal instability**, especially the growth behaviour, we construct now (for a special case) a solution sequence. At the same time, some analytical techniques can be sketched which are commonly used for spherical problems.
The mantle conductivity $\sigma(r)$ in (3.10) is specified to the often applied formula

$$\sigma(r) \;=\; \sigma_0\,(R_c/r)^\alpha\,, \quad \sigma_0 = \mathrm{const}\,, \tag{3.47}$$

(e.g. Stix, 1982), which approximates a more general exponential-type semi-conductor conductivity law. After applying some transformations to (3.10) a separation ansatz assuming a time-harmonic process gives the general solutions $u^k(r,t), k = 1,2,\ldots$

$$u^k(r,t) = \exp(ik\omega t)\; r^{-1/2}\left[C_1\,J_\nu(z_k\,r^{-\frac{\alpha-2}{2}}) + C_2\,J_{-\nu}(z_k\,r^{-\frac{\alpha-2}{2}})\right], \quad \nu = \frac{(2n+1)}{(\alpha-2)} \tag{3.48}$$

$$z_k = \frac{2}{\alpha-2}(-ik\omega\mu_0\sigma_0 R_c^\alpha)^{1/2}, \qquad C_1,\; C_2 \text{ constants}$$

where $J_\nu, J_{-\nu}$ are Bessel functions (Abramowitz & Stegun, 1965). Without loss of generality we consider here only the case $\alpha > 2$.
$u^k(r,t)$ fulfills the first boundary condition in (3.10) with an oscillating function

$$\phi^k(t) \;=\; A\,\exp(ik\omega t)\,, \qquad k = 1,2,\ldots \quad \text{at} \quad R_\sigma\,. \tag{3.49}$$

The second boundary condition consists only in an relation between the constants C_1 and C_2 and has no relevance for the following.
To see the growth of a sequence of functions starting at $r = R_\sigma$ it is necessary to introduce a normalization by defining

$$\bar{u}^k(r,t) := \exp(ik\omega t)\,\frac{u^k(r,t)}{u^k(R_\sigma,t)}, \qquad k = 1,2,\ldots \tag{3.50}$$

Via the decomposition into the Kelvin functions and using their exponential estimates (Abramowitz & Stegun, 1965) the lower bound

$$|\bar{u}^k(r,t)| \geq C\,\left(\frac{r}{R_\sigma}\right)^{\frac{\alpha}{4}-1} \exp\left(\frac{(\,2k\omega\,\mu_0\sigma_0 R_c^\alpha\,)^{1/2}}{\alpha-2}\,(r^{1-\alpha/2} - R_\sigma^{1-\alpha/2})\right), \qquad r < R_\sigma \tag{3.51}$$

can be derived whereas

$$|\bar{u}^k(R_\sigma,t)| = 1 \qquad \text{holds for} \qquad k = 1,2,\ldots\,. \tag{3.52}$$

Obviously, the modulus of $\bar{u}^k(r,t)$ grows up at least exponentially with the square root of the frequency $k\omega$. Moreover, for fixed k (frequency) and α (conductivity) the whole argument of the exponential function in (3.51) is increasing with decreasing r. Thus, the radial growth of the amplitude for a fixed frequency can also be estimated. The degree index n (see (3.10)) does not appear explicitly because its influence is only very weak due to the normalization. It is included into the constant C (Analogous growth examples can be found also on pp.19–20, Engl et al., 1996, for the standard differential equation).

3.7.3 Stability estimates

To make magnetic downward continuation to be a well-posed problem in the sense of Hadamard, the fulfillment of the third correctness criterion, the stability, is necessary. It can be established by imposing additional conditions ('a priori bounds') or other assumptions on the temporary smoothness of the solution $u(R_c,t)$. Numerous theoretical contributions exist on this topic (see citations in Ballani et al., 1999).

As the range of the spacial variable r is a closed finite interval, here $[R_c, R_\sigma]$, (under mathematical view point) two cases are distinguished:

(i) The position of r is located **in the interior** of this interval which enables stability estimates of the Hölder type.

(ii) The position of r is located **at the boundary** of the interval ($r = R_c$) leading only to the weaker logarithmic stability estimates.

Considering the **case (i)**, the interior of the radial interval, we adopt a theoretical result of Knabner & Vessella (1988) directly to our problem: With the assumptions

$$\|\phi\|_2 \leq \epsilon \qquad \text{and} \qquad \|u(R_c,.)\|_2 \leq E \qquad \text{(a priori bound)}, \tag{3.53}$$

$$\sigma(r) \in W^{2,\infty}(R_c,R_\sigma)\,, \qquad 0 < \gamma < \sigma(r) < \infty, \tag{3.54}$$

$$u(r,0) = 0 \quad \text{for} \quad R_c < r \leq R_\sigma \qquad \text{and} \qquad \frac{\partial u(R_\sigma,t)}{\partial r} = 0 \tag{3.55}$$

the Hölder estimate follows ($R_c < r \leq R_\sigma$):

$$\|u(r,.)\|_2 \leq C\,\epsilon^{1-K(r)/K(R_c)}(\epsilon^{K(r)/K(R_c)} + E^{K(r)/K(R_c)}) \quad \text{with} \quad K(r) = \int_r^{R_\sigma} (\mu_0\sigma(r))^{1/2}\,dr. \tag{3.56}$$

The proper content of such an estimate is the linking between differences, i.e. inserted (a small difference) for $\phi = \phi^0 - \phi^\delta$ in (3.53) gives an estimate for the corresponding difference $u^0 - u^\delta$ in (3.56).

The function $K(r)$ which appears in the controlling exponents in (3.56) represents in its squared form a physical quantity, the so-called electrical time constant of a radial symmetrically conducting layer of the mantle (Roberts, 1972).

Concerning **case(ii)**, an a priori bound for the time function $\|u(R_c,.)\|_2$,(R_c is one boundary of the radial interval) is, however, not sufficient to get a stability estimate (see counterexample in Remark 2.1, p. 403 Knabner & Vessella, 1987). More smoothness for the solution (than confining the function $\|u(R_c,.)\|_2$) has to be required, e.g. by a priori bounds for the radial or temporal derivatives. Moreover, instead of a Hölder estimate only the weaker logarithmic dependence on the Cauchy data of the order $O\left(1/log(1/\epsilon)\right)$ can be reached for $\|u(R_c,.)\|_2$ where ϵ is an upper bound for the data norm $\|\phi\|_2$. A theorem of Manselli & Vessella (1991, Theorem 1.1, p. 516) applied to our problem, confirms this situation:
If we prescribe the conditions

$$|u(R_\sigma,t)| \le \epsilon \qquad \text{and} \qquad \left|\frac{\partial u}{\partial r}(R_\sigma,t)\right| \le \epsilon (R_\sigma - R_c)^{-1} \tag{3.57}$$

and assume that for the interval boundary R_c with the a priori bound $E,\ E>0$, the relation

$$\max_{[R_c,R_\sigma]\times[0,T]} |u| + T^\alpha \sup_{t_1\neq t_2} \frac{|u(R_c,t_2)-u(R_c,t_1)|}{|t_2-t_1|^\alpha} \le E \tag{3.58}$$

is fulfilled for some $\alpha \in (0,1)$. Then, for a fixed $\beta \in (0,\frac{2}{3}\alpha)$, a constant ϵ_1 exists, such that the estimate

$$|u(R_c,t)| \le |log\,\epsilon|^{-\beta} \qquad \text{holds if} \qquad \epsilon \le \epsilon_1\ . \tag{3.59}$$

(ϵ_1 depends on $A,\beta,E,R_c,R_\sigma,\alpha$ with $A=\max\{(\mu_0\sigma(r))^{-1} : r\in[R_c,R_\sigma]\}$.)
However, the constants involved in such logarithmic estimates and especially the integrative influence of the electrical conductivity, can no longer be specified explicitly.
To overcome this numerically complicated situation concerning the stability at the important interval boundary (R_c) it is possible to choose different approaches:

(i) assuming additional a priori smoothness for the solution using theoretical founded regularization strategies, so that Hölder estimates become valid again, (Such estimations were shown for a simpler differential equation in Engl & Manselli, 1989) or

(ii) using a more general solution concept. We will follow this second way in the Sec. 4.1.

3.8 A sketch on the history of the geomagnetic nonharmonic downward continuation

From the Fifties of the twentieth century on, the main interest concerning the magnetic field of the deep earth interior referred above all to come step by step to a better data situation for the main field. An overview and detailed study of all potential field models was e.g. given by Mauersberger (1952). This phase was connected with the revealing of temporal changes: the secular variation. Important modelling initiatives in the Fifties and Sixties were basic developments on the generation of the earth magnetic field ('dynamo theory') (Bullard & Gellman, 1954), later on with the successful concept in this field by the group of Steenbeck, Krause and Rädler (beginning with the important paper of 1966 see, Krause & Rädler, 1980). With the modelling of the core-mantle coupling (Rochester, 1960, 1962) the link between earth rotation and geomagnetic field was taken into consideration. A survey of the whole temporal behaviour of the outer geomagnetic field was provided by studying geomagnetic spectra related to the magnetic signals generated within the core (Currie, 1967). The study of single temporal geomagnetic variations was focussed on the range of decadal periods, especially to the 60 years, 30 years and also 20 years oscillations.

Two topics, connected with upward and downward field continuation and external and internal induction, were at that time **of special interest**:

(i) to find estimates of the conductivity of the earth mantle and

(ii) the problem of the shielding properties of the earth mantle, i.e. which magnetic oscillations come from the earth interior and are still observable at the earth surface after having filtered by the electrically conducting earth mantle.

Initially, these tasks were treated by choosing special functions for the conductivity, e.g. a stratified mantle equipped with constant conductivities for the single layers or with the potential law for the conductivity $\sigma(r) = \sigma_0(R_c/r)^\alpha$. The solution of these problems was analytically possible in the highly developed frame of Bessel functions which is used until now (see Pinheiro & Jackson, 2008). Important papers of this early phase were given by McDonald (1957) and later on by Kolomitzeva (1972, 1982). However, a general mathematical downward continuation procedure in geomagnetism was not taken into consideration.

The task of the geomagnetic **upward** continuation for a spherical-symmetric conductivity was worked out by Smylie (1965). He used the Laplace transform with respect to the time variable and constructed a solution scheme working independently on the special given mantle conductivity $\sigma(r)$.

Currie (1967) has pointed to the importance of the possibility of the downward continuation (remark in (Rotanova et al., 1991)). At that time, it had become already clear that two effects in downward continuation had to be distinguished:

(i) a geometrical effect as was known for a long time by the harmonic downward continuation (by multiplying each spherical harmonic degree with a special power of r see (3.7));

(ii) a physical effect due to a (magnetic) diffusion which is described by the parabolic differential equation (3.26).

The **development of** a general **downward continuation methods** started in the second half of the seventies of the last century, mainly by three groups of authors. They worked independently of each other considering different geomagnetic aspects, but with restricted communication, partly due to a informational as well as a language barrier. Most pronouncedly, the following papers contain the ideas on nonharmonic downward continuation:

(A) Braginsky & Fishman (1977)

(B) Zhdanov et al. (1980)

(C) Benton & Whaler (1983)

We display some features on the publications (A), (B) and (C).

- On the publishing situation: (A) The authors gave afterwards further publication of the topic. (B) There exist probably also contributions prior to the cited paper, possibly related to the (oral) lecture for the induction workshop 1978 in Murnau/Germany. (C) No hint were found on any forerunner contribution on that topic.

- There are different theoretical starting points: (A) and (C) have based their investigation on the poloidal-toroidal decomposition. They formulate one-sided boundary value problems for the poloidal field (diffusion equation) with boundary values of first and second kind or first and third kind. For (C) the solution setup is initialized by an early paper on the inverse heat conduction problem presenting a perturbation theory (Burggraf, 1964). The analogies between different quantities in geomagnetism and heat conduction concerning the diffusion processes are established. Another way was selected by (B) who refer to the Helmholtz equation (not considering the poloidal-toroidal decomposition) and search the solution at the CMB for only one frequency, thus circumventing time-dependency, with the Fourier decomposition and synthesis in the background.

- (A) and (C) allow radially dependent mantle conductivities. Additionally, (A) require restrictively the conductivity concentrated near the CMB.
- The character of the mathematical task as an illposed (unstable) problem is specified by (B) and (C). Moreover, (B) even gives some possibilities for regularization. As a kind of regularization in (A) and (C) the scales are considered separately: For the two scales, spatially and temporally, smoothing average constants are introduced.
- (A),(B) and (C) have in common that they produce approximate solutions as series expansions for the field components at the CMB. The single terms of the series solutions of (A) and (C) depend with increasing index on corresponding number of temporal derivatives of the time-dependent Gauss coefficients (indices are here suppressed) $g(t), h(t), \dot{g}(t), \dot{h}(t), \ldots$ and so on. It is pointed out that rapid (high-frequency) field changes have to be excluded as they constitute the (numerical) instability of the task.
- As for the properties of the solutions, the authors of (A) already had found the effect that the three magnetic field components, being synchronously at the earth surface, but show different phase shifts at the CMB due to the magnetic diffusion. The method of (A) was applied by Rotanova et al. (1991) for studies of the secular variation, i.e. the temporal derivative of the geomagnetic field, for studies of the structure of the jerk 1970 at the CMB and an estimate for the conductivity of the lower mantle.

4 The NHDC method

4.1 Algorithm

The solving procedure formulates and handles the inverse problem (3.10) as a (Volterra) integral equation. The solution is set up as a finite-dimensional approximation relative to a prescribed function basis spanning the solution space and is searched as a minimum norm solution. The final determination of the unknown expansion coefficients is done with a special regularization variant. The precision of the data approximation and the smoothness of the solution can be accounted for by selecting suitable norms. Starting with the inverse problem in its original form (3.10), the following steps are executed:

(i) The initial-boundary value problem (3.10) is transformed by subtracting a stable value problem with homogeneous boundary conditions (at R_c: first kind, at R_σ: 3rd kind) and the given initial condition $\psi(r)$ so that the resulting difference problem has zero initial condition. The equivalent integral equation is then of Volterra type of the first kind

$$\phi(t) \;=\; \int_0^t k(t-\tau)\, f(\tau) d\tau + \phi_\psi(t), \qquad f(t) = u(R_c, t) \tag{4.1}$$

Here, $\phi_\psi(t)$ is the solution of eq. (3.10) at $r = R_\sigma$ with zero boundary values. In general, the kernel $k(t)$ is not explicitly (analytically) known and is not used in the algorithm.

(ii) That is the reason for approximating the right hand side of eq. (4.1) directly by a finite-dimensional operator A related to bases functions $e_k(t)$, $k = 1, \ldots, N$ in the solution space: With a finite setup for $f(t)$ there, the upward continuation is linearly related

$$f(t) \;=\; \sum_{k=1}^{N} f_k\, e_k(t) \qquad \xrightarrow{A} \qquad \phi(t) = \sum_{k=1}^{N} f_k A\left(e_k(t)\right) \;. \tag{4.2}$$

The still unknown term $A(e_k(t)) = u_k(R_\sigma, t)$ can be determined (because of uniqueness) by a sequence of k stable (two-side) initial-boundary value problems.

$$\frac{\partial^2 u_k}{\partial r^2} + \frac{2}{r}\frac{\partial u_k}{\partial r} - \frac{n(n+1)}{r^2} u_k \;=\; \mu_0 \sigma(r)\, \frac{\partial u_k}{\partial t}, \qquad R_\mathrm{c} < r < R_\sigma \tag{4.3}$$

$$u_k(R_\mathrm{c}, t) \;=\; e_k(t), \qquad \frac{\partial u_k}{\partial r}(R_\sigma, t) \;+\; \frac{n+1}{R_\sigma}\, u_k(R_\sigma, t) \;=\; 0, \qquad 0 \le t \le T \tag{4.4}$$

$$u_k(r, 0) \;=\; \psi_k(r) \;=\; \frac{e_k(0)}{\psi(R_c)} \psi(r) \;. \tag{4.5}$$

The initial conditions (4.5) ensure that $f(0) \;=\; \psi(R_c)$. With an arbitrary chosen basis $g_l(t), l \;=\; 1, \ldots, M$ in the data space, $\phi(t)$ and $u_k(R_\sigma, t)$ can be expand into

$$\phi(t) \;=\; \sum_{l=1}^{M} \phi_l g_l(t) \qquad \text{and} \qquad u_k(R_\sigma, t) \;=\; \sum_{l=1}^{M} a_{lk} g_l(t) \;. \tag{4.6}$$

Thus, the finite approximation of eq. (4.1) reads

$$\sum_{l=1}^{M} \phi_l g_l(t) \;=\; \sum_{l=1}^{M} \sum_{k=1}^{N} a_{lk} f_k g_l(t) \;, \tag{4.7}$$

which results (for linear independent $g_l(t)$) in

$$\phi_l \;=\; \sum_{k=1}^{N} f_k\, a_{lk} \;, \qquad l = 1, \ldots, M \;. \tag{4.8}$$

The determination of (a_{lk}) becomes very simple, if solution and data space are restricted to piecewise linear functions. This is a reasonable assumption, if the data are provided as $\{\phi(t_l)\}$ for an equally divided time space $[0,T]$, with $t_l = (l-1)\Delta t$, $l = 1,\ldots,M$, for example as monthly means. In this case, $g_l(t)$ are the triangle functions

$$g_l(t) \;=\; \begin{cases} 1 - \frac{|t-t_l|}{\Delta t} & |t-t_l| < 1 \\ 0 & \text{otherwise} \,. \end{cases}$$

With the same basis in the solution space, that is $e_k(t) = g_k(t)$, $k = 1,\ldots,M$, and $N = M$ the system (4.3, 4.4, 4.5) must be solved only twice. $A(e_1(t)$ has to be constructed from the boundary value $e_1(t)$ and the initial $\psi_1(r)$. This gives by means of eq. (4.6) the first column of the matrix (a_{lk}). All other solution $A(e_k(t))$ can be inferred from $A(e_2(t))$ by

$$A(e_k(t)) \;=\; A(e_2(t-(k-2)\Delta t)$$

because of $\psi_k(r) = 0$ for $k \geq 2$. Therefore, columns $2,\ldots,N$ of matrix (a_{lk}) form a submatrix of Toeplitz structure.

(iii) The proper unknowns for the (approximated) inverse problem are determined here by the regularization of the type

$$\min \|(f_k)\|_\beta \qquad \text{subject to} \qquad \|(a_{lk})(f_k) - (\phi_l)\|_\alpha \leq \epsilon \,. \tag{4.9}$$

This solution concept shall account for the non-uniform quality of the geophysical data being themselves results from an adjustment and smoothing process. The procedure is realized with the help of a quadratic programming tool of Hansen (1992, 1998) contained in the free MATLAB Regularization toolbox. The norms $\|\cdot\|_\alpha, \|\cdot\|_\beta$ can be selected as L_2 and W_2^1 norms.

After $u(R_c,t)$ having determined, it is available as lower boundary value. Together with the upper boundary of the third kind at R_σ (see the condition on the right of (4.4)), a stable (two-side) initial-boundary problem can be solved. This provides the function $u(r,t)$ at **intermediate radial values** $\boldsymbol{r_i}$, regularly spaced between R_c and R_σ, if using the finite-difference technique. Any irregular distribution of the points r_i can be achieved, if the finite-element solution method (FEM) is applied (see Sec. 4.2). By finite-difference approximation with these values then **partial derivatives** $\boldsymbol{\partial u(r,t)/\partial r}$ can determined, (near the point R_c only as one-side difference), which are needed for the tangential field components $\beta_{nm}^{\vartheta,\varphi}(r,t)$ (2.23). With a similar approach, partial derivatives of second order can be approximated, which are necessary, e.g. for diffusion calculations (see Sec. 8.3).

The **downward continuation** of the magnetic field **beneath the CMB** into the moving matter of the fluid outer core with a certain type prescribed velocity (see (2.25), (2.26), (2.28)) can be formulated as inverse problem in the same way as for the earth mantle ((3.10) and Sec. 3.1). The enlarged range for r is now $R_\sigma \geq r \geq R_p$ with $R_p < R_c$ (see Fig. 3.1). Initial and boundary conditions for each of the functions $S_{nm}^c(r,t)$, $S_{nm}^s(r,t)$ are added correspondingly. As an additional function, a velocity function $\omega(r), R_c \geq r \geq R_p$ has to be prescribed for the differential rotation in an upper layer of the fluid outer core. Concerning the solving algorithm a new formulation in a relatively simple way can be generated for (2.28) so that it is possible to use the same algorithm described above for the determination of pairs of functions $S_{nm}^c(R_p,t)$, $S_{nm}^s(R_p,t)$, $0 \leq t \leq T$. With the more formal complex combination $\bar{u} = S_{nm}^c + iS_{nm}^s$ the couple of differential equations (2.28) can be written as

$$\frac{\partial^2 \bar{u}}{\partial r^2} \;+\; \frac{2}{r}\frac{\partial \bar{u}}{\partial r} \;-\; \frac{n(n+1)}{r^2}\,\bar{u} - \mu_0\sigma(r)\,\frac{\partial \bar{u}}{\partial t} + im\mu_0\sigma(r)\omega(r)\bar{u} = 0 \,. \tag{4.10}$$

Thus, the structure of (3.10) is principally kept and all the steps (i) to (iii) can be carried out in the same way as described above, but now with complex quantities (bases functions $\bar{e}_k$, resulting matrix $\bar{a}_{lk}$). For the initial condition that solution of the differential equation (4.10) can be chosen which results if the time derivative terms are neglected. This calculation has to be done prior to step (i) (for results and details see Greiner-Mai et al., 2001).

4.2 Solution by finite elements

The **initial boundary problem**

$$u_{rr} + \frac{2}{r}u_r - \frac{k(k+1)}{r^2}u = \mu_0\,\sigma\,u_t\ , \tag{4.11}$$

$$u(R_c,t) = g(t)\ , \tag{4.12}$$

$$u_r(R_\sigma,t) + \frac{k+1}{R_\sigma}u(R_\sigma,t) = 0 \tag{4.13}$$

with $r \in [R_c, R_\sigma]$, which is used for the upward continuation in the downward continuation algorithm (see step (ii), Sec. 4.1, relations (4.3) to (4.5)), can be solved alternatively with the finite-element technique (FEM). We write the differential equation in a symmetric form

$$\frac{\partial}{\partial r}\left(r^2\frac{\partial}{\partial r}u\right) - k(k+1)u = \mu_0\,r^2\,\sigma\,u_t \tag{4.14}$$

corresponding to the the general form

$$-\frac{\partial}{\partial r}\left(a(r)\frac{\partial}{\partial r}u\right) + b(r)\,u = c(r)\,u_t \tag{4.15}$$

with sign chosen due to the convention for weak solutions of elliptical differential equations.

Crank-Nicolson time step

For a regular time discretisation $\{t_i\}$ with $\Delta t := t_{i+1} - t_i$ and $u^i := u(r,t_i)$ the temporal derivation of u is approximated by a setup with differences

$$u_t^{i+1/2} = \frac{u^{i+1}-u^i}{\Delta t} \qquad \text{with} \qquad u^{i+1/2} = \frac{1}{2}(u^{i+1}+u^i)\ . \tag{4.16}$$

With this, from (4.15) results an ordinary differential equation for $u^{i+1}(r)$ with known $u^i(r)$.

$$-\frac{\partial}{\partial r}\left(a(r)\frac{\partial}{\partial r}u^{i+1}\right) + \left[b(r) - \frac{2\,c(r)}{\Delta t}\right]u^{i+1} = \frac{\partial}{\partial r}\left(a(r)\frac{\partial}{\partial r}u^{i}\right) - \left[b(r) + \frac{2\,c(r)}{\Delta t}\right]u^{i}. \tag{4.17}$$

Setting in the following

$$u(r) := u^{i+1} \quad \text{and} \quad f(r) := \frac{\partial}{\partial r}\left(a(r)\frac{\partial}{\partial r}u^{i}\right) - \left[b(r) + \frac{2\,c(r)}{\Delta t}\right]u^{i}\ ,$$

gives now the differential equation which has to be solved

$$-\frac{\partial}{\partial r}\left(a(r)\frac{\partial}{\partial r}u\right) + \left[b(r) - \frac{2\,c(r)}{\Delta t}\right]u = f(r). \tag{4.18}$$

It has to be noted that the time of the solution $u(r)$ differs from that one of the right hand side $f(r)$. Boundary conditions are possibly needed for both times.

Weak solution

Considering boundary values of the first kind, requires the following decomposition of $u(r)$:

$$u(r) = u(r) - \bar{u} + \bar{u} = w(r) + \bar{u}\ . \tag{4.19}$$

$\bar{u}$ is an arbitrary function, matching $u(r)$ on that part of the boundary, where $u(r)$ has boundary values of the first kind (then there holds w(r)=0). It would be possible to choose a constant function $\bar{u}(r) = \bar{u}(R_c) = u(R_c)$. But we will go another way to simplify the FEM approximation with an alternative choice of $\bar{u}$. We multiply eq. (4.18) with an arbitrary function $v(r)$, which also vanishes there where $u(r)$ has

a boundary value of the first kind and hence on this part of the boundary being identically with $w(r)$. Integration in parts on these expressions can be carried out

$$-\int \frac{\partial}{\partial r}\left(a\frac{\partial}{\partial r}u\right)\, v\, dr + \int \left[b - \frac{2\,c}{\Delta t}\right] u\, v\, dr = \int f\, v\, dr, \tag{4.20}$$

which results in

$$\int a\frac{\partial(w+\bar{u})}{\partial r}\frac{\partial v}{\partial r} + \left[b - \frac{2\,c}{\Delta t}\right](w+\bar{u})\, v\, dr - a(R_\sigma)v(R_\sigma)\frac{\partial(w+\bar{u})}{\partial r}\Big|_{r=R_\sigma} = \int f\, v\, dr\ . \tag{4.21}$$

The weak solution of (4.18) is now that function $u(r) = w(r) + \bar{u}$ with $w(r)$, belonging to a special (corresponding) Hilbert space V, which fulfills for all $v(r) \in \mathrm{V}$ the variational equation (4.21) for $w(r)$. Expressed more abstractly: Find $w \in \mathrm{V}$ with

$$\Psi(w, v) = F(v), \quad \forall v \in \mathrm{V} \tag{4.22}$$

where $\Psi(w, v)$ is a bilinear form on $\mathrm{V} \times \mathrm{V}$, and $F(v)$ is a linear functional on V, thus $F \in \mathrm{V}'$, which is the dual Hilbert space to V. The detailed expressions of Ψ and F are (separation of known and unknown expressions)

$$\Psi(w, v) = \int a\frac{\partial w}{\partial r}\frac{\partial v}{\partial r} + \left[b - \frac{2\,c}{\Delta t}\right] w\, v\, dr - a(R_\sigma)v(R_\sigma)\frac{\partial w}{\partial r}\Big|_{r=R_\sigma}\ , \tag{4.23}$$

$$F(v) = \int f\, v\, dr - \int a\frac{\partial \bar{u}}{\partial r}\frac{\partial v}{\partial r} + \left[b - \frac{2\,c}{\Delta t}\right]\bar{u}\, v\, dr + a(R_\sigma)v(R_\sigma)\frac{\partial \bar{u}}{\partial r}\Big|_{r=R_\sigma}\ . \tag{4.24}$$

After inserting the boundary condition (4.13) we have

$$\Psi(w, v) = \int a\frac{\partial w}{\partial r}\frac{\partial v}{\partial r} + \left[b - \frac{2\,c}{\Delta t}\right] w\, v\, dr + a(R_\sigma)v(R_\sigma)\frac{k+1}{R_\sigma}w(R_\sigma)\ , \tag{4.25}$$

$$F(v) = \int f\, v\, dr - \int a\frac{\partial \bar{u}}{\partial r}\frac{\partial v}{\partial r} + \left[b - \frac{2\,c}{\Delta t}\right]\bar{u}v\, dr - a(R_\sigma)v(R_\sigma)\frac{k+1}{R_\sigma}\bar{u}(R_\sigma). \tag{4.26}$$

There exists a unique solution $w(r)$ of eq. (4.22), if $\Psi(w, v)$ is continuous and coercive (Lemma of Lax-Milgram, e.g. Evans, 1998; Hazewinkel, 2002). This is the case, if

$$c_1 \leq a(r) \leq c_2 \quad textwith \quad c_1,\, c_2 > 0\ , \tag{4.27}$$

$$0 < c_3 \leq b(r) - \frac{2\,c(r)}{\Delta t}\ . \tag{4.28}$$

For the poloidal magnetic field with $a(r) = r^2$, $b(r) = k(k+1)$ and $c(r) = -\mu_0\, r^2\, \sigma$ this is obviously fulfilled. It is (probably) sufficient that $\sigma(r) \in \mathrm{L}^2$ holds. Thus $\sigma(r)$ can have steps.

Remark: V is the vector space of all $v(r) \in \mathrm{L}^2(\mathrm{R_c}, \mathrm{R}_\sigma)$ with generalized first derivatives and vanishing boundary value at the end of the interval R_c. Equipped with the scalar product

$$(u, v) = \int u(r)v(r)\, dr + \int \frac{\partial u}{\partial r}\frac{\partial v}{\partial r}\, dr \tag{4.29}$$

V becomes a Hilbert space.

FEM formulation

The basic idea is to solve the variational equation (4.22) in an N-dimensional subspace $\mathrm{V_N} \subset \mathrm{V}$. Piecewise linear functions $u(r)$ defined over a (irregularly spaced) grid

$$\{r_0, r_1, r_2 \ldots r_N\}; \quad r_0 = R_c;\, r_N = R_\sigma$$

generate an $N+1$-dimensional vector space. One possible basis system are the triangle functions $\{\phi_i(r)\}$, $i = 0, \ldots, N$ ('form functions').

$$\phi_0(r) = \begin{cases} \frac{r_1 - r}{r_1 - r_0} & : \quad r \in [r_0, r_1] \\ 0 & : \quad \text{otherwise} \end{cases}$$

$$\phi_i(r) = \begin{cases} \frac{r-r_{i-1}}{r_i-r_{i-1}} & : \quad r \in [r_{i-1}, r_i] \quad i = 1, ..., N-1 \\ \frac{r_{i+1}-r}{r_{i+1}-r_i} & : \quad r \in [r_i, r_{i+1}] \quad i = 1, ..., N-1 \\ 0 & : \quad \text{otherwise} \end{cases}$$

$$\phi_N(r) = \begin{cases} \frac{r-r_{N-1}}{r_N-r_{N-1}} & : \quad r \in [r_{N-1}, r_N] \\ 0 & : \quad \text{otherwise} \end{cases}$$

With this holds

$$u(r) = \sum_{i=0}^{N} u_i \phi_i(r) \ , \tag{4.30}$$

when u_i denote the expansion coefficients . Obviously holds $u(r_i) = u_i$. We set $\bar{u}(r) = u_0\phi_0(r)$ and define $\mathrm{V_N}$ as the span of the bases functions $\{\phi_1 \ldots, \phi_N\}$. Now it is still necessary to insert

$$w(r) = \sum_{i=1}^{N} w_i \phi_i(r) \tag{4.31}$$

into eq. (4.22) (resp. (4.25) and (4.26)) and successively to choose for $v(r)$ the bases functions $\phi_i(r)$, $i = 1, \ldots, N$ of $\mathrm{V_N}$ (due to $v(R_\sigma) = 0$ is also $\phi_0(r)$ not necessary). This leads to a linear equation system

$$Aw = p \qquad \text{for} \qquad w = (w_1, ..., w_N)^T. \tag{4.32}$$

Considering in addition that in the Crank-Nicolson approximation the right hand side $f(r)$ in the $i+1$th time step of the equation (4.20) forms a linear operator (differential operator) of the solution in the ith step (comp. eq. (4.17)), then the linear equation system can be decomposed as follows

$$Aw(t_{i+1}) = Bw(t_i) + d \ . \tag{4.33}$$

Here $w(t_{i+1})$ is the searched solution vector at time t_{i+1}, while $w(t_i)$ is the preceding (known) solution vector at time t_i and d a vector, accounting for the boundary conditions of the first kind at both times. The matrices A and B have a similar structure. Their coefficients do not depend on time. They only depend on the grid spacing $\{r_0, r_1, r_2, \ldots, r_N\}$, the conductivity and the time step Δt.

The above formulae describe the procedure of *Ritz Galerkin*. Usually in the FEM-formulation, there are not considered the bases functions $\phi_i(r)$ but so-called 'form (shape) functions' $\psi_i(r)$ for the interval $[r_i, r_{i+1}]$, which are connected with the values at the knots w_i and w_{i+1}. Here

$$\psi_i(r) = [\phi_i(r)^+, \phi_{i+1}(r)^-] \tag{4.34}$$

is a two-dimensional vector and $\phi_i(r)^+$ the right(decending) part of $\phi_i(r)$ and $\phi_{i+1}(r)^-$ the left (ascending) part of $\phi_{i+1}(r)$. With this, the solution $w(r)$ in the interval $[r_i, r_{i+1}]$ becomes a scalar product of form (shape) functions and values at knots

$$w(r) = \left([\phi_i(r)^+, \phi_{i+1}(r)^-] \, , \, [w_i, w_{i+1}]\right) = (\psi_i(r) \, , \, [w_i, w_{i+1}]) \ . \tag{4.35}$$

Remark: The last discussed technical details giving at the end the same linear equation system. But their structural advantages actually appear in the multidimensional case, where it is easier to standardize the required integrations.

Determination of A, B and d

For the determination of the coefficients of A eq. (4.25) has to be evaluated. With $a(r) = r^2$, $b(r) = k(k+1)$ and $c(r) = -\mu_0 r^2 \sigma$ and the abbreviations

$$\begin{aligned} A^{(1)}_{pq} &= \int r^2 \frac{\partial \phi_p}{\partial r} \frac{\partial \phi_q}{\partial r} \, dr \ , \\ A^{(2)}_{pq} &= k(k+1) \int \phi_p \phi_q \, dr \quad (\text{plus} \ \ (k+1) r_N \quad \text{for} \ \ p = q = N) \ , \\ A^{(3)}_{pq} &= \frac{2\,\mu_0}{\Delta t} \int r^2 \, \sigma \phi_p \phi_q \, dr \end{aligned}$$

holds

$$A_{pq} = A^{(1)}_{pq} + A^{(2)}_{pq} + A^{(3)}_{pq} \; . \tag{4.36}$$

The term $(k+1)r_N$ in $A^{(2)}_{NN}$ results from the boundary condition $a(R_\sigma)v(R_\sigma)\frac{k+1}{R_\sigma}w(R_\sigma)$ in eq. (4.25). The matrix B only differs slightly

$$B_{pq} = -A^{(1)}_{pq} - A^{(2)}_{pq} + A^{(3)}_{pq} \; . \tag{4.37}$$

Evidently, the matrices A and B are symmetric because of the symmetry of the bilinear form Ψ and because of the special shape of the bases functions ϕ_i, which are tridiagonal matrices. The vector d results from the decomposition in (4.19) and due to $\bar{u}(r) = u_0\phi_0(r)$ it only contains entries in d_1 (for $v(r) = \phi_1(r)$)

$$d_1 = u_0 \left[\frac{2\,\mu_0}{\Delta t} \int r^2\, \sigma \phi_0 \phi_1 \, dr \; - \; \int r^2 \frac{\partial \phi_0}{\partial r} \frac{\partial \phi_1}{\partial r} \, dr \; - \; k(k+1) \int \phi_0 \phi_1 \, dr \right] \; . \tag{4.38}$$

The last term in eq. (4.26) vanishes because of $\bar{u}(R_\sigma) = u_0\phi_0(R_\sigma) = 0$. All the coefficients, which are independent of $\sigma(r)$, can be explicitly integrated. For instance holds:

$$\begin{aligned}
A^{(1)}_{pp} &= \frac{1}{3}(r_{p+1} - r_{p-1}) + \frac{r_p r_{p-1}}{r_p - r_{p-1}} + \frac{r_{p+1} r_p}{r_{p+1} - r_p} \quad p = 1, \ldots, N-1 && (4.39)\\
A^{(1)}_{NN} &= \frac{1}{3}(r_N - r_{N-1}) + \frac{r_N r_{N-1}}{r_N - r_{N-1}} && (4.40)\\
A^{(1)}_{pp+1} &= \frac{1}{3}(r_p - r_{p-1})^2 - \frac{1}{3}(r_{p+2} - r_{p-1})^2 + r_{p-1} r_p - r_{p+1} r_{p+2} \\
&- \frac{1}{3}(r_{p+1} - r_p) - \frac{r_{p+1} r_p}{r_{p+1} - r_p} \quad p = 1, ..., N-2 && (4.41)\\
A^{(1)}_{N-1N} &= \frac{1}{3}(r_{N-1} - r_{N-2})^2 + r_{N-2} r_{N-1} - \frac{1}{3}(r_N - r_{N-1}) - \frac{r_N r_{N-1}}{r_N - r_{N-1}} && (4.42)\\
A^{(2)}_{pp} &= k(k+1)\frac{1}{3}(r_{p+1} - r_{p-1}) \quad p = 1, ..., N-1 && (4.43)\\
A^{(2)}_{NN} &= k(k+1)\frac{1}{3}(r_N - r_{N-1}) + (k+1) r_N && (4.44)\\
A^{(2)}_{pp+1} &= k(k+1)\left[\frac{1}{2}(r_{p+2} - r_{p-1}) - \frac{1}{3}(r_{p+1} - r_p)\right] \quad p = 1, ..., N-2 && (4.45)\\
A^{(2)}_{N-1N} &= k(k+1)\frac{1}{6}(r_N + 2r_{N-1} - 3r_{N-2}) \; . && (4.46)
\end{aligned}$$

The above expressions were calculated with the 'Symbolic Toolbox' of MATLAB. Especially, the additional terms of eq. (4.25) at the boundary ($r = r_N$) have to be considered as well as the special integration intervals for the products of the 'test functions' at this boundary $\phi_N\phi_N$ resp. $\phi_{N-1}\phi_N$. In general, the coefficients $A^{(3)}_{pq}$ have to be integrated numerically, respectively they result from the special representations of σ. Often, a linear setup on the elements is sufficient, as

$$\sigma(r) = \sum_{i=0}^{N} \sigma_i \phi_i(r) \; .$$

In this way the finite-element discretisation and the behaviour of the function σ are coupled which can often be reasonable. However, possibly one loses the advantage of the finite element method (see Remark 3 below). For d_1 we obtain

$$\begin{aligned}
d_1 = {} & [u_0(t_{i+1}) + u_0(t_i)] \times \\
& \times \left[\frac{2\,\mu_0}{\Delta t} \int r^2\, \sigma \phi_0 \phi_1 \, dr \; + \frac{1}{3}(r_1 - r_0) + \frac{r_1 r_0}{r_1 - r_0} + k(k+1)\frac{1}{6}(3r_2 - 2r_1 - r_0) \right] \; ,
\end{aligned} \tag{4.47}$$

where $u_0(t_{i+1})$ and $u_0(t_i)$ are the boundary conditions of the first kind for the time values t_{i+1} and t_i.

Remarks

1. The numerical solution of eq. (4.33) should be use a LU decomposition of the system matrix A. This is necessary only once (for constant time step Δt). Therefore the processing applied (an algorithm of high precision) can more expensive, while at the same time it can be taken advantage of the properties of symmetry and tridiagonality. The numerical stability is sufficiently guaranteed by the diagonal dominance of A. This is supposed strongly to correlate with the requirements (4.27) and (4.28).

2. As further numerical test, it is still possible to solve the boundary value problem (4.18) (being in fact a virtual time step) with different conductivities σ with the boundary value solvers of MATLAB (see the Help for BVP). Having a look on the output of all integration points (which is nearly identical with the grid), provides the sense for the necessary (variable) density of the grid for given precision of the solution. The coefficients $A^{(1)}$ and $A^{(2)}$ can be tested easily. Here, it is sufficient to compare with the analytical solutions for $\sigma = 0 \rightarrow A^{(3)} = 0$.

3. Calculating $A^{(3)}_{pq}$ shows an 'advantage' of the FE method compared to normal finite differences (FD) procedures. Indeed, both methods work (in the simplest case) with piecewise linear setups for the solution. However the conductivity σ is treated differently. In the FD setup, the conductivity σ is (often implicitly) additionally polynomially approximated (often linearly) between the knots of the FD grid. In the FE procedure, the 'true' course of σ is incorporated in the coefficients of the system matrix via the integration. Thus, e.g. discontinuous σ can be considered without problems inside of one element. In the FD setup, this requires special efforts (discontinuities of σ have to be knots; the differential equation has to be 'appropriately discretized' at these places).

4. Let us consider eq. (4.16) with the solution u^{i+1} and the preceding solution u^i. Here, in fact, the progress amounts only to an half time step $\Delta t/2$. $u^{i+1/2}$ becomes again the 'right hand side' of eq. (4.33)!

5. Generally, the time dependent boundary function $g(t)$ in eq. (4.12) is given with fixed time steps (e.g. months). If this is also interpolated for the numerical solution (e.g. piecewise linear), then $u(R_\sigma, t)$ have to be determined also at these time points. The Crank-Nicolson procedure provides $u(R_\sigma, t)$ with a comparatively short temporal sampling ($\Delta t/2 \ll$ one month). But the needed monthly values for $u(R_\sigma, t)$ are not the values of the numerical solution at these monthly times. The solution with the many temporal knots then had to be developed for piecewise linear (month to month) functions (comp. left relation of (4.2)). That would lead once more to a simple tridiagonal equation system.

4.3 Error estimation

The evaluation of the regularized solution of the inverse boundary value problem (3.10) and of their geophysical relevance requires an error estimation or at least any upper bound for the error. Such information can be derived based on one of the different formulations of the problem (see Ch. 3). Connected with the algorithm described in Sec. 4.1, we use the chosen type of regularization (4.9). In detail, the effect of an error δ in the norm of data $\phi(t) = u(R_\sigma, t) = S^{cs}_{nm}(R_\sigma, t)$ on the solution $f(t) = u(R_\mathrm{c}, t) = S^{cs}_{nm}(R_\mathrm{c}, t)$ ((3.10) and (3.16)) has to be determined.

Applying **only the second regularization condition** in (4.9), both to 'exact' data ϕ and 'disturbed' data ϕ^δ, we have

$$\|Af - \phi\| \le \epsilon, \qquad \|Af^\delta - \phi^\delta\| \le \epsilon \qquad \text{with} \qquad \|\phi - \phi^\delta\| \le \delta, \tag{4.48}$$

where all f, f^δ are admitted as solutions, respectively, and the norm minimization in (4.9) is neglected. This leads to

$$\|A(f - f^\delta) - (\phi - \phi^\delta)\| \le 2\epsilon, \qquad \|\phi - \phi^\delta\| \le \delta, \tag{4.49}$$

for which it is sufficient to derive an estimate for $\sup \|f - f^\delta\|$.

Remark: The norm difference $\|f - f^\delta\|$ of the corresponding solutions f and f^δ has to be estimated. However, there seems not to exist an obvious relation between the difference of the minimum norm solutions and the minimum norm solution belonging to the difference of the data $\phi - \phi^\delta$. So we confine ourselves to derive an estimate for $\sup \|f - f^\delta\|$ in (4.49) with the data range fixed by $\|\phi - \phi^\delta\| \leq \delta$. We denote the difference of the solutions $f - f^\delta$ shortly by $\bar{f}^\delta$.

It can be seen, with the triangle inequality applied to (4.49), turning to squared norms and setting $\bar{f}^\delta = \sum_{k=1}^N f_k e_k$ with e_k orthonormal, that it is sufficient to consider the problem

$$\sup \left\{ \|\bar{f}^\delta\|^2 : \|A(\bar{f}^\delta)\|^2 \leq (2\epsilon + \delta)^2 \right\} = \sup \left\{ \sum_{k=1}^N f_k^2 : \sum_{i,j=1}^N f_i f_j (Ae_i, Ae_j) \leq (2\epsilon + \delta)^2 \right\} . \tag{4.50}$$

The matrix (Ae_i, Ae_j) is symmetric and regular as the functions Ae_k are linearly independent because of the uniqueness of the downward continuation problem. The transformation to principal axes of the quadratic form in the right hand side of (4.50) relates this quantity to the minimal eigenvalue λ_{min} of (Ae_i, Ae_j)

$$\sup \left\{ \sum_{k=1}^N g_k^2 : \sum_{l=1}^N g_k^2 \lambda_k \leq (2\epsilon + \delta)^2 \right\} = (2\epsilon + \delta)^2 \lambda_{min}^{-1} , \tag{4.51}$$

where $\lambda_k, k = 1, \ldots, N$ are the eigenvalues of the matrix (Ae_i, Ae_j), i.e. finally

$$\|A(\bar{f}^\delta)\| \leq 2\epsilon + \delta \qquad \text{gives} \qquad \|\bar{f}^\delta\| \leq (2\epsilon + \delta)\, \lambda_{min}^{-1/2} \tag{4.52}$$

as an upper bound for the assumed error of the downward continuation from R_σ to R_c.

An identical estimate was found for the analogous problem of regularization by the least squares collocation method in (Engl, 1982; Groetsch, 1984). The estimation (4.52) can be easily shown to be optimal in simple cases, and holds then even for the minimum norm solution, e.g. in the one-dimensional case or in the purely theoretical case if all eigenvalues are identical.

The influence of the model on the error bound depends on the dimension (number of bases functions), the time interval and the coefficient σ (conductivity distribution), which bears also the geometric dimensions of the spherical earth mantle shell. In general, however, to start with realistic error bars for the data forms the main problem. Including of the norm minimization, the first part in (4.9), in deriving an error estimation could improve the here generated upper error bound (see Remark above).

5 Special cases: Solutions for special function setups ('Simulations')

Simulation means here that – instead of the input of real data (first boundary value) in the downward continuation task – an analytical setup for the function in (3.10) $u = S_{nm}^{c,s}$ shall prescribe a specific spatial and temporal behaviour of the solution, especially at the CMB. This behaviour is realized by setting up a function of a certain function class (simple analytical functions and their combinations), which in most cases are multiplicatively put together with unknown r-dependent functions, and possibly equipped with free parameters or r-dependent parameter functions. Thus, the downward continuation task as an initial boundary value problem for a partial differential equation (3.10) is transferred to a pure initial value problem for an ordinary differential equation or a system of differential equations. Via the solutions $S_{nm}^{c,s}(R_c, t)$, the corresponding coefficients of the magnetic field components $\beta_{nm}^{r}(R_c, t)$, $\beta_{nm}^{\vartheta,\varphi}(R_c, t)$ (comp. (2.23)) can be derived.

Although both boundary values still are given only for **one** end of the radial interval (we will use here R_σ), the problem is now – contrary to the situation before with the partial differential equation – at least theoretically a well-posed one. That means, it has (it should have) no temporal instability. Nevertheless, it can be possibly still numerically badly conditioned in dependency of the parameter constellation.

The following list presents some of the most important cases for such setups:

- time polynomial setups

  $$u(r,t) = a(r), \quad u(r,t) = a(r) + b(r)\cdot t, \quad u(r,t) = a(r) + b(r)\cdot t + c(r)\cdot t^2$$

  generally $\quad u(r,t) = \sum_{k=0}^{N} a_k(r)\cdot t^k$

- oscillations (periodical Gauss coefficients)

  $$u(r,t) = g(r)\sin(2\pi t/T(r) + \alpha(r))$$

  or complex $\quad u(r,t) = g(r)\exp i(\omega(r)t + \alpha(r))$

- finite Fourier series

  $$u(r,t) = a(r) + g(r)\exp i(\omega(r)t + \alpha(r))$$

  $$u(r,t) = \sum_{k=0}^{N} a_k(r)\sin(2\pi kt/T + \alpha_k(r)) \quad \text{with} \quad t \in [0,T]$$

- further possible setups
  e.g. $u(r,t) = g(r)\exp(\alpha t)$

Remark: Not by far all basic function types are capable for such a setup, as e.g. the functions t^{-n} or $\ln t$.

5.1 Time polynomial setups

The first setup in the list above with a **time-independent** function

$$u(r,t) := a(r) \tag{5.1}$$

leads to the time-independent ordinary differential equation which does not depend on the conductivity

$$a_{rr} + \frac{2}{r}\, a_r - \frac{n(n+1)}{r^2}\, a = 0 \quad \text{with the solutions} \quad a^1(r) = C \cdot r^n, \quad a^2(r) = \frac{C}{r^{n+1}}\ . \tag{5.2}$$

Only the second solution fulfills the second boundary condition in (3.10)

$$a_r(R_\sigma) = -\frac{n+1}{R_\sigma} a(R_\sigma)\ . \tag{5.3}$$

Its continuation is the known case of the harmonic downward continuation (3.7) which keeps the time structure between top (R_σ) and down r-level (R_c).

Next, we study the case of the **temporal straight line** i.e., the setup

$$u(r,t) := a(r) + b(r) \cdot t. \tag{5.4}$$

The given boundary conditions are

$$a(R_\sigma) + b(R_\sigma) \cdot t \;=\; \Phi(t)\ , \tag{5.5}$$

$$a_r(R_\sigma) + b_r(R_\sigma) \cdot t \;=\; -\frac{n+1}{R_\sigma}\, a(R_\sigma) + b(R_\sigma) \cdot t\ . \tag{5.6}$$

The second one in (5.6) means immediately that the separated conditions are valid

$$a_r(R_\sigma) = -\frac{n+1}{R_\sigma}\, a(R_\sigma), \qquad b_r(R_\sigma) = -\frac{n+1}{R_\sigma}\, b(R_\sigma)\ . \tag{5.7}$$

Inserting the setup (5.4), the differential equation can be written as

$$a_{rr} + \frac{2}{r}\, a_r - \frac{n(n+1)}{r^2}\, a + (b_{rr} + \frac{2}{r}\, b_r - \frac{n(n+1)}{r^2}\, b) \cdot t = \mu_0\, \sigma(r)\, b\ . \tag{5.8}$$

For $b(r)$ a separate differential equation has to be fulfilled as the right hand side of the differential equation (5.8) does not depend on t,

$$b_{rr} + \frac{2}{r}\, b_r - \frac{n(n+1)}{r^2}\, b = 0, \tag{5.9}$$

which together with the boundary conditions (5.5) and (5.7) gives the solution

$$b(r) = \frac{C}{r^{n+1}} \quad \text{with a constant} \quad C \tag{5.10}$$

from (5.5),(see time-independent case (5.1)). Using this result we get finally

$$a_{rr} + \frac{2}{r}\, a_r - \frac{n(n+1)}{r^2}\, a = \mu_0\, \sigma(r)\, \frac{C}{r^{n+1}}\ . \tag{5.11}$$

This inhomogeneous equation with two boundary conditions for $a(r)$ from (5.5) and (5.7) can be analytically solved with a standard technique ('method of variation of constants or parameters', see e.g. Zwillinger, 1997).

Generalizing this approach for the straight line, it is possible to calculate the downward continuation of any **time polynomial** given by the setup

$$u(r,t) = \sum_{k=0}^{N} a^k(r) \cdot t^k \tag{5.12}$$

with the two boundary conditions specified for the polynomial

$$\Phi(t) = \sum_{k=0}^{N} a^k(R_\sigma) \cdot t^k \quad \text{and} \quad \sum_{k=0}^{N} a_r^k(R_\sigma) \cdot t^k = -\frac{n+1}{R_\sigma} \sum_{k=0}^{N} a^k(R_\sigma) \cdot t^k\ , \tag{5.13}$$

where $\Phi(t)$ is a given time polynomial. The second boundary condition can be split up into the individual ones

$$a_r^k(R_\sigma) = -\frac{n+1}{R_\sigma}\, a^k(R_\sigma), \qquad k = 0, \ldots, N\ . \tag{5.14}$$

Inserting our polynomial setup into the differential equation

$$\sum_{k=0}^{N} a_{rr}^k(r)\cdot t^k + \frac{2}{r}\sum_{k=0}^{N} a_r^k(r)\cdot t^k - \frac{n(n+1)}{r^2}\sum_{k=0}^{N} a^k(r)\cdot t^k = \mu_0\,\sigma(r)\sum_{k=0}^{N} k\cdot a^k(r)\cdot t^{k-1} \tag{5.15}$$

shows that the term with the highest power (N) of t on the left side have to satisfy a homogeneous partial differential equation

$$a_{rr}^N + \frac{2}{r}\,a_r^N - \frac{n(n+1)}{r^2}\,a^N = 0\,. \tag{5.16}$$

With the respective boundary conditions, we get the known solution $a^N(r) = C_N/r^{n+1}$ which can be inserted in the right side of eq. (5.15). Considering there only the terms connected with the power $N-1$ of t we obtain the inhomogeneous differential equation

$$a_{rr}^{N-1} + \frac{2}{r}\,a_r^{N-1} - \frac{n(n+1)}{r^2}\,a^{N-1} = \mu_0\,\sigma(r)\,N\,\frac{C_N}{r^{n+1}}\,. \tag{5.17}$$

Its solution $a^{N-1}(r)$, analogous to (5.11), can be again inserted in the right side of eq. (5.15). This procedure can be successively repeated until $k=0$ and all polynomial coefficient functions $a^k(r),\ k=0,\ldots,N$ have been determined. Their inserting into (5.12) with $r=R_c$ completes the downward continuation solution.

5.2 Periodical Gauss coefficients

5.2.1 Basics

We consider the coefficient function $u(r,t) := S_{nm}^{c,s}(r,t)$ in the downward continuation problem (3.10). Its connection with the Gauss coefficients $g_{nm}(t), h_{nm}(t)$ at the earth surface $r=R_E$ and their harmonic downward continuation to the level $r=R_\sigma$ is described by the relations (2.16), (3.7), (3.8) and (3.13).

For the periodical boundary condition

$$u(R_\sigma,t) \;=\; a\,e^{i(\omega t+\alpha)} = \phi(t) \tag{5.18}$$

with radially dependent amplitude $a=a(r)$, frequency $\omega=\omega(r)$ and phase shift $\alpha=\alpha(r)$, we choose the following setup for the solution of the differential equation

$$u(r,t) \;=\; a(r)\,e^{i(\omega(r)\,t+\alpha(r))}\,. \tag{5.19}$$

From the boundary conditions

$$\begin{aligned} u(R_\sigma,t) \;&=\; a\,e^{i(\omega(R_\sigma)t+\alpha(R_\sigma))}\,,\\ u_r(R_\sigma,t) \;&=\; [a_r(R_\sigma) \,+\, i\,a(R_\sigma)\,(\omega_r(R_\sigma)\,t \,+\, \alpha_r(R_\sigma))]\;e^{i(\omega(R_\sigma)t+\alpha(R_\sigma))}\\ &=\; -\,\frac{n+1}{R_\sigma}\,a(R_\sigma)\,e^{i(\omega(R_\sigma)t+\alpha(R_\sigma))} \end{aligned}$$

follows (dividing by $e^{i(\omega(R_\sigma)t+\alpha(R_\sigma))} \neq 0$, arranging according to real and imaginary parts and according to the powers of t)

$$\begin{aligned} a_r(R_\sigma) \;&=\; -\frac{n+1}{R}\,a(R_\sigma)\\ \omega_r(R_\sigma) \;&=\; 0\\ \alpha_r(R_\sigma) \;&=\; 0 \end{aligned}$$

Inserting of the derivatives,

$$\begin{aligned} u_r(r,t) \;&=\; [a_r \,+\, i\,a\,(\omega_r\,t \,+\, \alpha_r)]\;e^{i(\omega t+\alpha)},\\ u_{rr}(r,t) \;&=\; \left[a_{rr} \,+\, 2i\,a_r(\omega t \,+\, \alpha) \,+\, i\,a(\omega_{rr}t \,+\, \alpha_{rr}) - a(\omega_r t \,+\, \alpha_r)^2\right]\;e^{i(\omega t+\alpha)},\\ u_t \;&=\; i\,\omega\,a\,e^{i(\omega t+\alpha)}, \end{aligned}$$

into the differential equation (3.10) and division by $e^{i(\omega(r)t+\alpha(r))} \neq 0$ results in

$$\begin{aligned} & a_{rr} + 2ia_r\,(\omega_r t + \alpha_r) + ia\,(\omega_{rr}t + \alpha_{rr}) - a\,(\omega_r t + \alpha_r)^2 \\ & \quad + \frac{2}{r}\,[a_r + ia\,(\omega_r t + \alpha_r)] - a\left[\frac{n(n+1)}{r^2}\right] \\ & \quad = i\mu_0\sigma\,a\,\omega\,. \end{aligned} \tag{5.20}$$

Again, we rearrange the terms according to real and imaginary parts and according to powers of t, and we find the four equations

$$a_{rr} + \frac{2}{r}\,a_r - a\,\alpha_r^2 - \frac{n(n+1)}{r^2}\,a \;=\; 0, \tag{5.21}$$

$$2a_r\alpha_r + \frac{2}{r}\,a\,\alpha_r + a\,\alpha_{rr} \;=\; \frac{1}{r^2 a}\frac{d}{dr}\left(r^2a^2\alpha_r\right) \;=\; \mu_0\,\sigma\,\omega\,a, \tag{5.22}$$

$$a\,\omega_r^2 \;=\; 0, \tag{5.23}$$

$$-2a\,\alpha_r\omega_r + 2a_r\,\omega_r + a\,\omega_{rr} + \frac{2}{r}\,a\,\omega_r \;=\; 0. \tag{5.24}$$

With eq. (5.23) for nontrivial solutions $u(r,t)$ ($a(r) \neq 0$), the relation $\omega_r = 0$ can be derived and therefore holds

$$\omega(r) = \omega(R_\sigma)) = \text{const}\,. \tag{5.25}$$

With this, also eq. (5.24) is fulfilled.

Remark: For $\sigma(r) = 0$ eq. (5.22) and the above boundary conditions leads to $\alpha(\mathrm{r})_\mathrm{r} = 0$. Then eq. (5.21) provides the known amplitude amplification

$$a(r) = a(R_\sigma)\left(\frac{R_\sigma}{r}\right)^{n+1} \quad \text{(harmonic downward continuation)}\,. \tag{5.26}$$

To determine the functions $a(r)$ and $\alpha(r)$, we consider the remaining system (5.21) and (5.22). The implementation in MATLAB requires to transform this system of the order two into a system of the order one.

With $b(r) := a_r(r)$ and $\beta(r) := \alpha_r(r)$, the equations (5.21)–(5.22) passes on to the system (5.27)–(5.30) with the corresponding boundary conditions (added in the right column):

$$\alpha_r(r) \;=\; \beta(r), \qquad \alpha(R_\sigma) \;\text{(to be specified)}, \tag{5.27}$$

$$a_r(r) \;=\; b(r), \qquad a(R_\sigma) \;\text{(to be specified)}, \tag{5.28}$$

$$\beta_r(r) \;=\; \mu_0\,\sigma(r)\,\omega \;-\; \frac{2\,b(r)\,\beta(r)}{a(r)} \;-\; \frac{2\,\beta(r)}{r}, \qquad \beta(R_\sigma) \;=\; 0, \tag{5.29}$$

$$b_r(r) \;=\; -\frac{2\,b(r)}{r} \;+\; a\left[\beta^2(r) \;+\; \frac{n(n+1)}{r^2}\right], \qquad b(R_\sigma) \;=\; -\frac{n+1}{R_\sigma}\,a(R_\sigma)\,. \tag{5.30}$$

Remark: If one is interested only in the factor of the amplitude amplification and the phase shift, it should be simply selected $\alpha(R_\sigma) = 0$ and $a(R_\sigma) = 1$.

5.2.2 Amplitude and phase shift for B_r with a periodical setup at $r = R_\sigma$

We consider only one summand with fixed n and m in the magnetic field component given by $B_r(r,t)$ (2.20)

$$\left(B_r\right)_{nm} := \left(\frac{1}{r}S^c_{nm}(r,t)\cos m\varphi + \frac{1}{r}S^s_{nm}(r,t)\sin m\varphi\right) n(n+1)\;P_{nm}(cos\vartheta)\,. \tag{5.31}$$

For $r = R_\sigma$ this becomes

$$\left(B_r(R_\sigma,t)\right)_{nm} \;=\; \sin(\omega\,t)\,\frac{1}{R_\sigma}\,[\cos(m\,\phi) \;+\; \sin(m\,\phi)]\,(n+1)\,P_{nm}(\cos(\theta)), \tag{5.32}$$

where $S^c_{nm}(R_\sigma,t) = S^s_{nm}(R_\sigma,t) = \sin(\omega\,t)$ is assumed.

For arbitrary r, the functions $S^c_{nm}(r,t)$ and $S^s_{nm}(r,t)$ with $a(R_\sigma)=1$ and $\alpha(R_\sigma)=0$,

$$S^c_{nm}(r,t) = a(r)\,\sin(\omega\,t+\alpha(r)), \tag{5.33}$$
$$S^s_{nm}(r,t) = a(r)\,\sin(\omega\,t+\alpha(r)) \tag{5.34}$$

remain identical. So we get for eq. (5.31)

$$\Big(B_r(r,t)\Big)_{nm} = \frac{1}{r}\,[a(r)\,\sin(\omega\,t\,+\,\alpha(r))]\,[\cos(m\,\phi)\,+\,\sin(m\,\phi)]\,(n+1)P_{nm}(\cos(\theta))\;. \tag{5.35}$$

A comparison of eqs. (5.32) and (5.35) shows that the relative amplitude of *Sine* has the value $(R_\sigma/r)\,a(r)$. $\alpha(r)$ describes the phase shift dependent on the depth.

$a(r)$ and $\alpha(r)$ can be determined as solution of a differential equation system of first order ((5.27)–(5.30), Sec. 5.2.1) with the unknown functions

$$a(r), \qquad \alpha(r), \qquad \frac{\partial a(r)}{\partial r}, \qquad \frac{\partial \alpha(r)}{\partial r} \tag{5.36}$$

and the initial conditions

$$a(R_\sigma)=1, \qquad \alpha(R_\sigma)=0, \qquad \frac{\partial a(R_\sigma)}{\partial r} = -\frac{n+1}{R_\sigma}, \qquad \frac{\partial \alpha(r)}{\partial r} = 0\;. \tag{5.37}$$

.

Remark: Due to the relation

$$\dot{B}_r(r,t) = \omega\,B_r(r,t), \qquad r \le R_\sigma \tag{5.38}$$

valid for periodical setups, $B_r(R_\sigma,t) = A\sin(\omega\,t)$, the results for amplitude and phase shift can be also applied to all time derivatives of $B_r(r,t)$.

5.2.3 Amplitude and phase shift for B_ϑ with a periodical setup at $r = R_\sigma$

We consider only one summand with fixed n and m in the magnetic field component $B_\vartheta(r,t)$ (2.21)

$$\Big(B_\vartheta\Big)_{nm} := \left(\frac{1}{r}\frac{\partial}{\partial r}(r\;S^c_{nm}(r,t))\cos m\varphi + \frac{1}{r}\frac{\partial}{\partial r}(r\;S^s_{nm}(r,t))\sin m\varphi\right)\frac{dP_{nm}(cos\vartheta)}{d\vartheta}\;. \tag{5.39}$$

For $r = R_\sigma$ this becomes with

$$\frac{\partial S^{c,s}_{nm}(R_\sigma,t)}{\partial R_\sigma} = -\frac{n+1}{R_\sigma}S^{c,s}_{nm}(R_\sigma,t), \quad \text{(see (3.10))} \tag{5.40}$$
$$\Big(B_\vartheta(R_\sigma,t)\Big)_{nm} = -\sin(\omega\,t)\,\frac{n}{R_\sigma}\Big[\cos(m\,\phi)\,+\,\sin(m\,\phi)\Big]\frac{\partial P_{nm}(\cos(\vartheta))}{\partial\vartheta}, \tag{5.41}$$

where $S^c_{nm}(R_\sigma,t) = S^s_{nm}(R_\sigma,t) = \sin(\omega\,t)$ is assumed.

For arbitrary r, the functions $S^c_{nm}(r,t)$ and $S^s_{nm}(r,t)$ as well as their local derivatives remain identical. They have the following form:

$$S^c_{nm}(r,t) = a(r)\,\sin(\omega\,t+\alpha(r)), \tag{5.42}$$
$$S^s_{nm}(r,t) = a(r)\,\sin(\omega\,t+\alpha(r)), \tag{5.43}$$
$$\frac{\partial S^c_{nm}(r,t)}{\partial r} = \frac{\partial a(r)}{\partial r}\,\sin(\omega\,t+\alpha(r)) + \frac{\partial\alpha(r)}{\partial r}\,\cos(\omega\,t+\alpha(r))\cdot a(r), \tag{5.44}$$
$$\frac{\partial S^s_{nm}(r,t)}{\partial r} = \frac{\partial a(r)}{\partial r}\,\sin(\omega\,t+\alpha(r)) + \frac{\partial\alpha(r)}{\partial r}\,\cos(\omega\,t+\alpha(r))\cdot a(r), \tag{5.45}$$

with $a(R)=1$ and $\alpha(R)=0$. With the abbreviations

$$A(r) := a(r) + r\frac{\partial a(r)}{\partial r}, \tag{5.46}$$
$$B(r) := r\,\frac{\partial\alpha(r)}{\partial r}\cdot a(r) \tag{5.47}$$

eq. (5.39) reads

$$\Big(B_\theta(r,t)\Big)_{nm} = \frac{1}{r}\Big[A\,\sin(\omega\,t+\alpha(r)) \;+\; B\,\cos(\omega\,t+\alpha(r))\Big] \times \Big[\cos(m\,\phi) \;+\; \sin(m\,\phi)\Big]\frac{\partial P_{nm}(\cos(\theta))}{\partial\theta}\;. \tag{5.48}$$

Comparing eq. (5.41) and eq. (5.48), we see that the relative amplitude of *Sine* has the value $-(R_\sigma A(r))/(r\,n)$. The amplitude of the new developing term *Cosine* is $-(R_\sigma B(r))/(r\,n)$.

$a(r)$ and $\alpha(r)$ results from the solution of a differential equation system of first order with the unknown functions

$$a(r), \qquad \alpha(r), \qquad \frac{\partial a(r)}{\partial r}, \qquad \frac{\partial \alpha(r)}{\partial r} \tag{5.49}$$

with the initial conditions

$$a(R)=1, \qquad \alpha(R)=0, \qquad \frac{\partial a(R)}{\partial r}=-\frac{n+1}{R}, \qquad \frac{\partial \alpha(r)}{\partial r}=0\;. \tag{5.50}$$

We can summarize eq. (5.48) as follows

$$\Big(B_\theta(r,t)\Big)_{nm} = \frac{1}{r}\sqrt{A^2+B^2}\,\sin\left(\omega\,t+\alpha(r)+\arctan\frac{B}{A}+\pi\right) \times \Big[(\cos(m\,\phi) \;+\; \sin(m\,\phi))\Big]\frac{\partial P_{nm}(\cos(\theta))}{\partial\theta}\;. \tag{5.51}$$

The shift by π is a consequence of the positive amplitude. Thus, the dependence of the amplitude on the depth is given by the factor

$$\frac{1}{r}\,\sqrt{A(r)^2+B(r)^2} \tag{5.52}$$

and of the phase by

$$\alpha(r)+\arctan\frac{B(r)}{A(r)}+\pi\;. \tag{5.53}$$

Remarks

1. A short checkup concerning the shift by π is possible because for $r=R_\sigma$ from the initial conditions follows $A(R_\sigma)=-n$ and $B(R_\sigma)=0$. That means that all equations at $r=R_\sigma$ are identical (eq. (5.41); eq. (5.48); eq. (5.51)).

2. Due to the relation

$$\dot{B}_\vartheta(r,t) \;=\; \omega\,B_\vartheta(r,t), \qquad r\le R_\sigma \tag{5.54}$$

valid for periodical setups $B_\vartheta(R_\sigma,t) \;=\; A\sin(\omega\,t)$, the results for amplitude and phase shift can be also applied to all time derivatives of $B_\vartheta(r,t)$.

3. All relations derived here are analogously valid for the tangential component B_φ.

5.3 Finite Fourier series

Each time function given on a fixed interval $[0,T]$ can be (under very weak smoothness requirements) approximated by a finite Fourier series ($\omega=2\pi/T$)

$$f(t)=\frac{a_0}{2}+\sum_{k=1}^{N}(a_k\cos(k\omega t)+b_k\sin(k\omega t))=\frac{a_0}{2}+\sum_{k=1}^{N}c_k\sin(k\omega t+\phi_k) \tag{5.55}$$

with

$$a_k = \frac{2}{T}\int_0^T f(t)\cos(k\omega t)dt, \qquad k = 0,\ldots,N\ , \tag{5.56}$$

$$b_k = \frac{2}{T}\int_0^T f(t)\sin(k\omega t)dt, \qquad k = 1,\ldots,N \tag{5.57}$$

and

$$c_k = (a_k^2 + b_k^2)^{1/2}, \quad \tan\phi_k = \frac{a_k}{b_k}, \quad k = 1,\ldots,N\ , \tag{5.58}$$

where the single summands are orthogonal. In a more compressed notation (left side of (5.55)), which introduces the quantities of amplitude and phase $c_k,\ \phi_k$, the summands are also orthogonal.

As a setup for downward continuation of u(r,t) (see (3.10)) we choose the amplitude coefficients $g^k(r), k = 0,\ldots,N$ and the phases $\alpha_k(r), k = 1,\ldots,N$ as r-dependent functions.

$$u(r,t) = g^0(r) + \sum_{k=1}^{N} g^k(r)\sin(k\omega t + \alpha^k(r))\ . \tag{5.59}$$

Both boundary conditions at R_σ are ($\Phi(t)$ given)

$$u(R_\sigma,t) = g^0(R_\sigma) + \sum_{k=1}^{N} g^k(R_\sigma)\sin(k\omega t + \alpha^k(R_\sigma)) = \Phi(t) \tag{5.60}$$

and

$$\begin{aligned} g_r^0(R_\sigma) + \sum_{k=1}^{N}\Big[g_r^k(R_\sigma)\sin(k\omega t + \alpha^k(R_\sigma)) + g^k(R_\sigma)\cos(k\omega t + \alpha^k(R_\sigma))\,\alpha_r^k(R_\sigma)\Big] \\ = -\frac{n+1}{R_\sigma}\left[g^0(R_\sigma) + \sum_{k=1}^{N} g^k(R_\sigma)\sin(k\omega t + \alpha^k(R_\sigma))\right]\ . \end{aligned} \tag{5.61}$$

For the time independent part of the second boundary condition in (5.61) follows

$$g_r^0(R_\sigma) = -\frac{n+1}{R_\sigma}\, g^0(R_\sigma)\ . \tag{5.62}$$

For the time dependent part in (5.61) the validity of the individual second boundary conditions can only be fulfilled ($g^k(R_\sigma) \neq 0$ assumed, $k = 1,\ldots,N$) if $\alpha_r^k(R_\sigma) = 0, \quad k = 1,\ldots,N$, is chosen. This choice of this individual initial conditions is always possible. Then (5.61) can be decomposed due to the orthogonality of the trigonometric functions. The proof applies the usual trigonometric addition theorems. Thus we have single (second) boundary conditions for each $k = 1,\ldots,N$

$$g_r^k(R_\sigma) = -\frac{n+1}{R_\sigma}\, g^k(R_\sigma)\ . \tag{5.63}$$

Considering our setup (5.59), inserted into the differential equation, the time independent part can be split up easily fulfilling the homogeneous differential equation

$$g_{rr}^0 + \frac{2}{r}\, g_r^0 - \frac{n(n+1)}{r^2}\, g^0 = 0. \tag{5.64}$$

Together with the boundary conditions (5.60) and (5.62) results the unique solution $g^0(r) = C/r^{n+1}$. The detailed view onto the differential equation (3.10), now only for the time-dependent sinusoidal parts which are all arranged on one side of the equation and sorted for the *Sine* and *Cosine* parts, reads

$$\begin{aligned} \sum_{k=1}^{N}\Bigg(\cos(k\omega t + \alpha^k)\left[2g_r^k\alpha_r^k + (\frac{2}{r}\alpha_r^k - \mu_0\sigma(r)\omega + \alpha_{rr}^k)\, g^k\right] \\ +\ \sin(k\omega t + \alpha^k)\left[g_{rr}^k + \frac{2}{r}g_r^k - ((\alpha_r^k)^2 + \frac{n(n+1)}{r^2})\, g^k\right]\Bigg)\ =\ 0\ . \end{aligned} \tag{5.65}$$

Because of the orthogonality each coefficient has to vanish, i.e. we have the sets of nonlinear ordinary differential equations, for each index k two differential equations of order two:

$$g^k_{rr} + \frac{2}{r} g^k_r - \left((\alpha^k_r)^2 + \frac{n(n+1)}{r^2} \right) g^k = 0 \tag{5.66}$$

$$2 g^k_r \alpha^k_r + \left(\frac{2}{r} \alpha^k_r - \mu_0 \, \sigma(r) \, \omega + \alpha^k_{rr} \right) g^k = 0 \tag{5.67}$$

These are identical for each k with those ones, (5.21) and (5.22), respectively, which are already have been derived in Sec. 5.2.1 and can be solved separately, i.e. by a transfer to a system of first order as described there.

Data based setups: Approximative solutions

6

Unlike the pure simulation setups referring to special function types (see preceding chapter), we will now study the possibilities to include data functions in the solution setup to find approximative solutions (or sometimes 'perturbation' solutions) of our downward field continuation problems. Since the mathematical description of these problems is reduced to standard tasks for ordinary differential equations, they are no longer unstable but become stable problems.

Benton & Whaler (1983) presents a detailed study applying these approximative method to the downward continuation of the poloidal magnetic field, probably inspired by the methodically oriented paper of Burggraf (1964), one of the very early articles on inverse heat conduction problems (IHCP). Later on these problems with different mathematical and technical background were intensively studied (e.g. the surveys of Dinh & Gorenflo, 1991; Reinhardt & Seiffarth, 1993). These problems show a clear analogy to the geomagnetic downward continuation problem, as they are also (unstable) inverse boundary value problems for the diffusion/heat conduction differential equation.

For the function u in (3.10), a setup is chosen

$$u(r,t) = \sum_{k=0}^{N} f_k(r)\ \frac{d^k}{dt^k} g(t), \tag{6.1}$$

which can be understand as a generalized Taylor series of a certain Gauss coefficient $g(t)$ related to the time variable and with coefficients $f_k(r)$ being functions of the radius r. We want to demonstrate details and results for the upward and the downward continuation. The related tasks are all tasks for ordinary differential equations as in the previous chapter.

6.1 Up and downward continuation solution schemes

The boundary conditions for the **upward** continuation are given at both sides of the radial interval (let $g(t)$ any Gauss coefficient, degree n, given at R_c)

$$u(R_c,t) = g(t) \qquad \text{and} \qquad \frac{\partial u(R_\sigma,t)}{\partial r} = -\frac{n+1}{R_\sigma}\, u(R_\sigma,t)\ . \tag{6.2}$$

By the setup (6.1) they are split up into the sets of boundary conditions

$$f_0(R_c) = 1, \qquad f_k(R_c) = 0, \qquad k = 1,\dots,N \qquad \text{and} \tag{6.3}$$

$$\frac{df_k\,(R_\sigma)}{dr} = -\frac{n+1}{R_\sigma}\, f_k(R_\sigma), \qquad k = 0,\dots,N\ . \tag{6.4}$$

Inserting the setup (6.1) into the differential equation

$$\frac{\partial^2 u}{\partial r^2} + \frac{2}{r}\frac{\partial u}{\partial r} - \frac{n(n+1)}{r^2} u = \mu_0\, \sigma(r) \frac{\partial u}{\partial t} \tag{6.5}$$

and abbreviating the ordinary differential operator by the symbol D^2

$$D^2 := \frac{d^2(\cdot)}{dr^2} + \frac{2}{r}\frac{d(\cdot)}{dr} - \frac{n(n+1)}{r^2}\cdot(\cdot)\ , \tag{6.6}$$

we find the set of successively connected differential equations

$$D^2 f_0 = 0, \qquad D^2 f_k = \mu_0\, \sigma\, f_{k-1}, \quad k = 1,\dots,N\ , \tag{6.7}$$

which can be iteratively solved.

The determination of f_0, $(k = 0)$ consists of solving an homogeneous problem. There are two linear independent solutions

$$f_0^a = C_a \cdot r^n, \qquad f_0^b = C_b \cdot r^{-n-1} \,. \tag{6.8}$$

Only the second one $f_0^b = (R_c/r)^{n+1}$ fulfills the conditions (6.2) of the problem. Thus for the first approximation of u we get with

$$u(r,t) \,=\, g(t) \left(\frac{R_c}{r}\right)^{n+1} \tag{6.9}$$

the harmonic upward continuation. The next step, the determination of $f_1(r)$, requires to solve the following problem

$$D^2\, f_1(r) = \,\mu_0\, \sigma(r) \left(\frac{R_c}{r}\right)^{n+1} \quad \text{with} \quad f_1(R_c) = 0 \quad \text{and} \quad \frac{df_1(\,R_\sigma)}{dr} = -\frac{n+1}{R_\sigma}\, f_1(R_\sigma) \,. \tag{6.10}$$

This boundary value problem is sometimes classified as a so-called Sturm problem (see Heuser, 1991, No36, p.379), if the differential equation is reformulated as

$$\frac{\partial}{\partial r}\left(r^2\, \frac{\partial f_1(r)}{\partial r}\right) \,-\, n(n+1)\, f_1(r) \,=\, \mu_0\, \sigma(r)\, r^2 \left(\frac{R_c}{r}\right)^{n+1} \,. \tag{6.11}$$

Its complete analytical solution is possible by constructing Green's function

$$G(r,s) \,=\, \frac{1}{2n+1} \begin{cases} (R_c^{2n+1}\, r^{-n-1} - r^n)\, s^{-n-1} & : \quad R_c \le r \le s \le R_\sigma \\ (R_c^{2n+1}\, s^{-n-1} - s^n)\, r^{-n-1} & : \quad R_c \le s \le r \le R_\sigma \end{cases} \,. \tag{6.12}$$

Then the solution for $f_1(r)$ is found as

$$f_1(r) \,=\, \mu_0\, R_c^{n+1} \int_{R_c}^{R_\sigma} G(r,s)\sigma(s) s^{-n+1} ds \tag{6.13}$$

$$= \frac{\mu_0}{2n+1} \left(\frac{R_c}{r}\right)^{n+1} \left[\int_{R_c}^{r} \left(\frac{R_c^{2n+1}}{s^{2n}} - s\right) \sigma(s)\, ds \,+\, (R_c^{2n+1} - r^{2n+1}) \int_r^{R_\sigma} \frac{\sigma(s)}{s^{2n}}\, ds\right] \,. \tag{6.14}$$

The whole upward continuation result at R_σ reads as

$$u(R_\sigma, t) = \left(\frac{R_c}{R_\sigma}\right)^{n+1} \left[g(t) \,+ \dot{g}(t) \frac{\mu_0}{2n+1} \int_{R_c}^{R_\sigma} \left(\frac{R_c^{2n+1}}{s^{2n}} - s\right) \sigma(s)\, ds\right] \,. \tag{6.15}$$

This result is equivalent with the approximative solution in Backus (1983), which he constructed via some transformation steps and solving a Fredholm integral equation.

The **downward** continuation perturbation approach works formally with the same set of equations as the upward continuation problem concerning the decomposition of the boundary conditions and the differential equation. However, there is one decisive difference: The data (the Gauss coefficient $g(t)$) is taken now at the radius level of R_σ (formerly R_c). That means, the first and the second boundary condition both are prescribed for the same endpoint R_σ of the radius interval

$$u(R_\sigma, t) = g(t) \qquad \text{and} \qquad \frac{\partial u(R_\sigma, t)}{\partial r} = -\frac{n+1}{R_\sigma}\, u(R_\sigma, t) \,. \tag{6.16}$$

Thus, for the determination of the set of functions $f_k(r),\ k = 0, \ldots, N$ no longer boundary value problems, but **initial value problems** for ordinary differential equations with two initial values have to be solved. These initial values are given by

$$f_0(R_\sigma) = 1 \,, \qquad f_k(R_\sigma) = 0, \quad k = 1, \ldots, N \qquad \text{and} \tag{6.17}$$

$$\frac{df_0(R_\sigma)}{dr} = -\frac{n+1}{R_\sigma} \,, \qquad \frac{df_k(R_\sigma)}{dr} = 0, \quad k = 1, \ldots, N \,. \tag{6.18}$$

For $k = 0$, we find $f_0(r) = (R\sigma/r)^{n+1}$, and hence for the first approximation of u the harmonic downward continuation

$$u(r,t) \;=\; g(t)\,\left(\frac{R_\sigma}{r}\right)^{n+1} \quad . \tag{6.19}$$

The solution technique (for $k = 1,\ldots,$) uses the method of variation of parameters/constants and the Wronski determinant (Benton & Whaler, 1983). An explicit solution formula can be found, e.g. in Zwillinger (1997, No 95, p378). With the integral basis ($k = 1$)

$$\phi_1(r) \;=\; r^n, \;\; \phi_2(r) \;=\; r^{-n-1} \tag{6.20}$$

we find

$$f_1(r) \;=\; \frac{\mu_0}{2n+1}\left(\frac{R_\sigma}{r}\right)^{n+1}\left[\int_r^{R_\sigma} s\,\sigma(s)\,ds \;-\; r^{2n+1}\int_r^{R_\sigma}\frac{\sigma(s)}{s^{2n}}\,ds\right] \quad . \tag{6.21}$$

Summing up, the second approximation for u at R_c gives

$$u(R_c,t) \;=\; \left(\frac{R_\sigma}{R_c}\right)^{n+1}\left[g(t) \;+\dot g(t)\frac{\mu_0}{2n+1}\int_{R_c}^{R_\sigma}\left(s - \frac{R_c^{2n+1}}{s^{2n}}\right)\sigma(s)\,ds\right] \quad . \tag{6.22}$$

With the same procedure, $f_2(r)$ can be calculated to find the 3rd approximation of u at R_c:

$$\begin{aligned} f_2(r) = \left(\frac{\mu_0}{2n+1}\right)^2\left(\frac{R_\sigma}{r}\right)^{n+1}\Bigg[&\int_r^{R_\sigma}\int_y^{R_\sigma}(ys - y^{2n+2}s^{-2n})\,\sigma(s)\sigma(y)\,dy\,ds \\ &+r^{2n+1}\int_r^{R_\sigma}\int_y^{R_\sigma}(ys^{-2n} - y^{-2n}s)\,\sigma(s)\sigma(y)\,dy\,ds\Bigg] \quad . \end{aligned} \tag{6.23}$$

The integral terms for this third step contain four double integrals over weighted products of the conductivity. In (6.23) attention should be paid to the sequence of integration: first over y and followed by s. Because the variable y appears also as an integration boundary. For $r = R_c$ in $f_2(r)$ the third approximation of $u(R_c,t)$ can be determined and added to (6.22).

Remark: The perturbation setup (6.1) with summands, consisting of r-dependent and t-dependent factors, can be generalized by replacing the specific t-dependent quantities $d^k g(t)/dt^k$ by other time functions $p_k(t)$. The condition they have to fulfill is only the linear independency of the $p_k(t)$. It guarantees the decomposition of the basic differential equation as well as of the boundary conditions and thus the analytic handling of uncoupled tasks for different indices. Thus, many possibilities exist to modify this approach.

6.2 Upward and downward continuation of field components

From the results provided by the perturbation setups for upward and downward continuation, expressions for coefficients in the different magnetic components can be derived. Thus, we can compare their structures in regard to the difference between the results of upward and downward continuation and concerning to the difference between radial and tangential field components. The approximation of the perturbation solutions is limited here to the second order.

The approximation scheme for the **upward** continuation gives (let be the Gauss coefficient $g(t), u(R_c,t) = g(t)$ the lower input function with degree n)

$$u(R_\sigma,t) = f_0(R_\sigma)\,g(t) + f_1(R_\sigma)\,\dot g(t)\;. \tag{6.24}$$

From this, the coefficients of the field components at R_σ $\beta^r_{nm}(R_\sigma,t)$, $\beta^{\vartheta,\varphi}_{nm}(R_\sigma,t)$ (see (2.23)) have the form:

$$\beta^r_{nm}(R_\sigma,t) = \frac{f_0(R_\sigma)}{R_\sigma}\,g(t) + \frac{f_1(R_\sigma)}{R_\sigma}\,\dot g(t), \tag{6.25}$$

$$\beta^{\vartheta,\varphi}_{nm}(R_\sigma,t) = \left(\frac{f_0(R_\sigma)}{R_\sigma} + \frac{df_0(R_c)}{dr}\right)g(t) + \left(\frac{f_1(R_\sigma)}{R_\sigma} + \frac{df_1(R_c)}{dr}\right)\dot g(t). \tag{6.26}$$

Based on this, with (6.9) and (6.14) the expressions for the radial and tangential field coefficients at R_σ are found:

$$\beta^r_{nm}(R_\sigma,t) = \frac{1}{R_\sigma}\left(\frac{R_c}{R_\sigma}\right)^{n+1}\left[g(t) + \frac{\mu_0\,\dot g(t)}{2n+1}\int\limits_{R_c}^{R_\sigma}\sigma(s)\left(\frac{R_c^{2n+1}}{s^{2n}} - s\right)ds\right], \tag{6.27}$$

$$\beta^{\vartheta,\varphi}_{nm}(R_\sigma,t) = \frac{1}{R_\sigma}\left(\frac{R_c}{R_\sigma}\right)^{n+1}(-n)\left[g(t) + \frac{\mu_0\,\dot g(t)}{2n+1}\int\limits_{R_c}^{R_\sigma}\sigma(s)\left(\frac{R_c^{2n+1}}{s^{2n}} - s\right)ds\right]. \tag{6.28}$$

The approximation scheme for the **downward** continuation gives (let be $u(R_\sigma,t) = g(t)$ the upper input function, Gauss coefficient with degree n)

$$u(R_c,t) = f_0(R_c)\,g(t) + f_1(R_c)\,\dot g(t)\,. \tag{6.29}$$

From this the coefficients of the field components at R_c $\beta^r_{nm}(R_c,t)$, $\beta^{\vartheta,\varphi}_{nm}(R_c,t)$ (see (2.23)) can be derived

$$\beta^r_{nm}(R_c,t) = \frac{f_0(R_c)}{R_c}\,g(t) + \frac{f_1(R_c)}{R_c}\,\dot g(t), \tag{6.30}$$

$$\beta^{\vartheta,\varphi}_{nm}(R_c,t) = \left(\frac{f_0(R_c)}{R_c} + \frac{df_0(R_c)}{dr}\right)g(t) + \left(\frac{f_1(R_c)}{R_c} + \frac{df_1(R_c)}{dr}\right)\dot g(t)\,. \tag{6.31}$$

With this, using (6.19), (6.21) and by inserting, both field coefficients at R_c can be expressed as

$$\beta^r_{nm}(R_c,t) = \frac{1}{R_c}\left(\frac{R_\sigma}{R_c}\right)^{n+1}\left[g(t) + \frac{\mu_0\,\dot g(t)}{2n+1}\int\limits_{R_c}^{R_\sigma}\sigma(s)\left(s - \frac{R_c^{2n+1}}{s^{2n}}\right)ds\right], \tag{6.32}$$

$$\beta^{\vartheta,\varphi}_{nm}(R_c,t) = \frac{1}{R_c}\left(\frac{R_\sigma}{R_c}\right)^{n+1}(-n)\left[g(t) + \frac{\mu_0\,\dot g(t)}{2n+1}\int\limits_{R_c}^{R_\sigma}\sigma(s)\left(s + \left(1+\frac{1}{n}\right)\frac{R_c^{2n+1}}{s^{2n}}\right)ds\right]. \tag{6.33}$$

We find that all tangential magnetic field components (compared to the radial ones) have a factor $-n$ (the degree). A comparison shows that in both coefficients (for upward and downward continuation) the function $\sigma(s)$, which has to be integrated, is weighted with the same type of algebraic function of s. For the upward continuation, this weighting is identical for the radial and the tangential coefficients. In the case of the downward continuation, there are different weights (note the fraction term $1/(s^{2n})$!) in the radial and the tangential component. A more detailed consideration of the time structure between both coefficients provides for the downward continuation a time shift due to the different factors at the $\dot g$ terms. Therefore, contrary to the downward continuation, ((6.32) and (6.33)), the upward continuation provides no time shift between both components. The reason for this fact is the fulfillment of the second boundary condition of third kind at R_σ (6.2), which connects the function and its derivative.

Remark: The **diffusion time** of an oscillation of a certain geomagnetic field coefficient, degree n, between the core mantle boundary and the earth surface can be easily derived via the phase shift (see e.g. Stadelmann, 2001,2006; Stadelmann & Weidelt, 2005b,a).

6.3 Periodical perturbation setups: Amplitudes and phases

The method of perturbation or approximation for the nonharmonic downward continuation can help (as an alternative method) to find approximative solutions which have analytically transparent formulae. Thus, specific advantages can be used analyzing the amplitude-phase behaviour of oscillations (for the exact numerical case see above Sec. 5.2) and studying the influence of the radial conductivity function on the different geomagnetic components.

Setting for the Gauss coefficient at R_σ as first boundary value for $g(t) = \sin(\omega\,t)$ (corresponding to amplitude $= 1$, phase $= 0$) with $\omega = 2\pi/T$, the perturbation setup (6.29) gives for R_c

$$u(R_c,t) = f_0(R_c)\sin(\omega\,t) + f_1(R_c)\,\omega\,\cos(\omega\,t)\,. \tag{6.34}$$

The basic trigonometric identity

$$a\sin(\omega t) + b\cos(\omega t) = (a^2 + b^2)^{1/2}\sin(\omega t + \arctan(b/a)) \tag{6.35}$$

allows us to determine the (relative) amplitude and the phase shift for the downward continuation of $g(t) = \sin(\omega\, t)$. For the coefficients $\beta^r_{nm}(R_c, t)$ of B_r (6.32) and $\beta^{\vartheta,\varphi}_{nm}(R_c, t)$ of B_φ or B_ϑ (6.33), we get the corresponding phases $p_r, p_{\varphi,\vartheta}$, respectively (we suppress here the indices n,m , also for the amplitudes $A_r, A_{\vartheta,\varphi}$). For the tangents of the phases hold

$$\tan(p_r) = \frac{\mu_0\omega}{2n+1}\int\limits_{R_c}^{R_\sigma}\sigma(s)\left(s\, -\, \frac{R_c^{2n+1}}{s^{2n}}\right)ds\ , \tag{6.36}$$

$$\tan(p_{\varphi,\vartheta}) = \frac{\mu_0\omega}{2n+1}\int\limits_{R_c}^{R_\sigma}\sigma(s)\left(s\, +\left(1+\frac{1}{n}\right)\frac{R_c^{2n+1}}{s^{2n}}\right)ds\ . \tag{6.37}$$

The related amplitudes are

$$A_r = \frac{1}{R_c}\left(\frac{R_\sigma}{R_c}\right)^{n+1}\left[1+\left(\frac{\mu_0\,\omega}{2n+1}\int\limits_{R_c}^{R_\sigma}\sigma(s)\left(s-\frac{R_c^{2n+1}}{s^{2n}}\right)ds\right)^2\right]^{1/2}\ , \tag{6.38}$$

$$A_{\vartheta,\varphi} = \frac{1}{R_c}\left(\frac{R_\sigma}{R_c}\right)^{n+1} n\left[1+\left(\frac{\mu_0\,\omega}{2n+1}\int\limits_{R_c}^{R_\sigma}\sigma(s)\left(s+\left(1+\frac{1}{n}\right)\frac{R_c^{2n+1}}{s^{2n}}\right)ds\right)^2\right]^{1/2}\ . \tag{6.39}$$

Obviously the relation

$$A_r < A_{\vartheta,\varphi} \tag{6.40}$$

exists by the non-negativity of the conductivity function $\sigma(r)$. Due to the strictly increasing monotonicity of the arc tangent function the relation

$$p_r < p_\varphi \tag{6.41}$$

follows for a conductivity function with $\sigma(r) \not\equiv 0$, i.e. the phase shift at the CMB for the tangential components is stronger than for the radial one. The validity of these relations (6.40), (6.41) holds not universally, but is strongly connected to the approximative setups.

6.4 Downward continuation of temporally local extrema

The results of the downward continuation of u in eq. (6.29) and of the radial and tangential field coefficients $\beta^r_{nm}(R_c, t)$ and $\beta^{\vartheta,\varphi}_{nm}(R_c, t)$ in eqs. (6.32) and (6.33) can be used to study the time shifts of temporal local extrema for the downward continued quantities, respectively. For this we assume that the Gauss coefficient $g(t)$ at R_σ (for individual degree n) can be presented, e.g. as a temporal parabola in a certain fix time interval, e.g. as quadratic Taylor series, in abstract form

$$g(t) = c_2\, t^2 + c_1\, t + c_0\ . \tag{6.42}$$

Then, for an extremum holds $t^{R_\sigma}_{ex} = -c_1/2c_2$. Applying this parabola $g(t)$ to the downward continuation formula (6.32) (field coefficient $\beta^r_{nm}(R_c, t)$) we get again a quadratic time polynomial. Searching for the extremum $t^{R_c}_{ex,r}$ we find the relation

$$t^{R_c}_{ex,r} = t^{R_\sigma}_{ex,r} - \frac{\mu_0}{2n+1}\int\limits_{R_c}^{R_\sigma}\sigma(s)\left(s-\frac{R_c^{2n+1}}{s^{2n}}\right)ds\ . \tag{6.43}$$

It should account for the causality

$$t^{R_c}_{ex,r} < t^{R_\sigma}_{ex,r}\ . \tag{6.44}$$

In fact, this can be confirmed by the estimation

$$s^{2n+1} > R_c^{2n+1} \quad \longleftrightarrow \quad s - \frac{R_c^{2n+1}}{s^{2n}} > 0 \; . \tag{6.45}$$

For the tangential components, the analogous relation can be derived in a similar way

$$t_{ex,\vartheta,\varphi}^{R_c} = t_{ex,\vartheta,\varphi}^{R_\sigma} - \frac{\mu_0}{2n+1} \int\limits_{R_c}^{R_\sigma} \sigma(s) \left(s + \left(1 + \frac{1}{n} \right) \frac{R_c^{2n+1}}{s^{2n}} \right) ds \; . \tag{6.46}$$

It is interesting that these relations show the same integral expressions which appear for the phase shift of oscillations ((6.36)–(6.37)) with corresponding weight functions of $\sigma(r)$, however without the tangents function and independently of a period T. Thus, they can be – under certain aspect – considered as a very simple generalization of the oscillation studies.

Especially, these statements can be used for the secular variation with its components in jerk investigations. Jerks are sudden (trend) changes in the secular variation $\dot{\mathbf{B}}$ with a of duration some months to two years and which occur in irregular sequence (e.g. 1969, 1978, 1991, see Alexandrescu et al., 1995, 1996). The interest here concerns to the jerk occurrence times and time delays between earth surface and CMB (Ballani et al., 2010). A certain affinity to oscillations is suggested and approximative studies seems to be possible. However, it has to be remarked that these quantities, obtained by straight-line approximation, generally do not coincide with the maxima or minima of quadratic curves. The analytical shape of jerks in the secular variation component $\dot{B}_\varphi(R_E, t)$ was determined by Alexandrescu et al. (1995, 1996) for numerous geomagnetic stations. She tested as function-type half-parabolas $t^\alpha, t > 0$ and found for α a certain range between values of about 1.5 and 1.7. By the perturbation nonharmonic downward continuation formulae (6.32)–(6.33) it is possible to determine the negative time shift at the CMB, i.e. how much earlier the minimum of the approximating time curve occurs at the CMB compared with its appearance at the earth surface.

Let such a half-parabola have its minimum at the earth surface $t_{ex,\varphi}^{R_\sigma} = 0$. For R_c we have to find the minimum of the function (see formula (6.33) without constant factors):

$$t^\alpha + \alpha\, t^{\alpha-1}\, C \qquad \text{with} \qquad C = \frac{\mu_0}{2n+1} \int\limits_{R_c}^{R_\sigma} \sigma(s) \left(s + \left(1 + \frac{1}{n} \right) \frac{R_c^{2n+1}}{s^{2n}} \right) ds \; . \tag{6.47}$$

The condition of the vanishing first derivative provides

$$\alpha\, t^{\alpha-2} \left[t + (\alpha - 1)\, C \right] = 0 \; , \tag{6.48}$$

which leads to the only nonzero solution, depending on α and $\sigma(r)$,

$$t_{ex,\varphi}^{R_c} = -\,(\alpha\, -1)\, \frac{\mu_0}{2n+1} \int\limits_{R_c}^{R_\sigma} \sigma(s) \left(s + \left(1 + \frac{1}{n} \right) \frac{R_c^{2n+1}}{s^{2n}} \right) ds \; , \tag{6.49}$$

which is a clearly negative quantity, i.e. appears prior to the corresponding minimum assumed on the earth surface.

7 Impact of the conductivity function

As the NHDC method works in general as a numerical method, it does not show the explicit dependency of the solution on the specially chosen conductivity function $\sigma(r)$. Approximative (perturbation) solution methods as presented in Ch. 6 show analytical structures and thus can help to uncover this dependency. This applies the special cases derived with the setup (6.1), as single field coefficients β^{r}_{nm}, $\beta^{\vartheta,\varphi}_{nm}$ in Sec. 6.2, the temporal oscillations in Sec. 6.3 or time delays of extremal points in Sec. 6.4. More generally, all the possibilities can be addressed which could be generated by applying other bases functions as indicated in the remark at the end of Sec. 6.1.

The approximative downward continuation solutions derived from (6.1) ($k \geq 1$) are corrections of the harmonic solution ($k = 0$) which does not depend on the conductivity. The terms appearing for $k = 1$ are integrals over a weighted conductivity function σ in (6.22), for field components (6.32)–(6.33), for phases and amplitudes of oscillations (6.36)–(6.39) and for shifts of extremal values (6.43)–(6.46). For higher k, there result correspondingly k-fold integrals, as for $k = 2$ (6.23) and so on.

The cited formulae of Ch. 6 show the different influence of σ on the radial and tangential field components (also noted by Stadelmann, 2001,2006; Stadelmann & Weidelt, 2005b,a). The reason for this are different weight functions for the conductivity, depending on n,

$$w^{r}_{n}(r) = \frac{\mu_0}{2n+1}\left(r - \frac{R_c^{2n+1}}{r^{2n}}\right), \tag{7.1}$$

$$w^{\vartheta\varphi}_{n}(r) = \frac{\mu_0}{2n+1}\left(r + \frac{n+1}{n}\frac{R_c^{2n+1}}{r^{2n}}\right). \tag{7.2}$$

Both types are characterized by an opposite monotonous radial course concerning the magnitude, the growth and the curvature, which can be seen clearly in Fig. 7.1 with two examples for $n = 1$ and $n = 4$.

While for the radial type $w^{r}_{n}(r)$ the influence at the CMB is minimal ($w^{r}_{n}(R_c) = 0$) and increases towards larger radius values, the weight function for the tangential components $w^{\vartheta\varphi}_{n}(r)$ has its maximum value at the CMB and decreases monotonically for increasing radius values. We observe that the difference of the weight functions

$$w^{\vartheta\varphi}_{n}(r) - w^{r}_{n}(r) = \frac{\mu_0}{2n+1}\left(2 + \frac{1}{n}\right)\frac{R_c^{2n+1}}{r^{2n}} \tag{7.3}$$

presented in Fig. 7.1, shows its maximum value at the CMB together with $w^{\vartheta\varphi}_{n}(r)$. That means that the corresponding phase differences $p_{\vartheta\varphi} - p_r$ or the corresponding time delay differences $td_{\vartheta\varphi,n} - td_{r,n}$ can act as indicator for the conductivity in the **lower** mantle, especially the near CMB region. The opposite case is given by the pure r-component with the weight function $w^{r}_{n}(r)$ which is much more influenced by the upper mantle.

To demonstrate the sensitivity of $\boldsymbol{\sigma}$ on the whole $\boldsymbol{r}$-interval, a comparison can be made between radial and tangential component. We consider as test object a layer with bottom position (lower edge) at r and layer size $d(r)$ and ask what layer size originates a prescribed time delay td_0 of e.g. 0.1 yr. $d(r)$ has to satisfy the equation

$$td_0 = \int_{r}^{r+d(r)} \sigma(s)w(s)ds, \tag{7.4}$$

where $w(s)$ represents alternatively one of the functions $w^{r}_{n}(r)$ or $w^{\vartheta\varphi}_{n}(r)$. Fig. 7.3 shows exemplarily these quantities for three conductivities (Fig. 7.2) and the radial and tangential component (only the case $n = 1$).

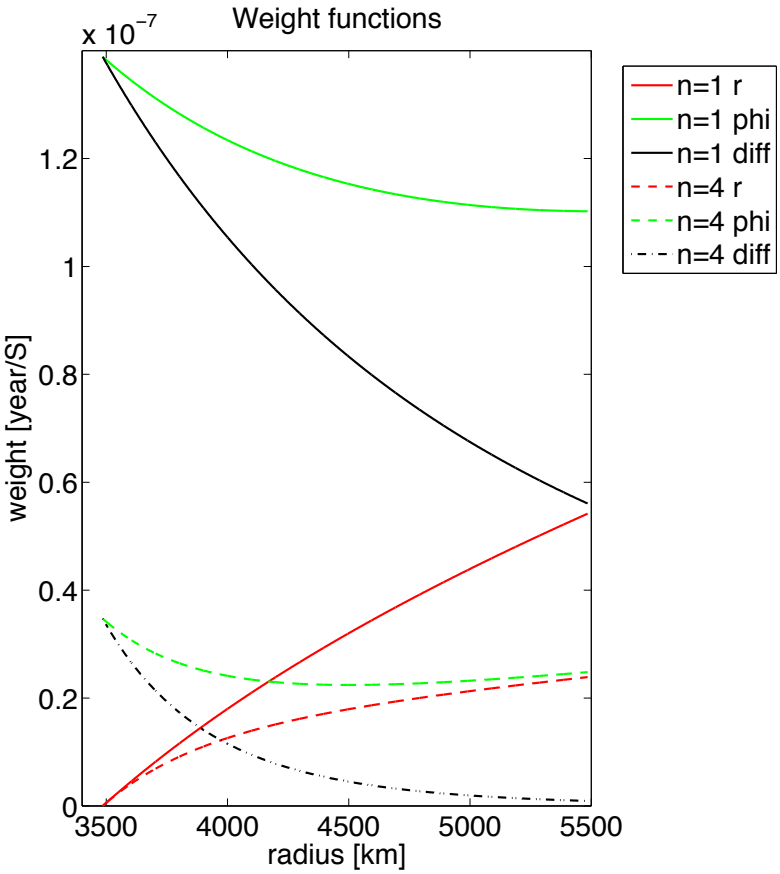

Figure 7.1: Weight functions $w_n^r(r)('\mathrm{r}'), w_n^{\vartheta\varphi}(r)$ ('phi') (see (7.1), (7.2)) and the differences $w_n^{\vartheta\varphi}(r) - w_n^r(r)$ ('diff') for the degrees $n = 1$ and $n = 4$ between $r = R_c$ and $r = R_\sigma$.

Because of the uncertainties in the lower mantle conductivity, we choose three alternative mantle conductivity functions. The details are (values in Sm^{-1})

$$\sigma_1(r) = \begin{cases} 0 & R_\sigma < r \\ 6 & R_c < r \le R_\sigma \end{cases},$$

$$\sigma_2(r) = \begin{cases} 0 & R_\sigma < r \\ 10 \cdot \left(\dfrac{R_c}{r}\right)^5 & R_c + 2\,\mathrm{km} < r \le R_\sigma \\ 1 \cdot 10^5 & R_c \le r \le R_c + 2\,\mathrm{km} \end{cases},$$

$$\sigma_3(r) = \begin{cases} 0 & R_D + 29\,\mathrm{km} \le r \\ 1 \cdot 10^3 \cdot \left(1 - \dfrac{r - R_D}{29}\right) & R_D \le r \le R_D + 29\,\mathrm{km} \\ 1 \cdot 10^3 & R_c < r \le R_D \end{cases}$$

with the radii: $R_c = 3485\,\mathrm{km}$, $R_\sigma = 5485\,\mathrm{km}$ and $R_D = 3670\,\mathrm{km}$ (7.5)

They can be shortly characterized by the following features:

σ_1 mantle low conducting; conductance $\approx 10^7 S$

σ_2 high conducting thin base layer above the CMB, decay by potential law through the mantle; conductance $\approx 2 \cdot 10^8 S$

σ_3 higher conducting D″ layer rapid dropping off to zero, mainly non-conducting mantle; conductance $\approx 2 \cdot 10^8 S$

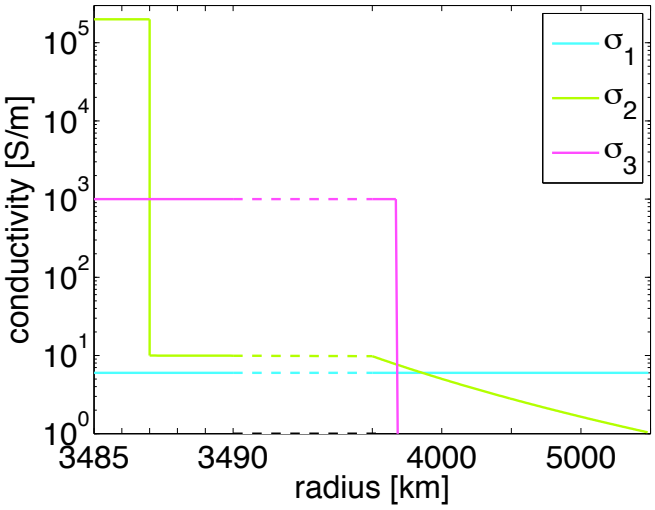

Figure 7.2: The mantle conductivity models $\sigma_1, \sigma_2, \sigma_3$ (logarithmic scales!)

While σ_1 marks some lower conductivity limit for the whole mantle, the models σ_2 and σ_3 especially cover possible situations in the near lower mantle zone above the CMB.

Fig.7.3 shows that for all the types of conductivity the φ-component is much more sensitive than the r-component. The sensitivity of the r-component increases near the earth surface. The comparison of the conductivities σ_1 and σ_2 (r-component) shows that the monotonous behaviour of the sensitivity (σ_1) can be changed due to the course of the conductivity (high values of σ_2 near the CMB). The high sensitivities for σ_3 (both components) are based on the conductivity concentration in near CMB lower mantle layer.

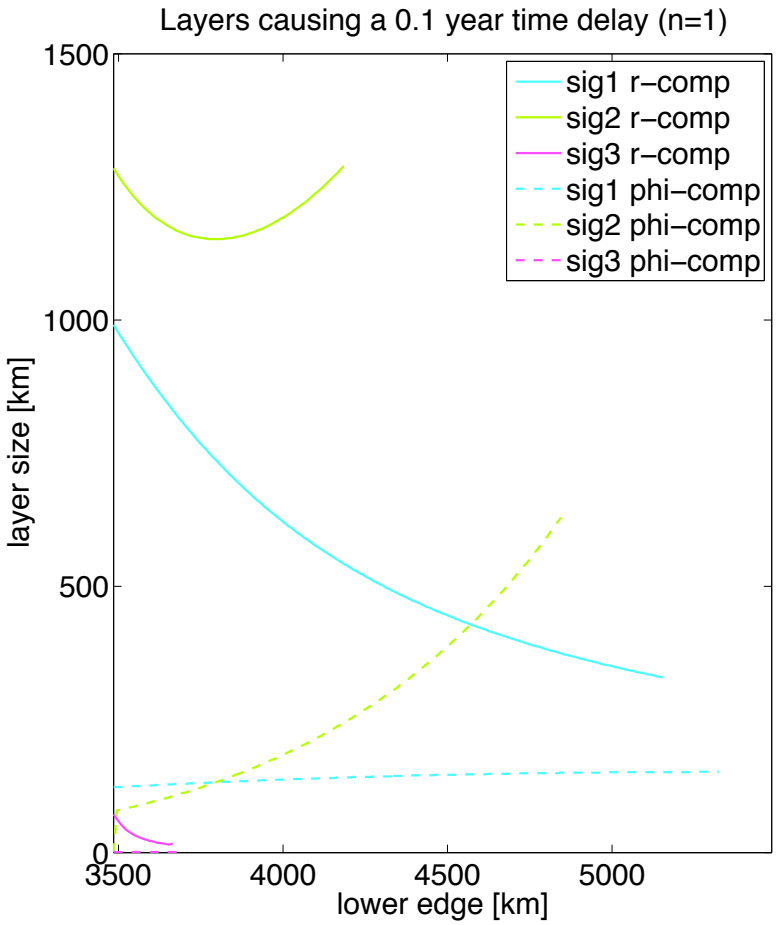

Figure 7.3: Solutions of $d(r)$ of equation (7.4) for the conductivities $\sigma_1, \sigma_2, \sigma_3$ (Fig. 7.2) and the geomagnetic r and φ components and $n = 1$. They describe the layer thickness of a conducting layer with the lower edge position at r which generates a time delay of 0.1 year in the corresponding geomagnetic component and the conductivity, respectively.

8 Applications

The following sections present special applications of the NHDC method which are of varied importance. They do not intend to be self-contained detailed investigations. Rather, they should be understood as methodically oriented possibilities (to have still to be worked out), demonstrating the applicability of the NHDC method in addition to our publications cited in the introduction.

8.1 Divergence of the geomagnetic field at the CMB

The vectorial induction equation (2.8) or (2.25), respectively, is completed by the Maxwell equation (see eq. (2.3) in Sec. 2.1)

$$\text{div } \mathbf{B} = 0. \tag{8.1}$$

For the applied global geomagnetic field models, valid in the earth outer space and especially for the earth surface, this condition is an intrinsic one, i.e. it is fulfilled with high precision. The method of NHDC determines (in dependency of the prescribed conductivity function σ) the generalized Gauss coefficients $g_{nm}(r,t), h_{nm}(r,t)$ or the quantities $S^{c,s}_{nnm}(r,t)$ at interpolation points $r = r_i$ between R_σ and R_c in a numerical, i.e. in an approximative way. In addition, the derivatives $\partial g_{nm}/\partial r$, $\partial h_{nm}/\partial r$, $\partial S^{c,s}_{nnm}(r,t)/\partial r$ and also derivatives of second order are generated by finite differences, which are near the CMB only supported by one side.

With one example, we demonstrate the typical quality of this numerical process for the approximated field components and first partial derivatives by recalculating the divergence condition at the earth surface ($r = R_E$) and the CMB ($r = R_c$). We have the expression

$$\text{div } \mathbf{B} = \frac{1}{r^2}\frac{\partial(r^2 B_r)}{\partial r} + \frac{1}{r\sin\vartheta}\frac{\partial(\sin\vartheta B_\vartheta)}{\partial\vartheta} + \frac{1}{r\sin\vartheta}\frac{\partial B_\varphi}{\partial\varphi} \tag{8.2}$$

and in more detail

$$\text{div } \mathbf{B} = \frac{2}{r}B_r + \frac{\partial B_r}{\partial r} + \frac{\cot\vartheta}{r}B_\vartheta + \frac{1}{r}\frac{\partial B_\vartheta}{\partial\vartheta} + \frac{1}{r\cos\vartheta}\frac{\partial B_\varphi}{\partial\varphi}\,. \tag{8.3}$$

For the components in (8.3), there are applied spherical-harmonic decompositions containing for each time the r-dependent coefficients or partial derivatives.

For the global field model C^{3}FM (Wardinski & Lesur, 2012), here considered up to the degree $n = 8$, we calculate globally the divergence for the time 2005.0 at the earth surface (R_E) and at the CMB (R_c), continued downward with the mantle conductivity model $\sigma_{5-250}(r)$, (values in $[\mathrm{S/m}]$)

$$\sigma_{5-250}(r) = \begin{cases} 0.3 & 5701\,\mathrm{km} - 6171\,\mathrm{km} \\ 1.0 & 4871\,\mathrm{km} - 5701\,\mathrm{km} \\ 5.0 & 3685\,\mathrm{km} - 4871\,\mathrm{km} \\ 250.0 & 3485\,\mathrm{km} - 3685\,\mathrm{km}\,. \end{cases} \tag{8.4}$$

We find the **global maxima** for the deviations of the divergence of zero:

$$\begin{aligned} &\text{for} \quad r = R_E \qquad 5\cdot 10^{-14}\,\mathrm{nT\,km} \\ &\text{for} \quad r = R_c \qquad 2\cdot 10^{-12}\,\mathrm{nT\,km}. \end{aligned} \tag{8.5}$$

8.2 Geomagnetic spectra and geomagnetic energy at the CMB

Spectra for the geomagnetic energy density at the earth surface were calculated independently at the same time by Mauersberger (1956) and Lucke (1957). Afterwards, Kautzleben (1963) showed the equivalence of both approaches, with some improvements and generated a universal formula being independent of the used normalisation. Lowes (1966, 1974) also considered the decomposition of mean square values on the sphere of spherical harmonic vector fields (the geomagnetic field, the geomagnetic secular variation) and considered its extrapolation down to the CMB. For the CMB, subsequently by several authors, geomagnetic or secular variation spectra were also considered and discussed, especially coupled with statistical view points. However, the background remained in every case the harmonic downward continuation, i.e. the assumption of a nonconducting mantle.

For a layered conducting mantle Stadelmann (2001,2006); Stadelmann & Weidelt (2005b,a) studied upward and downward continuation of magnetic field and secular variation by an analytical theory changing between time domain and frequency domain. In this context also a formula for the Mauersberger-Lowes spectrum at the CMB was derived (Stadelmann & Weidelt, 2005a).

The usage of the method of NHDC allows a new perspective: the integration of the effect of radial dependent mantle conductivity on spectra for field or secular variation at the CMB. Connected with the above shown approximative solutions for a CMB field (formulae in Ch. 6), revealing the conductivity influence analytically, further possibilities for forming and studying (approximative) spectra exist.

The **magnetic energy density** w for one point is given by (see Sec. 2.1 and Sommerfeld, 1961, vol III, p.108)

$$w = \frac{1}{2}(\mathbf{B}\cdot\mathbf{H}) \qquad \text{or} \qquad w = \frac{1}{2\mu}\mathbf{B}^2 \tag{8.6}$$

using the first relation in (2.5). The **magnetic energy** W itself is found by a volume integration of (8.6)

$$W = \int_V w\,dv \;=\; \frac{1}{2\mu}\int_V \mathbf{B}^2\,dv\;, \tag{8.7}$$

if V means the respective volume, e.g. the earth body.

For studying a **geomagnetic spectrum**, the energy density w is averaged over a spherical surface with radius $r = a$, i.e. expressed by

$$\langle\, w\,\rangle = \frac{1}{2\mu}\,\frac{1}{4\pi a^2}\int_0^{2\pi}\int_0^{\pi} w(a,\vartheta,\varphi,t)a^2\,\sin\,\vartheta\,d\vartheta\,d\varphi \tag{8.8}$$

(Mauersberger, 1956; Lowes, 1966). However, concerning the geomagnetic spectrum, most authors leave out the factor containing the permeability, $1/(2\mu)$.

We start in this way by integrating over the squared magnetic field decomposed in its spherical components (using the abbreviation MLK for the arising quantity)

$$MLK := \langle\,\mathbf{B}^2\,\rangle \;=\; \langle\,B_r^2\,\rangle \;+\; \langle\,B_\vartheta^2\,\rangle + \langle\,B_\varphi^2\,\rangle\;. \tag{8.9}$$

With the compressed representation of the magnetic components (see formulae (4;7),(4;8),(4:9) in Kautzleben, 1963, , p. 59)

$$B_r = \sum_{n=1}^{N}\sum_{m=0}^{n}\left[a_n^m(r)\cos m\varphi + b_n^m(r)\sin m\varphi\right]\;P_n^m(\vartheta)\;, \tag{8.10}$$

$$B_\vartheta = \sum_{n=1}^{N}\sum_{m=0}^{n}\left[g_n^m(r))\cos m\varphi + h_n^m(r)\sin m\varphi\right]\frac{dP_n^m(\vartheta)}{d\vartheta}\;, \tag{8.11}$$

$$B_\varphi = \sum_{n=1}^{N}\sum_{m=1}^{n}\left[g_n^m(r)\sin m\varphi - h_n^m(r)\cos m\varphi\right] m\;\frac{P_n^m(\vartheta)}{\sin\vartheta} \tag{8.12}$$

the author derived the general formula for MLK (eq. (4;41) in Kautzleben, 1963, , p. 65)

$$MLK = \frac{1}{2}\sum_{n=1}^{N}\left[n(n+1)(g_n^0(r))^2 + (a_n^0(r))^2\right](n_n^0)^2 + \\ + \frac{1}{4}\sum_{n=1}^{N}\sum_{m=1}^{n}\left[n(n+1)((g_n^m(r))^2 + (h_n^m(r))^2) + (a_n^m(r))^2 + (b_n^m(r))^2\right](n_n^m)^2 \,. \tag{8.13}$$

This formula holds for every radius r and is valid independently of the spherical harmonic normalisation. The input coefficients in (8.10) to (8.13) a_n^m, b_n^m, g_n^m, h_n^m act at the moment as formal quantities later to be specified. The normalisation factors $(n_n^m)^2$ are defined by

$$(n_n^m)^2 := \int_{-1}^{1} P_n^m(x)\, P_n^m(x)\, dx \,. \tag{8.14}$$

For the Ferrers-Neumann normalisation we have

$$(n_n^m)^2 = \frac{2}{2n+1}\frac{(n+m)!}{(n-m)!} \,, \tag{8.15}$$

for the Schmidt quasi-normalisation holds

$$(n_n^m)^2 = (2-\delta_{0m})\,\frac{2}{2n+1} \,. \tag{8.16}$$

The derivation of (8.13) requires for the tangential components B_ϑ, B_φ two special integral relations for the associated Legendre functions

$$\int_{-1}^{1}\frac{P_n^m(x)\,P_\nu^m(x)}{(1-x^2)}\,dx \,, \qquad \int_{-1}^{1}(1-x^2)\,\frac{d\,P_n^m(x)}{dx}\,\frac{d\,P_\nu^m(x)}{dx}\,dx \,. \tag{8.17}$$

One original derivation by Lucke (1957) was improved by Kautzleben (1963) and enlarged for any normalisation.

The most important and interesting point in the derivation of the universal expression (8.13) is the fact that, after summed up all terms for both tangential components, all product terms $g_\nu^m\, g_\mu^m, \mu \neq \nu$ (and analogously for the h-coefficients), which would mix the influence of **different scales**, cancel out mutually.

We will specify the general expression for the quantity (8.13) for two usual normalisations: the Ferrers-Neumann (FN) case (here already used as our standard case) and the Schmidt quasi-normalisation (SchmQ) as the international geomagnetic data standard.

For the first case (FN), we compare the coefficients of the magnetic components ((2.20), (2.21), (2.22)) with their representations given in ((8.10),(8.11),(8.12)). With the normalisation factor $(n_n^m)^2$ specified in (8.15), we find for MLK

$$MLK(FN,r,t) = \sum_{n=1}^{N}\frac{n\,(n+1)}{2n+1}\sum_{m=0}^{n}\left[\frac{1}{\lambda_{nm}^2}\left\{\left(\frac{S_{nm}^c}{r}+\frac{\partial S_{nm}^c}{\partial r}\right)^2 + \left(\frac{S_{nm}^s}{r}+\frac{\partial S_{nm}^s}{\partial r}\right)^2 + \right.\right. \\ \left.\left. + \,n\,(n+1)\left(\left(\frac{S_{nm}^c}{r}\right)^2 + \left(\frac{S_{nm}^s}{r}\right)^2\right)\right\}\right] \,. \tag{8.18}$$

Here we have used the convention $S_{n0}^s \equiv 0$. λ_{nm} is Schmidt's quasi-normalization coefficient given in (3.5).

To treat the second case (SchmQ), we enlarge the concept of the Gauss coefficient by an r-dependency in a way that it is compatible for the nonharmonic downward continuation. We define

$$g_{nm}(r,t) := \frac{n}{\lambda_{nm}\,R_E}\,S_{nm}^c(r,t) \,, \tag{8.19}$$

$$h_{nm}(r,t) := \frac{n}{\lambda_{nm}\,R_E}\,S_{nm}^s(r,t) \tag{8.20}$$

with the connections to the usual Gauss coefficients valid for the earth surface

$$g_{nm}(R_E,t) = g_{nm}(t)\ , \tag{8.21}$$
$$h_{nm}(R_E,t) = h_{nm}(t) \tag{8.22}$$

The magnetic field components expressed by these enlarged Gauss coefficients have the form

$$B_r = R_E \sum_{n=1}^{N}\sum_{m=0}^{n}\left(\frac{g_{nm}}{r}\cos m\varphi + \frac{h_{nm}}{r}\sin m\varphi\right)(n+1)\ P_{nm}(cos\vartheta)\ , \tag{8.23}$$

$$B_\vartheta = R_E \sum_{n=1}^{N}\sum_{m=0}^{n}\left(\left(\frac{g_{nm}}{r}+\frac{\partial g_{nm}}{\partial r}\right)\cos m\varphi + \left(\frac{h_{nm}}{r}+\frac{\partial h_{nm}}{\partial r}\right)\sin m\varphi\right)\frac{1}{n}\frac{dP_{nm}(cos\vartheta)}{d\vartheta}\ , \tag{8.24}$$

$$B_\varphi = R_E \sum_{n=1}^{N}\sum_{m=0}^{n}\left(\left(\frac{h_{nm}}{r}+\frac{\partial h_{nm}}{\partial r}\right)\cos m\varphi - \left(\frac{g_{nm}}{r}+\frac{\partial g_{nm}}{\partial r}\right)\sin m\varphi\right)\frac{m}{n}\frac{P_{nm}(cos\vartheta)}{\sin\vartheta}\ . \tag{8.25}$$

With the SchmQu normalisation factor $(n_n^m)^2$ ((8.14), (8.16)) then MLK (for this normalisation) can be expressed as

$$MLK(SchmQ,r,t) = R_E^2 \sum_{n=1}^{N}\frac{n+1}{n\,(2n+1)}\sum_{m=0}^{n}\left\{\left(\frac{g_{nm}}{r}+\frac{\partial g_{nm}}{\partial r}\right)^2 + \left(\frac{h_{nm}}{r}+\frac{\partial h_{nm}}{\partial r}\right)^2 + \right.$$
$$\left. + n\,(n+1)\left(\left(\frac{g_{nm}}{r}\right)^2 + \left(\frac{h_{nm}}{r}\right)^2\right)\right\}\ . \tag{8.26}$$

Here, again the convention $h_{n0} \equiv 0$ is used.

The proper spectrum for both cases (8.18), (8.26) respectively, are the summands of the first sum, plotted for each n. The connection with the usual standard spectrum for the harmonic downward continuation (convention $h_{n0}(t) \equiv 0$)

$$MLK(SchmQ(harmonic),r,t) = \sum_{n=1}^{N}\left(\frac{R_E}{r}\right)^{2n+4}(n+1)\sum_{m=0}^{n}\left[(g_{nm}(t))^2 + (h_{nm}(t))^2\right] \tag{8.27}$$

can be tested by setting (for the SchmQ case)

$$g_{nm}(r,t) := \left(\frac{R_E}{r}\right)^{n+1} g_{nm}(t)\ , \tag{8.28}$$
$$h_{nm}(r,t) := \left(\frac{R_E}{r}\right)^{n+1} h_{nm}(t) \tag{8.29}$$

or (for the FN case)

$$S_{nm}^{cs}(r,t) := \left(\frac{R_E}{r}\right)^{n+1} S_{nm}^{cs}(R_E,t)\ . \tag{8.30}$$

We want now to investigate the **influence of the conductivity** $\sigma(r)$ on the quantity MLK, i.e. on the spectrum, and limit the radial coordinate r to the CMB, i.e. $r = R_c$. With the results of Ch. 6 this is possible **in an approximative sense**.

If we define (analogous to (2.23)) the coefficients $\beta_{nm}^{\vartheta\varphi,g}$, $\beta_{nm}^{\vartheta\varphi,h}$ of the field components B_ϑ, B_φ in eqs. (8.24) and the coefficients $\beta_{nm}^{r,g}$, $\beta_{nm}^{r,h}$ of the r-component in eq. (8.23), then the quantity $MLK(SchmQ,r,t)$ (8.26) can be written in the form

$$MLK(SchmQ,R_c,t) = R_E^2 \sum_{n=1}^{N}\frac{n+1}{n(2n+1)}\sum_{m=0}^{n}\left\{\left(\beta_{nm}^{\vartheta\varphi,g}(R_c,t)\right)^2 + \left(\beta_{nm}^{\vartheta\varphi,h}(R_c,t)\right)^2 + \right.$$
$$\left. + n(n+1)\left(\left(\beta_{nm}^{r,g}(R_c,t)\right)^2 + \left(\beta_{nm}^{r,h}(R_c,t)\right)^2\right)\right\}\ . \tag{8.31}$$

Instead of the conductivity interval $[R_\sigma, R_c]$ we can also choose without any changes the larger interval $[R_E, R_c]$. Then our field component coefficients with the approximations derived in Ch. 6 by the perturbation theory are

$$\beta_{nm}^{r,g}(R_c,t) = \frac{1}{R_c}\left(\frac{R_E}{R_c}\right)^{n+1}\left[g_{nm}(t) + \frac{\mu_0\,\dot g_{nm}(t)}{2n+1}\int\limits_{R_c}^{R_E}\sigma(s)\left(s - \frac{R_c^{2n+1}}{s^{2n}}\right)ds\right], \tag{8.32}$$

$$\beta_{nm}^{\vartheta\varphi,g}(R_c,t) = \frac{1}{R_c}\left(\frac{R_E}{R_c}\right)^{n+1}(-n)\left[g_{nm}(t) + \frac{\mu_0\,\dot g_{nm}(t)}{2n+1}\int\limits_{R_c}^{R_E}\sigma(s)\left(s + \left(1+\frac{1}{n}\right)\frac{R_c^{2n+1}}{s^{2n}}\right)ds\right] \tag{8.33}$$

and $\beta_{nm}^{r,h}(R_c,t)$, $\beta_{nm}^{\vartheta\varphi,h}(R_c,t)$ analogous with $h_{nm}(t)$,$\dot h_{nm}(t)$. With the abbreviations

$$I^r(\sigma,n) := \frac{\mu_0}{2n+1}\int\limits_{R_c}^{R_E}\sigma(s)\left(s - \frac{R_c^{2n+1}}{s^{2n}}\right)ds\,, \tag{8.34}$$

$$I^{\vartheta\varphi}(\sigma,n) := \frac{\mu_0}{2n+1}\int\limits_{R_c}^{R_E}\sigma(s)\left(s + \left(1+\frac{1}{n}\right)\frac{R_c^{2n+1}}{s^{2n}}\right)ds \tag{8.35}$$

we get for (8.32), (8.33) the formulae in condensed form

$$\beta_{nm}^{r,g}(R_c,t) = \frac{1}{R_c}\left(\frac{R_E}{R_c}\right)^{n+1} g_{nm}(t)\left[1 + \frac{\dot g_{nm}(t)}{g_{nm}(t)}\,I^r(\sigma,n)\right], \tag{8.36}$$

$$\beta_{nm}^{\vartheta\varphi,g}(R_c,t) = (-n)\frac{1}{R_c}\left(\frac{R_E}{R_c}\right)^{n+1} g_{nm}(t)\left[1 + \frac{\dot g_{nm}(t)}{g_{nm}(t)}\,I^{\vartheta\varphi}(\sigma,n)\right] \tag{8.37}$$

and analogous with $h_{nm}(t)$, $\dot h_{nm}(t)$ the coefficients $\beta_{nm}^{r,h}(R_c,t)$, $\beta_{nm}^{\vartheta\varphi,h}(R_c,t)$.

Inserting these quantities in (8.31) we find

$$\begin{aligned} &MLK(SchmQ,R_c,t) \approx \\ &\approx R_E^2\sum_{n=1}^{N}\frac{n+1}{n\,(2n+1)}\sum_{m=0}^{n}\Bigg[n^2\left\{g_{nm}^2\left[1+\frac{\dot g_{nm}}{g_{nm}}\,I^{\vartheta\varphi}(\sigma,n)\right]^2 + h_{nm}^2\left[1+\frac{\dot h_{nm}}{h_{nm}}\,I^{\vartheta\varphi}(\sigma,n)\right]^2\right\} + \\ &\qquad + n\,(n+1)\left\{g_{nm}^2\left[1+\frac{\dot g_{nm}}{g_{nm}}\,I^{r}(\sigma,n)\right]^2 + h_{nm}^2\left[1+\frac{\dot h_{nm}}{h_{nm}}\,I^{r}(\sigma,n)\right]^2\right\}\Bigg]. \end{aligned} \tag{8.38}$$

It is easy to see that the case $\sigma(r) \equiv 0$ gives for (8.38) the standard MLK for the harmonic downward continuation (8.27). Some slight changes of (8.38) lead to our final expression

$$\begin{aligned} &MLK(SchmQ,R_c,t) \approx \\ &\approx R_E^2\sum_{n=1}^{N}\frac{n(n+1)}{(2n+1)}\sum_{m=0}^{n}\Bigg[g_{nm}^2\left\{\left[1+\frac{\dot g_{nm}}{g_{nm}}\,I^{\vartheta\varphi}(\sigma,n)\right]^2 + (1+\frac{1}{n})\left[1+\frac{\dot g_{nm}}{g_{nm}}\,I^{r}(\sigma,n)\right]^2\right\} + \\ &\qquad + h_{nm}^2\left\{\left[1+\frac{\dot h_{nm}}{h_{nm}}\,I^{\vartheta\varphi}(\sigma,n)\right]^2 + (1+\frac{1}{n})\left[1+\frac{\dot h_{nm}}{h_{nm}}\,I^{r}(\sigma,n)\right]^2\right\}\Bigg]. \end{aligned} \tag{8.39}$$

The square of each Gauss coefficient is controlled by a pair of squared brackets, each containing a conductivity integral $I^r(\sigma,n)$, $I^{\vartheta\varphi}(\sigma,n)$, respectively, which are governed however by oppositely monotonous weight functions (see Ch. 7). Thus, the main effect comes from the magnitude of the conductivity in the range near the ends of the r-interval (earth surface, CMB) combined with the different temporal behaviour of the single Gauss coefficients.

8.3 Diffusion studies

For the mantle, the CMB and the fluid outer core the expanded induction equation containing the Lorentz term with the fluid velocity $\mathbf{v}$

$$\mathrm{curl}\,\big(\frac{1}{\mu_0\,\sigma(r)}\;\mathrm{curl}\;\mathbf{B}\big) - \mathrm{curl}(\mathbf{v}\times\mathbf{B}) = -\frac{\partial}{\partial t}\mathbf{B} \tag{8.40}$$

has to be applied (see Sec. 2.2). The main interest here shall be limited to the diffusion in the mantle connected with the poloidal field $\mathbf{B_p}$ ((2.9) in Sec. 2.1)

$$\mathbf{B} \;=\; \mathbf{B_t} \;+\; \mathbf{B_p}\;. \tag{8.41}$$

The vectorial induction equation for $\mathbf{B_p}$ holds

$$\mathrm{curl}\big(\frac{1}{\mu_0\,\sigma(r)}\;\mathrm{curl}\;\mathbf{B_p}\big) \;=\; -\frac{\partial}{\partial t}\mathbf{B_p} \tag{8.42}$$

which can be transformed by

$$\Delta\,\mathbf{B} \;=\; \mathrm{grad}\;\mathrm{div}\;\mathbf{B} \;-\; \mathrm{curl}\;\mathrm{curl}\;\mathbf{B} \qquad \text{and} \qquad \mathrm{div}\;\mathbf{B} \;=\; 0 \tag{8.43}$$

into

$$\frac{1}{\mu_0\,\sigma(r)}\;\mathrm{curl}\;\mathrm{curl}\;\mathbf{B_p} \;=\; -\frac{\partial}{\partial t}\mathbf{B_p} \tag{8.44}$$

and finally into

$$\frac{1}{\mu_0\,\sigma(r)}\,\Delta\,\mathbf{B_p} \;=\; -\frac{\partial}{\partial t}\mathbf{B_p}\;. \tag{8.45}$$

The left side of this identity represents in vectorial form the quantity of diffusion. Without the common coefficient $1/(\mu_0\,\sigma(r))$ we get for the spherical components the detailed expressions where the symbol Δ now denotes the scalar Laplace operator

$$(\Delta\,\mathbf{B})_r = \Delta\,B_r - \frac{2}{r^2}B_r - \frac{2}{r^2\sin\vartheta}\frac{\partial B_\varphi}{\partial\varphi} - \frac{2}{r^2}\frac{\partial B_\vartheta}{\partial\vartheta} - \frac{2\cot\vartheta}{r^2}B_\vartheta\;, \tag{8.46}$$

$$(\Delta\,\mathbf{B})_\vartheta = \Delta\,B_\vartheta + \frac{2}{r^2}\frac{\partial B_r}{\partial\vartheta} - \frac{2\cot\vartheta}{r^2\sin\vartheta}\frac{\partial B_\varphi}{\partial\varphi} - \frac{B_\vartheta}{r^2\sin^2\vartheta}\;, \tag{8.47}$$

$$(\Delta\,\mathbf{B})_\varphi = \Delta\,B_\varphi + \frac{2}{r^2\sin\vartheta}\frac{\partial B_r}{\partial\varphi} + \frac{2\cot\vartheta}{r^2\sin\vartheta}\frac{\partial B_\vartheta}{\partial\varphi} - \frac{B_\varphi}{r^2\sin^2\vartheta}\;. \tag{8.48}$$

In the following we consider only the diffusion for the r-component. Thus we focus on the relation (8.46). Its detailed form reads as

$$(\Delta\,\mathbf{B})_r \;=\; \frac{\partial^2 B_r}{\partial r^2} + \frac{4}{r}\frac{\partial B_r}{\partial r} + \frac{2}{r^2}B_r + \frac{1}{r^2}\left(\frac{\partial^2 B_r}{\partial\vartheta^2} + \cot\vartheta\frac{\partial B_r}{\partial\vartheta} + \frac{1}{\sin^2\vartheta}\frac{\partial^2 B_r}{\partial\varphi^2}\right) + . \tag{8.49}$$

The first three summands belong to the radial part

$$(\Delta\,\mathbf{B})_{r,rad} = \frac{\partial^2 B_r}{\partial r^2} + \frac{4}{r}\frac{\partial B_r}{\partial r} + \frac{2}{r^2}B_r\;, \tag{8.50}$$

while the remaining three ones are responsible for the tangential part

$$(\Delta\,\mathbf{B})_{r,tan} = \frac{1}{r^2}\left(\frac{\partial^2 B_r}{\partial\vartheta^2} + \cot\vartheta\frac{\partial B_r}{\partial\vartheta} + \frac{1}{\sin^2\vartheta}\frac{\partial^2 B_r}{\partial\varphi^2}\right)\;. \tag{8.51}$$

Accounting for the radial part of the basic vectorial equation $\div\mathbf{B} = 0$ the relation (8.46) can be written in the advantageous shorter form

$$(\Delta\,\mathbf{B})_r = \Delta\,B_r + \frac{2}{r}\frac{\partial B_r}{\partial r} + \frac{2}{r^2}B_r\;. \tag{8.52}$$

Chulliat & Olsen (2010) give for the diffusion the equivalent expression

$$D = \frac{1}{\mu_0 \sigma(r)} \left(\frac{1}{r}\right) \Delta\,(rB_r)\ . \tag{8.53}$$

Amit & Christensen (2008) choose for the whole r-component of the poloidal induction equation the representation

$$\dot{B}_r = \frac{1}{\mu_0 \sigma(r)} \left(\frac{1}{r^2}\frac{\partial^2}{\partial r^2}(r^2 B_r) + \Delta\, B_r\ - \frac{1}{r^2}\frac{\partial}{\partial r}(r^2 \frac{\partial B_r}{\partial r})\right)\ . \tag{8.54}$$

The r-component of the expanded vectorial induction equation (8.40) has the known form

$$\dot{B}_r = -\nabla_H (u_H\, B_r) + \frac{1}{\mu_0 \sigma(r)} \left(\frac{1}{r}\Delta\,(rB_r)\right)\ , \tag{8.55}$$

where the index H means the horizontal components, respectively. Usually, for large (core) conductivity values the second term on the right hand side is neglected (additionally there is also a scale argument), and the fluid flow studies for the CMB are done using the relation (see for example Wardinski, 2005,?; Wardinski & Lesur, 2012)

$$\dot{B}_r = -\nabla_H (u_H\, B_r)\ . \tag{8.56}$$

With (8.55) instead of (8.56), the traditional fluid flow determination (specified with the different constraints) can account for the diffusion term, i.e. for the effect of the mantle conductivity above the CMB.

Summing up, except for the coefficient $1/(\mu_0 \sigma(r))$ the quantities (8.46), (8.49), (8.52), (8.53) and (8.54) are identical. For the calculation of the diffusion of the radial component immediately above the CMB, there exist different possibilities: The total quantity D, (8.53), can be calculated directly by the secular variation quantity $\dot{B}_r$, determined with NHDC, due to (8.45 and (8.54). A further possibility provides (8.49) by the calculation of all single terms at the CMB and their summation. With this a separated calculation of both parts, the radial diffusion (8.50) and the tangential diffusion (8.51), can be reached, in analogy to the application of dynamo studies of Amit & Christensen (2008).

Without the intention to present here a detailed study, the Figures 8.1–8.4 show one example for the diffusion of the field component B_r, downward continued to the CMB under different aspects. For the data model C^{3}FM (Wardinski & Lesur, 2012), used up to the degree $n = 8$ and the mantle conductivity model $\sigma_{5-250}(r)$ (see Sec. 8.1), the time 2005.0 is considered. Fig. 8.1 shows the total diffusion calculated corresponding to the identical relations (8.53), (8.54). The difference of left and right hand side of (8.54), $\dot{B}_r - D$, is presented in Fig. 8.2 (with other scale than in Fig.8.1!), illustrating the quality of approximation the diffusion directly by the secular variation $\dot{B}_r$ at the CMB instead of the calculation by the single terms. The difference amounts here e.g. to about 5%. Figs. 8.3 and 8.4 demonstrate the splitting of the total diffusion into radial and tangential parts, corresponding to the relations (8.50) and (8.51). Especially, we notice the wide difference between the scales for the total diffusion in Fig. 8.1 and its radial and tangential parts in Figs. 8.3 and 8.4, which cancel each other for the most part.

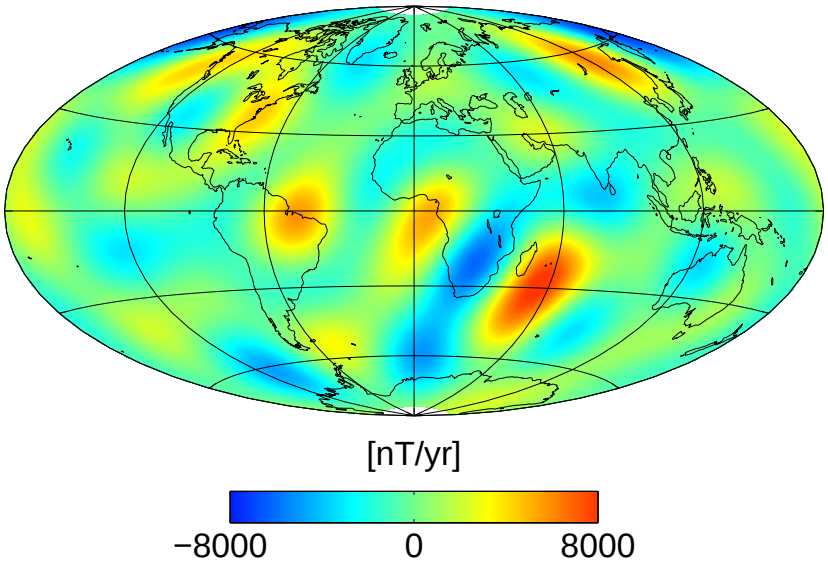

Figure 8.1: Total diffusion at the CMB (8.53) for 2005.0. Calculated with NHDC from the data model C^{3}FM (Wardinski & Lesur, 2012) up to the degree $n = 8$ using the mantle conductivity model $\sigma_{5-250}(r)$ (8.4).

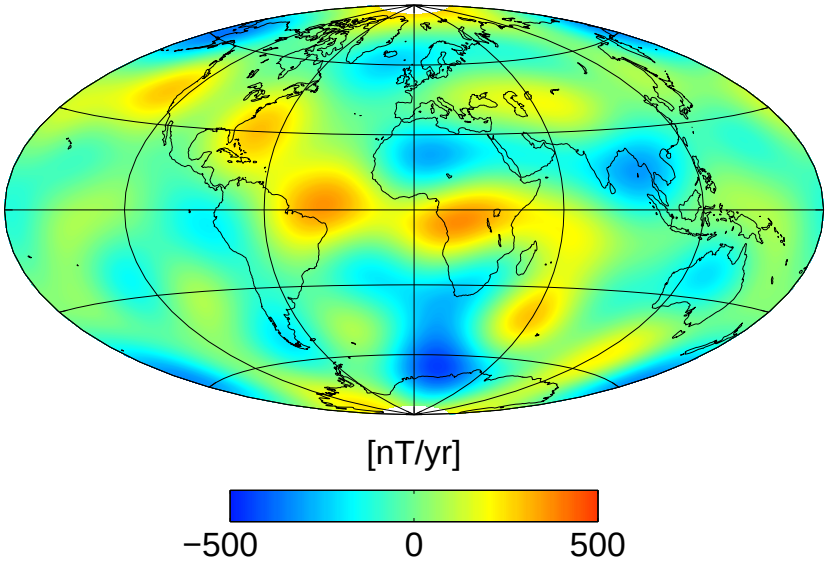

Figure 8.2: Difference $\dot{B}_r - D$, D from (8.53), at the CMB (8.53) for 2005.0. Both quantities calculated with NHDC from the data model C^{3}FM (Wardinski & Lesur, 2012) up to the degree $n = 8$ using the mantle conductivity model $\sigma_{5-250}(r)$ (8.4).

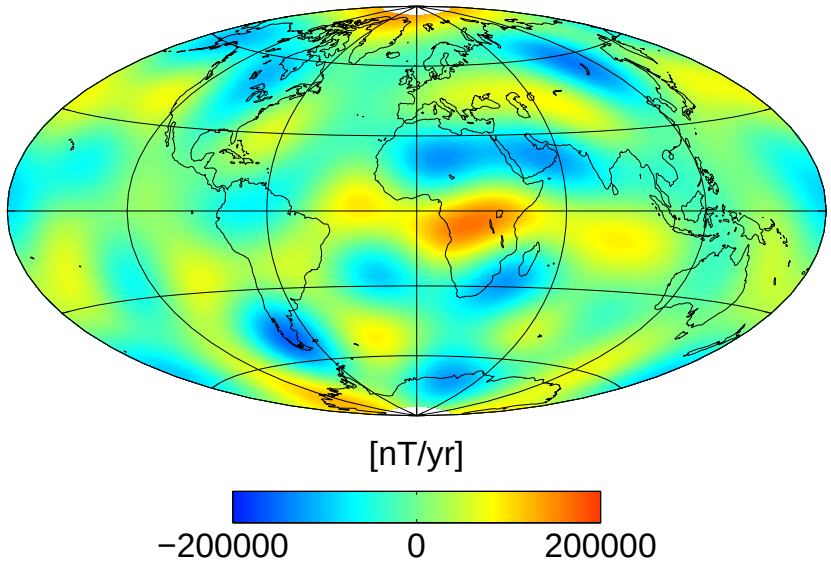

Figure 8.3: Radial diffusion at the CMB (8.50) for 2005.0. Calculated with NHDC from the data model C^{3}FM (Wardinski & Lesur, 2012) up to the degree $n = 8$ using the mantle conductivity model $\sigma_{5-250}(r)$ (8.4).

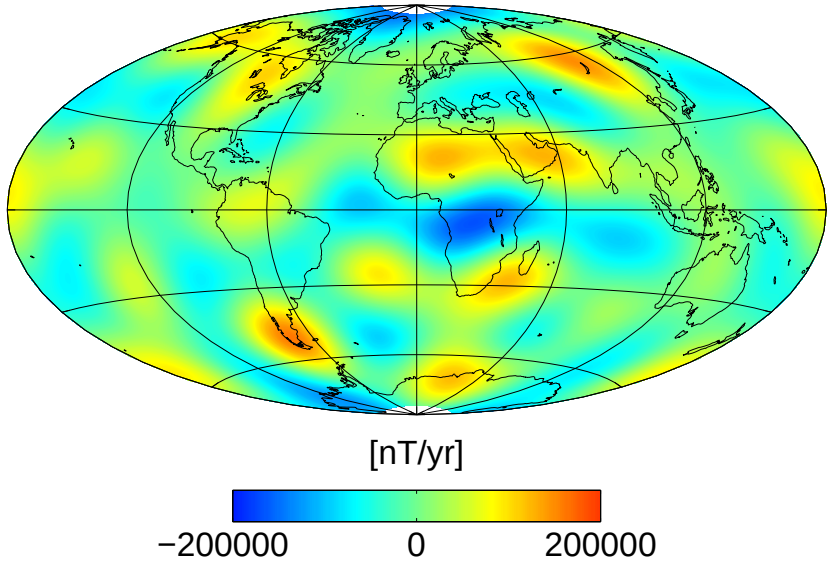

Figure 8.4: Tangential diffusion at the CMB (8.51) for 2005.0. Calculated with NHDC from the data model C^{3}FM (Wardinski & Lesur, 2012) up to the degree $n = 8$ using the mantle conductivity model $\sigma_{5-250}(r)$ (8.4).

9 Overcoming the limitations

The nonharmonic downward continuation (NHDC) represents a theoretically rigorous method to determine the geomagnetic field at the CMB which accounts for a given mantle conductivity model. Due to the temporal instability concerning higher frequencies it needs regularization. In addition, this downward continuation task can be approximatively solved by certain setups. Supplementary, this approach enables some insight into some dependencies of involved parameters. For the field produced near the CMB, the divergence-free condition (as part of the Maxwell equations) keeps fulfilled with high precision. The spacial-temporal resolution for interesting areas, especially the CMB zone, can be adapted by the finite-element technique.

The benefit of the method is manifold, e.g. the calculations of the electromagnetic core-mantle coupling or detailed diffusion studies. Moreover, the NHDC can be used for a new estimate of bound for the Ohmic heating in the core (Backus et al., 1996). In connection with the components of jerks, calculated at the CMB, and their time shift differences, constraint for the deep mantle conductivity can be derived. The behaviour of jerks, calculated in different depths of the fluid upper core layer, can help to find arguments concerning the origin of jerks. Also the investigation of jerks in terms of moving energy acceleration patterns can give hints for active areas in the fluid outer core.

The limitation of the presented NHDC method consists mainly in its one-dimensionality, which is based on the assumption $\sigma = \sigma(r)$. On the other hand, it is just this condition which is responsible for the advantageous separability of poloidal and toroidal field part. Some indications show that the lateral (θ, ϕ) dependency of the electrical mantle conductivity is much weaker than the radial one so that our approach is justified up to a certain order of magnitude. Nevertheless, significant exceptions exist in several regions with strong lateral anomalies, e.g. beneath the southern Africa.

One way to study lateral inhomogeneous problems with the existing theoretical frame (NHDC) is their transformation to locally limited areas. This requires (in analogy to existing methods as done at developing the spherical cap harmonic analysis by Thébault et al., 2006) new theoretical derivations which secure a new self-contained method which can decompose inhomogeneous areas with controlled boundary effects.

The development of the mathematical formulation as an adjoint problem or the enlargement to a assimilation problem which can be connected with other fields can provide advantages. From the background mathematical point of view, for the inverse heat equation in two or three dimensions, some theoretical work on stability etc. already exists (e.g. Vessella, 1997; Knosowski et al., 1999; Berntsson & Eldén, 2001). For the upward continuation in three dimension Hamano (2002) has derived a formalism which uses Gauss coefficients given at the CMB and a prescribed inhomogeneous conductivity. On this systematic studies of the effect of special cases preliminary work could base for further development of the inverse problem. A two- or three-dimensional formalism for the earth magnetic field downward continuation would require a coupled treatment of poloidal and toroidal field parts. The lacking of boundary values for the toroidal field outside the earth body can be only compensated by additional assumptions. One possibility accounting for the physical background is the modelling by its (the field) sources, the generating velocities in the fluid outer core (Hagedoorn et al., 2010). This means a shifting and possibly enlargement of the original inverse problem. Those velocities existing directly on the core-mantle boundary, i.e. on the surface of the core, can be approximatively ('frozen flux approximation') related to the field there and are relatively often determined, however, using different types of additional assumptions necessary to diminish non-uniqueness (Bloxham & Jackson, 1991; Wardinski, 2005; Wardinski & Lesur, 2012).

A more comprehensive inverse modelling of the earth interior means above all the inclusion of dynamical aspects: In the fluid outer core, the induction law as the field equation, can be coupled with the

Navier-Stokes equation, which describes the fluid dynamics in different approximations, or also possibly coupled with thermodynamic and rheological laws. The concerning inverse problems with the aim to determine field components and fluid motion based on observed data can be entitled as 'inverse dynamo problems' (see e.g. Stefani & Gerbeth, 2000; Matsushima & Honkura, 1989). However, the main effort made in this field today is to calculate geodynamo models under different conditions, which consists in solving direct initial and boundary value problems.

Another possibility of coupling different geophysical quantities is the relation between magnetic field and earth rotation: A correlation is observed in the decadal period range. Thus it is e.g. assumed that the responsible electromagnetic coupling torque between core and mantle (Lorentz torque) is balanced by the relative rotation of a fluid outer core layer for which some parameter information can be concluded by the joint inversion of magnetic and earth rotation data. However a fully consistent modelling between magnetic field and earth rotation without any contradictions exist up to now only for partial aspects (Hagedoorn & Greiner-Mai, 2008; Greiner-Mai & Hagedoorn, 2008; Hagedoorn et al., 2012). Further improvement of the input data (i.e. temporally higher resolved and better coverage of the earth surface with the planned SWARM mission, including additional older data, special campaigns on the earth surface to fill gaps), will allow to study higher frequency, suddenly or episodic events (e.g. jerks) in greater detail and will lead to the determination of improved (more constraint) parameter bounds in the deep earth interior.

Acknowledgement

We thank our colleague Ingo Wardinski for his permanent help with advices, his readiness for discussions and his support with data and software. One of the authors (J.M. Hagedoorn) was supported by the DFG research unit 584, 'Earth Rotation and Global Dynamic Processes'.

References R

Abramowitz, M., Stegun, I. A., 1965. Handbook of Mathematical Functions. New York: Dover Publications.

Alexandrescu, M., Gibert, D., Hulot, G., Le Mouël, J., Saracco, G., 1995. Detection of geomagnetic jerks using wavelet analysis. J. geophys. Res. 100, 12557–12572.

Alexandrescu, M., Gibert, D., Hulot, G., Le Mouël, J., Saracco, G., 1996. Worldwide wavelet analysis of geomagnetic jerks. J. geophys. Res. 101, 21975–21994.

Amit, H., Christensen, U. R., 2008. Accounting for magnetic diffusion in core flow inversions from geomagnetic secular variation. Geophys. J. Int. 175, 913 – 924.

Backus, G., Parker, R., Constable, C., 1996. Foundations of Geomagnetism. Cambridge University Press.

Backus, G. E., 1983. Application of mantle filter theory to the magnetic jerk of 1969. Geophys. J. R. astr. Soc. 74, 713–746.

Backus, G. E., 1986. Poloidal and toroidal fields in geomagnetic field modeling. Rev. Geophys. 24, 75–109.

Ballani, L., Greiner-Mai, H., Stromeyer, D., 1995. Über ein nicht-charakteristisches Cauchy-Problem bei der geomagnetischen Kern-Mantel-Kopplung. Zeitschr. f. Angew. Math. Mech. (ZAMM) 75 (SII), S613 – S614.

Ballani, L., Greiner-Mai, H., Stromeyer:, D., 1999. Determining the magnetic field in the earth's deep mantle by an inverse boundary value problem. Scientific Technical Report STR99/12, GFZ Potsdam, Germany, DOI: 10.2312/GFZ.b103-99127

Ballani, L., Greiner-Mai, H., Stromeyer, D., 2002. Determining the magnetic field in the core-mantle boundary zone by non-harmonic downward continuation. Geophys. J. Int. 149, 374–389.

Ballani, L., Hagedoorn, J. M., Wardinski, I., Stromeyer, D., Greiner-Mai, H., 2010. The 1991 geomagnetic jerk as seen at the earth's surface and the core-mantle boundary. Geophys. J. Int. 183 (2), 659–680.

Benton, E. R., Whaler, K. A., 1983. Rapid diffusion of the poloidal geomagnetic field through the weakly conducting mantle: a perturbation solution. Geophys. J. R. astr. Soc. 75, 77–100.

Berntsson, F., 1999. A spectral method for solving the sideways heat equation. Inverse Problems 15, 891–906.

Berntsson, F., Eldén, L., 2001. Numerical solution of a Cauchy problem for the Laplace equation. Inverse Problems 17, 839–853.

Bloxham, J., Jackson, A., 1991. Fluid flow near the surface of the Earth's outer core. Rev. Geophys. 29, 97–120.

Braginsky, S. I., Fishman, V. M., 1977. Screening of the magnetic field in the mantle under electrical conductivity concentrated close to the core boundary. Geomag. Aeron. 17 (5), 907–915.

Bronshtein, I. N., Semendyayev, K. A., Musiol, G., Muehlig, H., 2004. Handbook of Mathematics, 4. Edition. Springer-Verlag Berlin Heidelberg.

Bullard, E. C., Gellman, H., 1954. Homogeneous dynamos and terrestrial magnetism. Philos. Trans. R. Soc. London A 247, 213–278.

Burggraf, O. R., 1964. An exact solution of the inverse problem in heat conduction theory and aplications. J. Heat Transfer 86C, 373 – 382.

Cannon, J. R., 1984. The One-Dimensional Heat Equation. Vol. 23 of Encyclopedia of Mathematics. Addison-Wesley, Reading, Mass..

Carslaw, H. S., Jaeger, J. C., 1992. Conduction of heat in solids. Oxford: Clarendon Press.

Chulliat, A., Olsen, N., 2010. Observation of magnetic diffusion in the Earth's outer core from Magsat, Ørsted, and CHAMP data. J. geophys. Res. 115, doi:10.1029/2009JB006994.

Currie, R. G., 1967. Magnetic shielding properties of the Earth's mantle. J. geophys. Res. 72, 2623–2633.

Dinh, N. H., Gorenflo, R., 1991. A noncharacteristic Cauchy problem for the heat equation. Acta Appl. Math. 24, 1–27.

Dinh Nho Hào, 1994. A noncharacteristic Cauchy problem for linear parabolic equations and related inverse problems I: Solvability. Inverse Problems 10 (2), 195 – 315.

Doetsch, G., 1937. Theorie und Anwendung der Laplace-Transformation. Vol. XLVII of Grundlehren der Mathematischen Wissenschaften. Berlin: Julius Springer.

Eldén, L., 1983. The numerical solution of a non-characteristic Cauchy problem for a parabolic equation. In: Deuflhard, P., Hairer, E . (Eds.), Numerical Treatment of Inverse Problems in Differential and Integral Equations. Birkhäuser: Boston, Basel, Stuttgart, pp. 246–268.

Eldén, L., 1995. Numerical solution of the sideways heat equation. In: Engl, H., Rundell, W. (Eds.), Inverse Problems in Diffusion Processes. Philadelphia: SIAM, pp. 130–150.

Engl, H. W., 1982. On least-squares collocation for solving linear integral equations of the first kind with noisy right-hand side. Boll. Geod. Sci. Aff. 41, 291 – 313.

Engl, H. W., Hanke, M., Neubauer, A., 1996. Regularization of Inverse Problems. Kluwer Academic Publishers, Dordrecht/Boston/London.

Engl, H. W., Manselli, P., 1989. Stability estimates and regularization for an inverse heat conduction problem in semi-infinite and finite time intervals. Numer. Funct. Anal. Optim. 10, 517–540.

Evans, L., 1998. Partial Differential Equations. AMS.

Francini, E., 2000. Stability results for solutions of a linear parabolic noncharacteristic Cauchy problem. J. Inv. Ill-Posed Problems 8 (3), 255 – 272.

Greiner-Mai, H., 1993. Decade variations of the earth's rotation and geomagnetic core-mantle coupling. J. Geomag. Geoelectr. 45, 1333–1345.

Greiner-Mai, H., Ballani, L., Stromeyer, D., 2001. Continuation of the earth's magnetic field into a core layer with differential rotation. Sci. Techn. Rep. GFZ Potsdam, STR01/09, http://ebooks.gfz-potsdam.de/pubman/item/escidoc:8524:1/component/escidoc:8523/0109.pdf.

Greiner-Mai, H., Ballani, L., Stromeyer, D., 2004. The poloidal geomagnetic field in a differentially rotating upper core layer. Geophys. J. Int. 158, 864–873.

Greiner-Mai, H., Hagedoorn, J., 2008. Core-Mantle Coupling - Part II: Topographic coupling torques. Sci. Techn. Rep. GFZ Potsdam, STR 08/11 http://ebooks.gfz-potsdam.de/pubman/item/escidoc:8774:2/component/escidoc:8773/0811.pdf.

Greiner-Mai, H., Hagedoorn, J., Ballani, L., Wardinski, I., Stromeyer, D., Hengst, R., 2007. Axial poloidal electromagnetic core-mantle coupling torque: A re-examination for different conductivity and satellite supported geomagnetic field models. Studia geophys.geod. 51 (4), 491–513.

Groetsch, C. W., 1984. The Theory of Tikhonov Regularization for Fredholm Equations of the First Kind. Boston: Pitman.

Gubbins, D., 1996. A formalism for the inversion of geomagnetic data for core motions with diffusion. Phys. Earth Planet. Inter. 98, 193–206.

Hagedoorn, J., Greiner-Mai, H., 2008. Core-Mantle Coupling - Part I: Electromagnetic coupling torques. Sci. Techn. Rep. GFZ Potsdam, STR 08/06, http://ebooks.gfz-potsdam.de/pubman/item/escidoc:8764:3/component/escidoc:18014/Component%20escidoc:18014.

Hagedoorn, J., Greiner-Mai, H., Ballani, L., 2010. Determining the time-variable part of the toroidal geomagnetic field in the core-mantle boundary zone. Phys. Earth Planet. Inter. 178, 56–67.

Hagedoorn, J., Greiner-Mai, H., Ballani, L., 2012. Core-Mantle Coupling - Part III: Gravitational coupling torques. Sci. Techn. Rep. GFZ Potsdam, STR 12/01, http://ebooks.gfz-potsdam.de/pubman/faces/viewItemFullPage.jsp?itemId=escidoc:61143.

Hamano, Y., 2002. A new time-domain approach for the electromagnetic induction problem in a three-dimensional heterogeneous earth. Geophys. J. Int. 150, 753–769.

Hansen, P. C., 1992, 1998. Regularization Tools. A Matlab Package for Analysis and Solution of Discrete Ill-Posed Problems. Lyngby, Denmark, 109 pp.

Hazewinkel, M. (Ed.), 2002. Encyklopaedia of Mathematics. Springer-Verlag Berlin.

Heuser, H., 1991. Gewöhnliche Differentialgleichungen: Einführung in Lehre und Gebrauch, 2. Edition. Mathematische Leitfäden. Stuttgart: Teubner.

Holme, R., 1998. Electromagnetic core-mantle coupling I: Explaining decadal variations in the Earth's length of day. Geophys. J. Int. 132, 167–180.

Jacobs, J. (Ed.), 1987a. Geomagnetism. Vol. 1. Academic Press, London.

Jacobs, J. (Ed.), 1987b. Geomagnetism. Vol. 2. Academic Press, London.

Kautzleben, H., 1963. Die analytische Darstellung des geomagnetischen Hauptfeldes und der Säkularvariation. Abhandlung, Geomagnetisches Institut Potsdam, Deutsche Akademie der Wissenschaften zu Berlin Nr. 32, 96pp.

Kautzleben, H., 1965. Kugelfunktionen. B.G. Teubner Verlagsgesellschaft, Leipzig.

Knabner, P., Vessella, S., 1987. Stabilization of ill-posed Cauchy problems for parabolic equations. Ann. Mat. Pura Appl. 149, 393–409.

Knabner, P., Vessella, S., 1988. The Optimal Stability Estimate for some Ill-posed Cauchy Problems for a Parabolic Equation. Math. Meth. Appl. Sci. 10, 575–583.

Knosowski, Y., von Lieres, B., Schneider, A., 1999. Regularization of a non-characteristic Cauchy problem for a parabolic equation in multiple dimensions. Inverse Problems 15, 731 – 743.

Kolomitzeva, G. I., 1972. On the distribution of the electrical conductivity in the Earth mantle by secular variation data of the geomagnetic field (Russian). Geomagnetizm i Aeronomiya 12, 1082 – 1085.

Kolomitzeva, G. I., 1982. About screen properties of the mantle and extrapolation of the variation field to the core-mantle boundary (Russian). Geomagnetizm i Aeronomiya 22 (2), 287 – 291.

Krause, F., Rädler, K.-H., 1980. Mean-Field Magnetohydrodynamics and Dynamo Theory. Akademie-Verlag, Berlin / Pergamon Press, Oxford.

Kuvshinov, A., 2012. Deep electromagnetic studies from land, sea, and space: progress status in the past 10 years. Surv. Geophys. 33, 169–209.

Lowes, F. J., 1966. Mean-square values on sphere of spherical harmonic vector fields. J. geophys. Res. 71, 2179.

Lowes, F. J., 1974. Spatial power spectrum of the main geomagnetic field, and extrapolation to the core. Geophys. J. R. astr. Soc. 36, 717–730.

Lucke, O., 1957. Über Mittelwerte von Energiedichten der Kraftfelder. Wiss. Z. Pädagog. Hochschule Potsdam. Math Nat. Reihe 3 (1), 39 – 46.

Manselli, P., Miller, K., 1980. Calculation of the surface temperature and heat flux on one side of a wall from measurements on the opposite side. Ann. Mat. Pura Appl. 123, 161–83.

Manselli, P., Vessella, S., 1991. On Continuous Dependence, on Noncharacteristic Cauchy Data, for Level Lines of Solutions of the Heat Equation. Forum Math. 3, 513–521.

Matsushima, M., Honkura, Y., 1989. Large-scale fluid motion in the earth's outer core estimated from non-dipole magnetic field data. J. Geomag. Geoelectr. 41, 963 – 1000.

Mauersberger, P., 1952. Betrachtungen über die zeitliche Änderung der Parameter des geomagnetischen Feldes auf Grund der vorliegenden Potentialentwicklungen. Abhandlungen Geophysikalisches Institut Potsdam No. 5, 5 – 58.

Mauersberger, P., 1956. Das Mittel der Energiedichte des geomagnetischen Hauptfeldes an der Erdoberfläche and seine säkulare Änderung. Gerlands Beitr. Geophys. 65, 207–215.

McDonald, K. L., 1957. Penetration of the geomagnetic secular field through a mantle with variable conductivity. J. geophys. Res. 62, 117–141.

Olsen, N., 2002. A model of the geomagnetic field and its secular variation for epoch 2000 estimated from Ørsted data. Geophys. J. Int. 149, 455–463.

Pinheiro, K., Jackson, A., JUN 2008. Can a 1-D mantle electrical conductivity model generate magnetic jerk differential time delays? Geophys. J. Int. 173 (3), 781–792.

Reigber, C., Lühr, H., Schwintzer, P., 2002. CHAMP mission status. Adv. Space Res. 30, 129–134.

Reinhardt, H.-J., Seiffarth, F., 1993. On the Approximate Solution of Illposed Cauchy Problems for Parabolic Differential Equations. In: Inverse Problems: Principles and Applications in Geophysics, Technology, and Medicine. Vol. 74 of Mathematical Research. Anger, G. et al (eds), Berlin: Akademie-Verlag, pp. 284–298.

Roberts, P. H., 1972. Electromagnetic core-mantle coupling. J. Geomag. Geoelectr. 24, 231–259.

Rochester, M. G., 1960. Geomagnetic westward drift and irregularities in the Earth's rotation. Philos. Trans. R. Soc. London A 252, 531–555.

Rochester, M. G., 1962. Geomagnetic core-mantle coupling. J. Geophys. Res. 67, 4833 – 4836.

Rotanova, N. M., Fishman, V. M., Abramova, D. J., Bondar, T. N., 1991. On analytical continuation of the geomagnetic secular variation field to the core boundary (Russian). Geomagnetism and Aeronomiya 31(3), 513 – 520.

Schmitt, B. J., 1995. The poloidal-toroidal representation of solenoidal field in spherical domains. Analysis 15 (3), 257–277.

Smylie, D. E., 1965. Magnetic diffusion in a spherically-symmetric conducting mantle. Geophys. J. R. astr. Soc. 9, 169–184.

Sommerfeld, A., 1961. Elektrodynamik, vol. III Vorlesungen über Theoretische Physik. Akadem. Verl.-Ges. Leipzig.

Spanier, J., Oldham, K. B., 1987. An Atlas of Functions. Washington et al: Hemisphere Publishing Corporation.

Stadelmann, J., 2001,2006. Diffusion der Säkularvariation durch den Erdmantel: Diffusionszeiten für radiale und tangentiale Magnetfelder. In: Hoerdt, A. , Stoll, J. (Ed.), Protokoll über das 19. Kolloquium "Elektromagnetische Tiefenforschung" Burg Ludwigstein 1.-5.10.2001. Deutsche Geophysikalische Gesellschaft e. V., [Bibliothek des Wissenschaftsparks Albert Einstein] [Vertrieb], [Potsdam], pp. 253 – 262.

Stadelmann, J., Weidelt, P., 2005a. Diffusion of the geomagnetic secular variation through the heterogeneous mantle. Final report, DFG Priority Program 1097: Geomagnetic Variations; proposal We 1048/6-2, Institute of Geophysics and Extraterrestrial Physics, Technical University of Braunschweig, Germany.

Stadelmann, J., Weidelt, P., 2005b. Electromagnetic time constants of the earth's mantle. In: Ritter, O., Brasse, H. (Eds.), Protokoll über das 21. Kolloquium "Elektromagnetische Tiefenforschung" Haus Wohldenberg, Holle 3.-7.10.2005. Deutsche Geophysikalische Gesellschaft e. V., [Bibliothek des Wissenschaftsparks Albert Einstein] [Vertrieb], Potsdam, pp. 91 – 110.

Stefani, F., Gerbeth, G., 2000. Can we look inside a dynamo? Astron. Nachr. 312, 235–247.

Stix, M., 1982. On electromagnetic core-mantle coupling. Geophys. Astrophys. Fluid Dynamics 21, 303–313.

Thébault, E., Schott, J. J., Mandea, M., 2006. Revised spherical cap harmonic analysis (R-SCHA): Validation and properties. J. geophys. Res. (Solid Earth) 111, 1102.

Tsutsumi, A., 1965. A remark on the uniqueness of the noncharacteristic cauchy problem for equations of parabolic type. Proc. Japan Acad. Ser. A Math. Sci. 41, 65 – 70.

Vessella, S., 1997. Stability estimates in an inverse problem for a three-dimensional heat equation. SIAM J. Math. Anal. 28, 1354–1370.

Wardinski, I., 2005. Core surface flow models from decadal and subdecadal secular variation of the main geomagnetic field. Sci. Techn. Rep. STR05/07, GFZ Potsdam, http://ebooks.gfz-potsdam.de/pubman/faces/viewItemFullPage.jsp?itemId=escidoc:8672:3.

Wardinski, I., Lesur, V., 2012. An extended version of the C^{3}FM geomagnetic field model: application of a continuous frozen-flux constraint. Geophys. J. Int. 189, 1409–1429.

Zhdanov, M. S., Rotanova, N. M., Chernova, T. A., 1980. On analytical continuation of the main geomagnetic field and its secular variation (Russian). Geomagnetism and Aeronomiya 20, 718 – 725.

Zwillinger, D., 1997. Handbook of Differential Equations, 3. Edition. Academic Press, San Diego.

ISSN 1610-0956